Nuriye Arslansoy

M.Sc. Thesis

AGU 2024

BIOSYNTHESIS OF HIGH VALUE-ADDED CAROTENOIDS BY ENGINEERED MICROORGANISMS

M.Sc. THESIS
SUBMITTED TO THE DEPARTMENT OF BIOENGINEERING
AND THE GRADUATE SCHOOL OF ENGINEERING AND SCIENCE
OF ABDULLAH GUL UNIVERSITY
IN PARTIAL FULFILLMENT OF THE REQUIREMENTS
FOR THE DEGREE OF
MASTER OF SCIENCE

By
Nuriye Arslansoy
August 2024

BIOSYNTHESIS OF HIGH VALUE-ADDED CAROTENOIDS BY ENGINEERED MICROORGANISMS

A THESIS
SUBMITTED TO THE DEPARTMENT OF BIOENGINEERING
AND THE GRADUATE SCHOOL OF ENGINEERING AND SCIENCE OF
ABDULLAH GUL UNIVERSITY
IN PARTIAL FULFILLMENT OF THE REQUIREMENTS
FOR THE DEGREE OF
MASTER OF SCIENCE

By
Nuriye Arslansoy
August 2024

SCIENTIFIC ETHICS COMPLIANCE

I hereby declare that all information in this document has been obtained in accordance with academic rules and ethical conduct. I also declare that, as required by these rules and conduct, I have fully cited and referenced all materials and results that are not original to this work.

Name-Surname: Nuriye Arslansoy
Signature:

REGULATORY COMPLIANCE

M.Sc. thesis titled Biosynthesis of High Value-added Carotenoids by Engineered Microorganisms has been prepared in accordance with the Thesis Writing Guidelines of the Abdullah Gül University, Graduate School of Engineering & Science.

Prepared By	Advisor
Nuriye Arslansoy	Asst. Prof. Özkan Fidan

Head of the Bioengineering Program
Asst. Prof. Emel Başak Gencer Akçok

ACCEPTANCE AND APPROVAL

M.Sc. thesis titled Biosynthesis of High Value-added Carotenoids by Engineered Microorganisms and prepared by Nuriye Arslansoy has been accepted by the jury in the Bioengineering Graduate Program at Abdullah Gül University, Graduate School of Engineering & Science.

19 /08/ 2024

(Thesis Defense Exam Date)

JURY:

Advisor: Asst. Prof. Özkan Fidan

Member: Asst. Prof. İsmail Akçok

Member: Prof. Dr. Oğuz Bayraktar

APPROVAL:

The acceptance of this M.Sc. thesis has been approved by the decision of the Abdullah Gül University, Graduate School of Engineering & Science, Executive Board dated ….. /….. / 2024 and numbered ……..…….

…….. /…….. / 2024

Graduate School Dean
Prof. Dr. İrfan ALAN

ABSTRACT

BIOSYNTHESIS OF HIGH VALUE-ADDED CAROTENOIDS BY ENGINEERED MICROORGANISMS

Nuriye Arslansoy
MSc. in Bioengineering
Advisor: Asst. Prof. Özkan Fidan
August 2024

Carotenoids are pigment molecules that play an important role in coloring plants, algae, and other organisms. These molecules exhibit various biological activities such as anticancer, antiviral and antioxidant activities. They have a huge market size and are mainly used in the food, feed, and cosmetic industries. The current supply chain for carotenoids is mostly relied on the extraction from plants and/or chemical synthesis for certain carotenoids. However, these strategies have various bottlenecks and disadvantages such as being affected by climate change, more difficult and costly extraction processes, and environmental issues. These can be overcome with microbial biosynthesis, which not only addresses the previous problems but also provides advantages of producing in a short time and scale-up for industrial production. In this research, we aimed to biosynthesize the high value-added carotenoids by engineered microorganisms. The genome of a native producer of zeaxanthin diglucoside, identified as endophytic *Pseudomonas* sp. 102515, was first edited by CRISPR-Cas9 to knock out zeaxanthin glucosyltransferase (CrtX), lycopene β-cyclase (CrtY) and beta-carotene hydroxylase (CrtZ). This led to Δ*crtX*, Δ*crtY* and Δ*crtZ* mutant strains of *Pseudomonas* sp. 102515. On the other hand, overexpression plasmids carrying *crtW*, *CaZEP* and *CaZEP-CaCCS*$_{m40}$ genes were constructed and transformed to Δ*crtX* mutant to synthesize astaxanthin, violaxanthin and capsanthin/capsorubin. HPLC analysis of extracts from mutant strains and overexpression strains revealed that all the engineered strains produced the corresponding carotenoids such as zeaxanthin, β-carotene, and lycopene. Thus, this study paved the way for the biosynthesis of valuable carotenoids in the engineered endophytic bacteria.

Keywords: Carotenoids, Biosynthesis, Pseudomonas, Genetic Engineering, CRISPR-Cas9

ÖZET

TASARLANMIŞ MİKROORGANİZMALAR İLE KATMA DEĞERİ YÜKSEK KAROTENOİDLERİN BİYOSENTEZİ

Nuriye Arslansoy
Biyomühendislik Anabilim Dalı Yüksek Lisans
Tez Yöneticisi: Dr. Öğr. Üyesi Özkan Fidan
Ağustos 2024

Karotenoidler, bitkiler, algler ve diğer organizmaları renklendirmede önemli rol oynayan pigment moleküllerdir. Bu moleküller, antikanser, antiviral ve antioksidan aktiviteler gibi çeşitli biyolojik aktiviteler sergiler. Büyük bir market büyüklüğüne sahiptirler ve ağırlıklı olarak gıda, yem ve kozmetik endüstrilerinde kullanılırlar. Karotenoidlerin mevcut tedarik zinciri, çoğunlukla bitkilerden ekstraksiyon ve/veya belirli karotenoidler için kimyasal senteze dayanır. Ancak, bu stratejiler iklim değişikliğinden etkilenme, daha zor ve maliyetli ekstraksiyon süreçleri ve çevresel sorunlar gibi çeşitli kısıtlamalar ve dezavantajlara sahiptir. Mikrobiyal biyosentez bu sorunları aşmak ve aynı zamanda kısa sürede, endüstriyel ölçekte üretim için avantajlar sağlayan etkili bir yöntemdir. Bu araştırmada, genetik olarak tasarlanmış mikroorganizmalar kullanarak yüksek katma değerli karotenoidleri biyosentezle üretmeyi amaçladık. Doğal bir zeaksantin diglukozit üreticisi olarak keşfedilmiş endofitik *Pseudomonas* sp. 102515'in genomu, CRISPR-Cas9 ile düzenlenerek zeaksantin glukoziltransferaz (CrtX), likopen β-siklaz (CrtY) ve β-karoten hidroksilaz (CrtZ) genleri nakavt edildi. *Pseudomonas* sp. 102515'in Δ*crtX*, Δ*crtY* ve Δ*crtZ* mutant suşları elde edildi. Diğer yandan, *crtW*, *CaZEP* ve *CaZEP-CaCCS*$_{m40}$ genlerini taşıyan aşırı ekspresyon plazmidleri oluşturuldu ve Δ*crtX* mutantına astaksantin, violaksantin ve kapsantin/kapsorubin sentezlemek üzere transforme edildi. Mutant suşlardan ve aşırı ekspresyon suşlarından elde edilen ekstraktların HPLC analizi, genetik olarak tasarlanmış suşların zeaksantin, β-karoten ve likopen gibi ilgili karotenoidi ürettiğini ortaya koydu. Böylece, bu çalışma, genetik mühendislik ile endofitik bakterilerde değerli karotenoidlerin biyosentezi için bir yol açtı.

Anahtar kelimeler: Karotenoidler, Biyosentez, Pseudomonas, Genetik Mühendisliği, CRISPR-Cas9

Acknowledgements

First and foremost, I would like to express my gratitude to my advisor, Dr. Özkan Fidan, for giving me this opportunity and providing invaluable guidance throughout the journey. I am deeply appreciative of his patience and genuine interest as an advisor. Additionally, I want to thank him for his accessibility, which is an essential quality of an outstanding advisor.

I would like to thank TÜBİTAK for supporting our project under 3501-Career Development Program (Project No: 221Z280). Also, I would like to express my sincere thanks to TÜBİTAK for financially supporting me as a scholar under this project (Project No: 221Z280) through my master studies and by BİÇABA-Birlikte Çalışıp Birlikte Başaracağız Scholarship Program for 12 months.

I want to extend my heartfelt thanks to my entire family, who consider my aspirations and support my career at every step. Especially, I would like to thank my mom, Fatma Arslansoy, who encouraged me to pursue my studies and has continuously shaped the direction of my life for the better since my birth. I am deeply grateful to my beloved sisters, Ayşe and Tuba Arslansoy, and my little brother, Muhammed Talha Arslansoy, who have made me the person I am today by sharing their diverse perspectives and creating joyful moments in my life.

I would also like to express my gratitude to my dear friends, Medine Daş Ağgedik and Elif Yaren, who have been by my side through every difficulty in this journey, offering their unwavering support and patience. I am deeply grateful for the kindness and guidance of Didem Bayraktaroğlu Serin, my first labmate at AGU, who played a crucial role in helping me establish order from scratch at the Fidan Lab during the long, hot days of summer. Lastly, I want to give a special shoutout to my little branch, Sena Sıla Odakan, who is always eager to learn from me and shows incredible patience during my difficult days.

TABLE OF CONTENTS

LIST OF FIGURES

LIST OF TABLES

LIST OF ABBREVIATIONS

AMD	Age-related Macular Degeneration
CCS	Capsanthin/capsorubin Synthase
CRISPR	Clustered Regularly Interspaced Short Palindromic Repeats
CrtI	Carotene Isomerase
CrtW	β-carotene Ketolase
CrtX	Zeaxanthin Glucosyltransferase
CrtY	Lycopene β-cyclase
CrtZ	B-carotene Hydroxylase
DMAPP	Dimethylallyl Diphosphate
DNA	Deoxyribonucleic Acid
DXP	1-deoxy-D-xylulose 5-phosphate
FPP	Farnesyl Pyrophosphate
FW	Fresh Weight
G3P	D-glyceraldehyde-3-phosphate
GGPP	Geranylgeranyl Pyrophosphate
GPP	Geranyl Pyrophosphate
HDR	Homology Directed Repair
HMG-CoA	3-hydroxy-3-methylglutaryl-CoA
HPLC	High Performance Liquid Chromatography
IPP	Isopentenyl Diphosphate
LB	Luria Bertani
LDL	Low Density Lipoproteins
LYC-b	Lycopene β-cyclase
LYC-e	Lycopene ε-cyclase
ME	2-*C*-methyl-D-erythritol
MEP	2-*C*-methyl-D-erythritol 4-phosphate
MVA	Mevalonate
OE PCR	Overlapping-extension Polymerase Chain Reaction
PCR	Polymerase Chain Reaction
PDS	Phytoene Desaturase

PPPP	Prephytoene Diphosphate
ROS	Reactive Oxygen Species
TLC	Thin Layer Chromatography
UV	Ultraviolet
ZEP	Zeaxanthin Epoxidase

To all the women,
who are struggling
the challenges of
this unequal world.

Chapter 1

Introduction

Carotenoids are a natural group of lipid-soluble pigments [1]. They consist of polyunsaturated isoprene units (C5H8) and have 30-50 carbons in their structure with conjugated double bonds [2]. These conjugated double bonds provide the color formation in carotenoid molecules [3]. The most naturally abundant carotenoids are C40 carotenoids and the functional groups at the end of the chain diversify the carotenoids, leading to the formation of more than 750 carotenoid molecules [2,3]. Depending on oxygen presence, carotenoids are divided into two groups: carotenes consisting of only carbon and hydrogen, and xanthophylls containing oxygen in their structures [3]. Carotenoids are mainly biosynthesized in photosynthetic organisms such as plants, algae, some bacteria, and fungi species [3]. However, animals and humans cannot synthesize carotenoids, thus they must obtain them from dietary sources [4].

Carotenoids play a significant role in photosynthesis due to two main functions: as photoprotective agents and as light harvesting pigments [5]. In addition, carotenoids have exhibited various biological activities such as antioxidant, anticancer, anti-atherosclerotic properties [6]. Also, it was shown that increased carotenoid consumption was correlated with a lower risk of chronic diseases [4]. Another important aspect of carotenoids is their role as provitamin A. Vitamin A is involved in various processes, including vision, reproduction, cell differentiation and proliferation, and immunity. Vitamin A deficiency can cause several symptoms, such as xerophthalmia, increased susceptibility to severe infections, increased mortality, and detrimental effects on growth and fetal development [7]. β-carotene, α-carotene and β-cryptoxanthin exhibit provitamin-A activity and thus, are useful to combat with vitamin A deficiency [7]. Apart from all these health benefits, a study revealed that long term supplementation of β-carotene has increased the cognitive abilities of the men subjects [8]. Overall, carotenoids play a significant role in human health due to their biological activities.

1.1 Biosynthesis of Carotenoids

Carotenoids are mainly found in photosynthetic organisms and synthesized from plastids [9]. The most abundant carotenoids are the C40 carotenoids, and their biosynthesis starts from 5-carbon isoprenoid units as isopentenyl diphosphate (IPP) and dimethylallyl diphosphate (DMAPP) [9]. These two precursors are synthesized from one of the two non-homologous pathways: the mevalonate (MVA) pathway and the 2-*C*-methyl-D-erythritol 4-phosphate (MEP) pathway [2,10]. In the first step of MVA pathway, three acetyl-CoA molecules are condensed to yield 3-hydroxy-3-methylglutaryl-CoA (HMG-CoA), which is subsequently reduced to MVA via the catalysis of HMG-CoA reductase. The phosphorylation of MVA twice and subsequent decarboxylation result in the formation of IPP, and through the catalysis of IPP isomerase, IPP is converted to DMAPP. On the other hand, the starting point of MEP pathway is the synthesis of 1-deoxy-D-xylulose 5-phosphate (DXP) from pyruvate and D-glyceraldehyde-3-phosphate (G3P) by head-to-head condensation of these two molecules, catalyzed via DXP synthase. Intramolecular rearrangement of DXP results in formation of 2-*C*-methyl-D-erythritol (ME) and the subsequent reduction of ME generates MEP. Finally, MEP is converted to IPP and DMAPP via four intermediates [11].

The complete biosynthesis of certain carotenoids is shown in Figure 1.1 . The two precursors, IPP and DMAPP, first form the C10 molecule geranyl pyrophosphate (GPP) via head-to-tail condensation. GPP and IPP condensed together to yield C15 molecule farnesyl pyrophosphate (FPP). The further addition of one more IPP molecule to FPP results in the formation of C20 intermediate precursor geranylgeranyl pyrophosphate (GGPP). The head-to-head condensation of two GGPP molecules leads to prephytoene diphosphate (PPPP), which forms phytoene via the removal of the diphosphate group and stereospecific proton abstraction. Phytoene is a colorless molecule with three conjugated double bonds and provides the C40 skeleton of carotenoids. It is the primary precursor to synthesize C40 carotenoids. For the formation of phytoene from IPP, there are four enzymes to catalyze the steps. These enzymes are IPP isomerase for isomerization of IPP to DMAPP, GPP synthase to convert IPP and DMAPP into GPP, GGPP synthase to catalyze conversion of IPP and DMAPP to GGPP and lastly, phytoene synthase which catalyzes the formation of phytoene from GGPP [9].

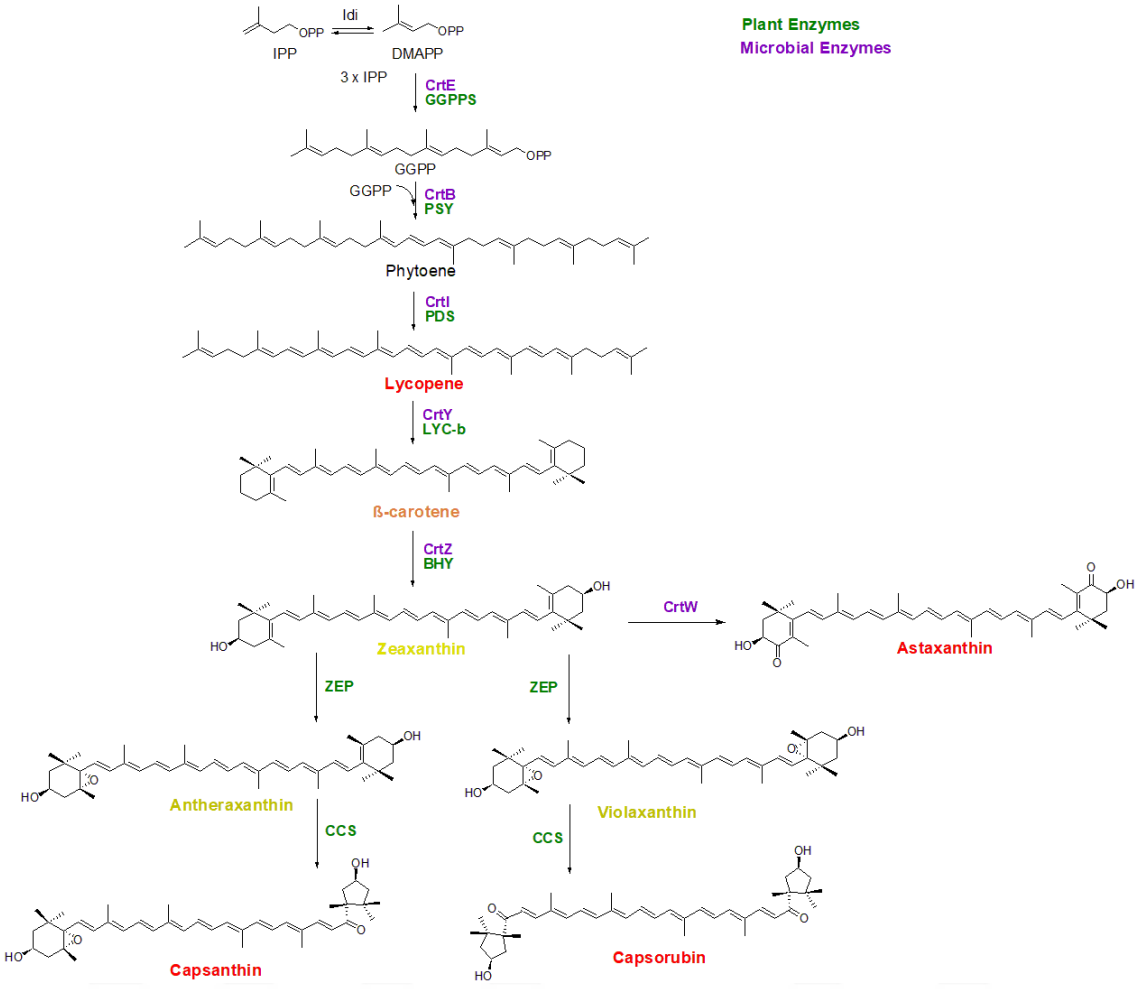

Figure 1.1 Biosynthetic pathway of carotenoids.

Conjugated carbon-carbon double bonds provide the required chromophore structure for carotenoid coloration. Desaturation of phytoene by phytoene desaturase (PDS) in higher plants, and carotene isomerase (CrtI) in bacteria and fungi leads to the formation of lycopene at four steps by introducing one desaturation at each step [9]. Increased number of conjugated carbon-carbon double bonds gives rise to red colored lycopene [2,9]. Phytoene is found as 15-*cis* isomer in higher plants while lycopene is observed as all-*trans*, that indicates the isomerization which is facilitated by light and catalyzed by plant desaturases at some point [9].

Lycopene is the precursor for the synthesis of cyclic and bicyclic carotenoids which is catalyzed by lycopene cyclases [2]. At first, cyclization of lycopene by lycopene-β-cyclase (LYC-b) by the introduction of β-rings and lycopene-ε-cyclase (LYC-e) by the introduction of ε-rings yields to β-carotene and α-carotene, respectively. Further

modifications of carotenes via β-carotene ketolase and β-carotene hydroxylase generate several C40 carotenoids that belong to the xanthophylls group [2]. The first xanthophylls formed from β-carotene are β-cryptoxanthin and zeaxanthin which are obtained via hydroxylation on C-3 and C-3' positions of the β-rings by β-carotene hydroxylase. Zeaxanthin epoxidase (ZEP) modifies 3-hydroxy β-rings of zeaxanthin by introducing 5,6-epoxy groups and yields antheraxanthin and violaxanthin. Finally, capsanthin/capsorubin synthase (CCS) forms cyclopentane rings (κ-rings) from 3-hydroxy-5,6-epoxy β-rings of antheraxanthin and violaxanthin, and results in capsanthin and capsorubin which are the ketolated carotenoids [9]. Astaxanthin is synthesized by β-carotene ketolase, catalyzing the conversion of zeaxanthin into astaxanthin [12]. C50 and C30 carotenoids are rare and C50 carotenoids are synthesized through the addition of two DMAPP molecules on C40 carotenoids [13], while C30 carotenoids are synthesized by two ways: by the condensation of FPP molecules or from the oxidative cleavage of C40 carotenoids [2,14].

1.2 Dietary Sources of Carotenoids

Carotenoids cannot be synthesized by humans and must be obtained through daily dietary intake. Most important sources of carotenoids in the human diet are fruits and vegetables, which provide almost 50 different carotenoids. Various carotenoids can be detected in human blood plasma, including zeaxanthin, β-cryptoxanthin, lutein, lycopene, β-carotene, and α-carotene [15]. A study revealed that the highest carotenoid containing fruits and vegetables are red peppers, carrots, apricots, nectarines, plums, peaches and the lowest in cherries [16]. Table 1.1 summarizes some of the fruits and vegetables and their carotenoid contents as μ/100 g vegetable or fruit.

Due to its provitamin A activity, β-carotene is considered one of the most important carotenoids. Mainly, apricot, carrot, mango and pumpkin species are rich in β-carotene and also contains a portion of α-carotene [17]. 60-70% of total carotenoids of apricot is determined as β-carotene [18]. Orange vegetables such as carrots, and dark green leafy vegetables like lettuce and spinach, are other sources rich in β-carotene [19,20]. According to the database (https://fdc.nal.usda.gov/fdc-app.html#/?component=1122), lycopene is found in tomato (46 mg/100 g FW (fresh weight)), watermelon (1.6-3.5

mg/100 g FW), papaya (1.8-4.2 mg/100 g FW) and guava (3.2-7.0 mg/100g FW) [21]. 80-90% of the total pigments in tomato is determined to be lycopene, making tomato and tomato-based products such as ketchup and sauce significant sources of lycopene [22,23]. Gac fruit aril is not included in the database, yet. However, gac fruit aril is determined as the highest β-carotene (20.5 mg/100 g FW) and lycopene (146.6 mg/100 g FW) containing fruit [24].

Table 1.1 Carotenoid contents of different fruits and vegetables according to information from [21]**.**

Carotenoid	Description	Carotenoid per 100 g (µg)
Lycopene	Tomato powder	46300
	Tomato, sun-dried	45900
	Catsup	12100
	Rose Hips, wild (Northern Plains India)	6800
	Guavas, common, raw	5200
β-carotene	Peppers, sweet, red, freeze-dried	42900
	Carrot, dehydrated	34000
	Grape leaves, raw	16200
	Sweet potato, frozen, cooked, baked, without salt	12500
	Tomato powder	10300
α-carotene	Carrot, dehydrated	14300
	Peppers, sweet, red, freeze-dried	6930
	Pumpkin, raw	4020
β-cryptoxanthin	Species, pepper, red or cayenne	6250
	Species, paprika	6190
	Papayas, raw	589
	Peppers, sweet, red, raw	490
Zeaxanthin	Eggs, Grade A, Large, egg yolk	546
	Spinach, mature	466
	Spinach, baby	191
Lutein	Spinach, mature	7450
	Spinach, baby	5830
	Eggs, Grade A, Large, egg yolk	612

Corn seeds and egg yolks are good sources of lutein and zeaxanthin due to their high content of these carotenoids [23]. 21.8 μg/g FW lutein and 13.4 μg/g FW zeaxanthin were determined in egg yolk [25]. The lutein and zeaxanthin content of egg yolk is coming from corn seeds hence chicken diet is primarily depending on corn seeds [23]. Total lutein and zeaxanthin contents from four different corn cultivar were determined between 947-2758 μg/100 g [26]. Spinach (11.93 mg/100 g) and kale (39.55 mg/100g) are found as high-level lutein and zeaxanthin containing vegetables [27]. Carotenoids can exist in esterified form among plants. For instance, the high level of zeaxanthin dipalmitate (35.7 mg/g FW) was determined in goji berry at fully ripe stage, while 5% of total carotenoids was estimated as β-cryptoxanthin monopalmitate (2.2 mg/g FW) [28]. β-cryptoxanthin is provitamin A xanthophyll and major carotenoid found in mandarins and oranges [15]. β-cryptoxanthin was determined in both skin (283-1254 μg/g FW) and pulp (76.5-287 μg/g FW) of the persimmon with different levels depending on the cultivar [29].

In addition to plants, carotenoids are also synthesized via various microorganisms, including certain algae, bacteria, and fungi species. Algae are pigment-producing photosynthetic organisms and perceived as a good source of bioactive compounds including carotenoids [30]. Astaxanthin is a red carotenoid with an antioxidant activity ten times higher than other carotenoids [31]. Main microalgae species producing astaxanthin are *Haematococcus pluvialis, Chlorella zofingiensis*, and *Chlorococcum* sp. [32]. The richest source of astaxanthin is *H. pluvialis* with 80% (relative to biomass) of the total carotenoids and *H. pluvialis* is the primary industrial source for the production of astaxanthin [30,32]. Halotolerant green algae *Dunaliella salina* synthesizes carotenoids such as β-carotene, α-carotene, lutein, and lycopene [33]. Relatively, 86% of total carotenoids from *D. salina* was determined as β-carotene that makes *D. salina* the richest source of β-carotene [33]. Lutein and zeaxanthin are synthesized via algal species such as *Scenedesmus* spp., *Chlorella* spp. *Rhodophyta* spp., or *Spirulina* spp. *Chlorella* genus is the best source for industrial level lutein production. β-carotene, β-cryptoxanthin and zeaxanthin are synthesized by *Spirulina platensis* [30]. Generally, algae species produce various carotenoids, and they are the most suitable organisms for industrial scale-up processes to produce carotenoids.

Despite the high yield of microalgal carotenoid biosynthesis, the cost of carotenoid biosynthesis via microalgae in an industrial process is higher than that of bacteria since the microalgae require longer cultivation time and depend on light to produce carotenoids [34]. Some bacterial species are also natively capable of biosynthesizing carotenoids and gain attention for carotenoid production due to shorter cultivation time [34]. In literature, *Brevibacterium linens* was reported as high β-cryptoxanthin (0.3 mg/mL) producing bacteria [35], while *Paracoccus zeaxanthinifaciens* was reported as high zeaxanthin (13.8 mg/L) producer [36] and *Paracoccus carotinfaciens* (E-396) was reported for high astaxanthin producer (19.9 mg/L) [37]. Besides, some endophytic bacteria species are identified as native carotenoid producers. For instance, *Pseudomonas* sp. 102515 was isolated from the leaves of *Taxus chinensis* and capable of producing an antioxidant natural product, zeaxanthin diglucoside (380 ± 12 mg/L) [38].

1.3 Antioxidant Potential and Health Benefits of Carotenoids

1.3.1 Functional Roles of Different Carotenoid Molecules

Carotenoids have various functions in nature, including light-harvesting, photoprotection, coloration for sexual purposes, and protection in animals, as well as provitamin A activity in vertebrates [39]. All carotenoids possess light-harvesting and photoprotection properties due to conjugated double bonds, which can exhibit $\pi \rightarrow \pi^*$ transition following light-absorption and subsequent high-energy excitation [39]. This light-harvesting property of carotenoids increases the spectral range of photosynthesis in plants [40]. Besides, light absorption and excitation result in color formation and carotenoids exhibit yellow-orange or red color which are in the visible spectrum with wavelengths 400-500 nm [39].

In the presence of at least 9 conjugated double bonds, molecules exhibit singlet oxygen quenching activity and radical scavenging activity that provides carotenoids antioxidant properties. In addition, the linear system of conjugated C-C double bonds

renders carotenoids potent antioxidants via high reducing potential in lipid formation via oxidation. When carotenoid molecules interact with membranes or dissolve in lipid structures, they can protect these structures from oxidative damage caused by aggressive radical species, thereby preventing irreversible destruction [40]. The effective neutralization of reactive oxygen species and other free radicals by carotenoids in both photosynthetic and non-photosynthetic organisms provides the protection from oxidative damage. This makes carotenoids excellent candidates as natural antioxidants [41].

1.3.2 Role of Carotenoids in Reducing Oxidative Stress via Antioxidant Properties

Reactive oxygen species (ROS) are formed by cells for normal cellular functions, such as intracellular signaling and redox regulation. ROS molecules are derived from oxygen and can be extremely reactive in different forms such as hydroxyl radical, or less reactive like superoxide and hydrogen peroxide. Intracellular free radicals, which have unpaired electrons, are often considered as ROS. The excessive formation of ROS is called as oxidative stress and cause severe damage in cellular structures [42,43]. ROS and free radicals start a chain reaction by interacting with biomolecules like lipids, proteins, and DNA, and form free radicals readily [42,43]. Newly formed free radicals further react with another free radical to eliminate the unpaired electron or with a free radical scavenger, a primary antioxidant, to break the chain [42]. Antioxidant is defined as "any substance that delays, prevents or removes oxidative damage to a target molecule" [44]. Antioxidants are investigated under two groups as enzymatic antioxidants and non-enzymatic antioxidants [43] or as preventative and chain-breaking antioxidants [45].

Carotenoids are non-enzymatic, chain-breaking, and lipid soluble antioxidants due to their hydrophobic nature [45,46]. Hydrophobic scavengers are located on the cellular membrane or found in lipoproteins, preventing lipid peroxidation by interrupting chain reactions of ROS or free radicals [47]. Chain-breaking antioxidants interfere the chain reaction via trapping the chain-carrying radicals [45]. Chain-breaking antioxidants such as α-tocopherol, tend to donate hydrogen atom to trap free radicals [48]. However, a study investigated the radical scavenging activity of four carotenoids; astaxanthin, β-carotene,

canthaxanthin and zeaxanthin, to reveal the radical scavenging mechanism of carotenoids and concluded that carotenoids demonstrated the antioxidant activity via the addition of radicals to conjugated polyene chain in their structure unlike the other natural antioxidants. The conjugated polyene chain stabilizes the free radicals by the resonance of conjugated double bonds under low oxygen pressure similar to physiological tissue environment [48].

Carotenoids are secondary free radical scavengers and physical singlet oxygen quenchers [47]. Singlet oxygen ($^1O_2$) is an excited state of oxygen where an electron changes spin and yields two unpaired electrons with opposite spins. It is responsible for $^1O_2$ dependent lipid peroxidation and DNA damage [49,50]. Vitamin-E (α-tocopherol) is the most efficient peroxyl radicals' scavenger in cellular membrane phospholipid bilayer structure [47]. Importantly, the inhibition of $^1O_2$ dependent lipid peroxidation was also achieved by carotenoids including β-carotene, astaxanthin and lycopene, due to their $^1O_2$ scavenging activity as great as that of α-tocopherol [49]. An *in vitro* study to show the protection of cells from lipid peroxidation via singlet oxygen quenching activity of carotenoids concluded that the highest protection was provided by lycopene, followed by astaxanthin and then, β-carotene [51]. Basically, carotenoids prevent lipid peroxidation and cellular damage through radical scavenging or singlet oxygen quenching activities, rendering carotenoids effective natural antioxidants and important dietary supplements for health.

1.3.3 Potential Health Benefits Associated with Carotenoid Consumption

In human plasma, 12 carotenoids have been detected, including lutein, zeaxanthin, lycopene, α-carotene, β-carotene, and β-cryptoxanthin [52]. It has been hypothesized that dietary carotenoids could reduce cancer rate, and several studies have been conducted to test this hypothesis. These studies considered different types of cancer and revealed that a high consumption of carotenoid-rich vegetables and fruits was associated with a decreased risk of cancer [53]. Epidemiological studies investigated the mechanism behind reduced risk of cancer associated with carotenoids and showed that the supplementation

of vitamin A does not decrease the risk of cancer, unlike carotenoids. This suggests that carotenoids may exert their anticancer effects through mechanisms other than those related to vitamin A activity [54]. The antioxidant activity of carotenoids is well-known for their ability to scavenge radicals and quench singlet oxygen. Both radicals and singlet oxygen can damage biomolecules in cells through mechanisms such as lipid peroxidation or DNA damage. Since the genetic changes caused by DNA damage can led to cancer formation, carotenoids can decrease the risk of cancer through their antioxidant activities [34,53]. For instance, a study showed that there was an inverse relationship between developing prostate cancer and the consumption of lycopene rich tomato and tomato-based products. This suggests that lycopene has a significant impact to reduce the prostate cancer development risk [55]. In an *in vitro* study on breast cancer, it was demonstrated that carotenoids, including astaxanthin, β-carotene and lutein, exhibited synergistic effects with anticancer drug doxorubicin. These carotenoids increased the ROS-mediated apoptosis of cancer cells while showing no toxicity to healthy cells [56]. Overall, various carotenoids exhibit anticancer activity attributed to their radical scavenging and singlet oxygen quenching capabilities. The supplementation of carotenoids holds promise for the treatment and prevention of several cancer types.

Oxidative stress may contribute to the pathogenesis of Alzheimer's disease. Astaxanthin was reported with its antioxidant activity as well as *in vivo* and *in vitro* neuroprotective effects. In a study investigating the neuroprotective effect of astaxanthin for Alzheimer's disease using HT22 cells, it was found that astaxanthin could be beneficial for the treatment of neurological diseases such as Alzheimer's disease, since it was significantly suppressed the accumulation of ROS in HT22 cells and involved in the regulation of other biomolecules implicated in the progression of the disease [57]. In the case of subarachnoid hemorrhage, neuronal apoptosis plays a significant role in the development of pathogenesis. The administration of astaxanthin after subarachnoid hemorrhage was shown to reduce the neuronal apoptosis and mitigate secondary brain injury, thereby alleviating brain dysfunction. This neuroprotective effect of astaxanthin involves the modulation of the Akt/Bad pathway [58]. In addition, oxidative stress also involves in ageing and reduces cognitive abilities such as memory and language [59]. In 2013, a study revealed that serum lutein levels were significantly associated with better cognitive abilities in the subjects over 80 years old. Additionally, serum levels of lutein, zeaxanthin, and β-carotene were all correlated with better cognitive abilities in subjects

over 100 years old. Besides, it was found that brain lutein and β-carotene levels are associated with better cognitive abilities [59]. It may be concluded that carotenoids are also beneficial for improving cognitive abilities and preventing neurodegenerative diseases.

Macula is a part of the eye which contains high density of cone cells and provides vision. It is exposed to light and oxidative stress on a regular basis. Age-related macular degeneration (AMD) is a chronic disease that progresses to blindness and oxidative stress aids the manifestation of AMD. Zeaxanthin and lutein are accumulating on human macula to protect macula through scavenging light-induced radicals and reducing oxidative stress. Previous studies indicated that the antioxidant activity of carotenoids in macula reduces the ROS levels and prevents damage caused from oxidative stress, which ultimately helps to reduce the risk of AMD. It was concluded that the supplementation of lutein and zeaxanthin is a preventative treatment against AMD [60]. Skin is the largest organ in the human body and exposed continuously to light and solar radiation, like eyes. The solar radiation and light exposure cause the generation of wrinkles, pigmentation, and premature aging as well as ROS formation [34]. Lycopene and β-carotene supplementation was reported to provide protection against UV-induced skin damage while elevated dietary intake of these carotenoids protected the skin from UV-induced erythema in humans [61].

Lutein is mainly suggested for eye-related disorders, but it has a higher antioxidant potential than β-carotene and lycopene which makes it a suitable target for the prevention and treatment of cardiovascular diseases. It has been showed that lutein exhibits anti-atherosclerotic activity. Lutein involves in the regulation of certain pathways related to antioxidant enzyme production and reduces ROS via both direct antioxidant activity and expression of antioxidant enzymes. Low density lipoproteins (LDL) play a key role in the development of atherosclerosis and lutein reduces the distribution of LDL particles in plasma and the accumulation of LDL particles in aorta. There are several other mechanisms that lutein involves and prevents cardiovascular disorders and thus, it is a good candidate to prevent or delay atherosclerosis [62]. Several studies demonstrated that lycopene exhibits similar mechanisms of action to other carotenoids, including the modulation of oxidative stress through the regulation of different pathways. Additionally, various cleavage products of lycopene was shown to interact with transcription factors

and regulate the overexpression of antioxidants [63]. Lycopene was also considered as a promising molecule for the treatment and prevention of cardiovascular diseases, neurodegenerative diseases and various cancer types due to its high antioxidant activity [63].

1.4 Industrial Demand and Limitations of Traditional Carotenoid Production Methods

All these activities provide a wide range of uses in various industries and increase the demand for carotenoids. Carotenoids have huge market size and the expansion of the market size due to increased demand is projected from USD 1.5 billion in 2017 to USD 2 billion by 2026 [64]. The current supply chain for carotenoids is dependent on extraction from plants and chemical synthesis. However, these strategies have some disadvantages and bottlenecks [65]. Use of organic solvents for both the chemical synthesis and plant extraction cause environmental problems and also, climate change and seasonal differences affect the plants availability. In addition, growing a plant is a costly and time-consuming process. Since the synthetic carotenoids produced by chemical synthesis might lead to health problems such as toxicity and increased allergenicity, there is an increased tendency for microbial production and extraction from plants [64].

Microbial production can overcome these disadvantages and bottlenecks therefore it is found to be the most efficient strategy for industrial scale production. The use of microbial production is fundamental to meet with the demand at industrial level since it is possible to produce large scale production in short time with lower costs [64]. Currently, microalgae, bacteria and fungi species are commonly used for this purpose [64]. As an alternative to native carotenoid producer microorganisms, metabolic engineering strategies offer the production of carotenoids in other engineered microorganisms [66]. Besides, yield improvement can also be performed through the genetic engineering techniques [64].

1.5 Objectives and Scope of the Thesis

In this study, we aimed to biosynthesize zeaxanthin, lycopene, beta-carotene, astaxanthin, violaxanthin and capsanthin/capsorubin by genetically engineering an endophytic bacterium which is determined as *Pseudomonas* sp. 102515, a native zeaxanthin diglucoside producer [38]. Zeaxanthin glucosyltransferase (CrtX), lycopene beta-cyclase (CrtY) and beta-carotene hydroxylase (CrtZ) genes from the genome of *Pseudomonas* sp. 102515 were knockout by CRISPR-Cas9 system to obtain Δ*crtX*, Δ*crtY and* Δ*crtZ* knockout strains which are producing zeaxanthin, lycopene and beta-carotene, respectively. Beta-carotene ketolase (CrtW), zeaxanthin epoxidase (ZEP) and capsanthin/capsorubin synthase (CCS) from *Capsicum annuum* were constructed as overexpression plasmid and transformed to Δ*crtX* mutant to produce astaxanthin, violaxanthin and capsanthin/capsorubin. Synthesized carotenoids via engineered strains were extracted and confirmed by TLC and HPLC analysis.

Chapter 2

Materials and Methods

2.1 Strains, Media, and Plasmids

Strains and plasmids are shown in Table 2.2. Generally, *E. coli* Top10 cells was used for cloning experiments and *Pseudomonas* sp. 102525 isolate [38] was used for carotenoid production. Luria Bertani (LB) medium (Condalab) was utilized for bacterial growth in all steps, 20 g/L bacteriological agar (Condalab) and antibiotics added whenever required. LB medium was supplemented with kanamycin (50 µg/mL, Kan50 for *E. coli* and 30 µg/mL, Kan30 for *Pseudomonas* sp. 102515), ampicillin (100 µg/mL, Amp100), gentamicin (35 µg/mL, Gen35), tetracycline (10 µg/mL, Tet10 for *E. coli* and 25 µg/mL, Tet25 for *Pseudomonas* sp. 102515) and chloramphenicol (25 µg/mL, Chl25 for *E. coli*). Culture conditions were 37˚C and 28˚C; with 220 rpm agitation for *E. coli* Top10 and *Pseudomonas* sp. 102525, respectively.

Table 2.2 Strains and Plasmids used in this study.

Strain or Plasmid	Description	Source
Strains		
E. coli Top10	F- mcrA Δ(mrr-hsdRMS-mcrBC) φ80 lacZΔM15Δ lacX74 recA1 araΔ139Δ(ara-leu)7697 galU galK rpsL (StrR) endA1 nupG	Lab stock
E. coli BL21(DE3)	BF^{-} ompT gal dcm lon $hsdS_B$ (r_B^{-} m_B^{-}) λ (DE3 [lacI lacUV5-T7p07 ind1 sam7 nin5]) $[malB^{+}]_{K-12}(\lambda^S)$	Lab stock
Pseudomonas sp. 102515	Wild type, zeaxanthin diglucoside producing strain	[38]
Pseudomonas sp. 102515Δ*crtX*	Zeaxanthin producing knockout strain	This study

Pseudomonas sp. 102515 Δ*crtY*	Lycopene producing knockout strain	This study
Pseudomonas sp. 102515 Δc*rtZ*	B-carotene producing knockout strain	This study
Pseudomonas sp. 102515Δ*crtX*/pNAr18	Astaxanthin producing overexpression strain	This study
Pseudomonas sp. 102515Δ*crtX*/pNAr17	Violaxanthin producing overexpression strain	This study
Pseudomonas sp. 102515Δ*crtX*/pNAr20	Capsanthin/capsorubin producing overexpression strain	This study
Plasmids		
pCas9	Recombineering plasmid with constitutively expressed *cas9* and the araBAD promoter expressing *αβγ*	[67]
pJOE_pvdJ	*P. putida* KT2440 suicide plasmid with repair template for *pvdJ* knockout	[67]
pNAr7	*P. putida* KT2440 suicide plasmid with repair template for *crtX* knockout	This study
pNAr10	*P. putida* KT2440 suicide plasmid with repair template for *crtY* knockout	This study
pNAr14	*P. putida* KT2440 suicide plasmid with repair template for *crtZ* knockout	This study
pgRNAtet-IvaA	Guide RNA plasmid targeting *lvaA*	[67]
pNAr8	Guide RNA plasmid targeting *crtX*	This study
pNAr9	Guide RNA plasmid targeting *crtY*	This study
pNAr15	Guide RNA plasmid targeting *crtZ*	This study
pJET1.2	Cloning vector	Lab Stock
pNAr11	Blunt-ended beta carotene ketolase gene *crtW* cloned into pJET1.2	This study
pNAr16	Blunt-ended *CaZEP* gene cloned into pJET1.2	This study
pNAr12	Blunt-ended $CaCCS_{m40}$ gene cloned into pJET1.2	This study

pMiS1-ges-mva	*P. putida* KT2440 expression vector pMiS1 with geraniol synthase gene *ges* and 6 MVA pathway genes	[68]
pMF541	pUClac vector with pMB1 ori carrying $CaCCS_{m40}$ and *CaZEP* genes	[69]
pUC-CaZEP-RBS5000	pUClac vector with pMB1 ori carrying *CaZEP* gene	[70]
pNAr17	*P. putida* KT2440 expression vector pMiS1 with *CaZEP* gene	This study
pNAr18	*P. putida* KT2440 expression vector pMiS1 with beta carotene ketolase gene c*rtW*	This study
pNAr20	*P. putida* KT2440 expression vector pMiS1 with *CaZEP-*$CaCCS_{m40}$ genes	This study
pAC-LYCipi	Lycopene producing plasmid	Addgene plasmid #: 53279
pAC-BETAipi	β-carotene producing plasmid	Addgene plasmid #: 53277
pAC-ZEAXipi	Zeaxanthin producing plasmid	Addgene plasmid # 53287
pAC-VIOL	Violaxanthin producing plasmid	Addgene plasmid #53087

2.2 Plasmid Construction

Phusion DNA Polymerase (ThermoFisher Scientific) was always used for polymerase chain reaction (PCR) and all primers are listed in Table 2.2 . PCR reaction was prepared with final volume of 20 µL including 0.5 µM forward primer, 0.5 µM reverse primer, 1x buffer, 200 µM dNTPs, 3% DMSO, variable amount of template, 0.02 U/µL Phusion DNA Polymerase and dH_2O up to 20 µL. The reaction conditions were set for 35 cycles: 1 min at 98˚C for initial denaturation, 10 sec at 98˚C for denaturation, 30 sec at 50-75˚C for annealing, 30 sec/kb at 72˚C for extension and finally, 10 min 72˚C for final extension.

Different protocol had been developed for overlapping-extension (OE) PCR: 0.25 µM forward primer, 0.25 µM reverse primer, 1x buffer, 400 µM dNTPs, 3% DMSO, variable amount of template, 0.02 U/µL Phusion DNA Polymerase and dH_2O up to 20 µL. First, reaction conditions were set for 20 cycles without primers as follows: 1 min at 98˚C for initial denaturation, 10 sec at 98˚C for denaturation, 30 sec at 65-80˚C for annealing, 30 sec/kb at 72˚C for extension and finally, 10 min 72˚C for final extension. After the completion of first 20-cycle, primers were added and conditions were set as 1 min at 98˚C for initial denaturation, 10 sec at 98˚C for denaturation, 30 sec at 50-75˚C for annealing, 30 sec/kb at 72˚C for extension and finally, 10 min 72˚C for final extension.

Table 2.2 List of all the primers used in this study.

Primer No.	Oligo Name	Oligonucleotide Sequence 5'-3'
1	CrtX-Uphom-F-PmlI	AACACGTGACGCCCTGTTCTTCGCGCAGCA
2	CrtX-Uphom-R	CGACATGGCGCGCAACTGCCCATGGTGTTCGACCA
3	CrtX-Downhom-F	GAACACCATGGGCAGTTGCGCGCCATGTCGGCGATCA
4	CrtX-Downhom-R-BamHI	AAGGATCCATCGTGCATCTCAATCCC
5	CrtY-Uphom-F-PmlI	TGCACGTGCAGCACCAGCACGTGGTGGCGCGATTGCCTTCG
6	CrtY-Uphom-R	AGGTGCGCTTATCCTCTCCGGCAAACCGC
7	CrtY-Downhom-F	CGGAGAGGATAAGCGCACCTCGTAGCCG
8	CrtY-Downhom-R-BamHI	GGCCGCTTTGGTCCCGGATCCAGGTGTTCGACCTGATGATGCG
9	CrtZ-Uphom-F-PmlI	TGCACGTGCAGCACCAGCACGTGCTCAATGGCAAGGAAACCGG
10	CrtZ-Uphom-R	GGAAACCGAAGCATGATGTACTTGTGCGACC
11	CrtZ-Downhom-F	TACATCATGCTTCGGTTTCCTGCTGGCG
12	CrtZ-Downhom-R-BamHI	GGCCGCTTTGGTCCCGGATCCGCGATAAACGGGTCGGATTA
13	pgRNAtet-CrtX-F-SpeI	ACTAGTGGGCTCGCGATTCATCGGCAGTTTTAGAGCTAGAAAT
14	pgRNAtet-CrtX-R	ATTATACCTAGGACTGAGCTAGCTG
15	pgRNAtet-F	GCTTGGATTCTCACCAATAAAAAAC
16	pgRNAtet-R	ACTAGTATTATACCTAGGACTGAGC
17	pgRNAtet-CrtYZ-R	GGTGAGAATCCAAGCGCCTCCGCCCTGCGGCCT
18	pgRNAtet-CrtY-F	AGGTATAATACTAGTCTGTTCTTCGCGCAGCACCTGTTTTAGAGCTAGA

19	pgRNAtet-CrtZ-F	AGGTATAATACTAGTCCCTGGGCAATGCC GGCTATGTTTTAGAGCTAGA
20	ColonyPCR-CrtX-F	AGTCCAGCTCCGGACGGGTTTG
21	ColonyPCR-CrtX-R	TGCGGTGCCCATAGTGGCCGACA
22	ColonyPCR-CrtY-F	AGGGTGGTGGCGATGCCGGC
23	ColonyPCR-CrtY-R	GCCGAACGCTTCGTGCCCAT
24	ColonyPCR-CrtZ-F	CGAATGGGAAGGCGAATTCC
25	ColonyPCR-CrtZ-R	TCGATCCCTTCGACGAGCAG
26	CrtW-OE-PmeI-F	AAGTTTAAACATGGTCCAGTGCCAGCCGT C
27	CrtW-OE-SpeI-R	AAACTAGTTTACAGCGAGATTTTGTGTGC TT
28	CaZEP-OE-PmeI-F	AAGTTTAAACATGTATAGCACCGTGTTTT ATAC
29	CaZEP-OE-HindIII-SpeI-R	AAAGCTTATCATCATCACTAGTTTACGCG GTGCCAACCAC
30	CaCCSM40-OE-SpeI-F	AACTAGTATGTTTCATTATCGTAACAAAA G
31	CaCCSM40-OE-HindIII-R	AAAAGCTTTTACAGGCTTTCAATCGCCAG ATTGC

2.2.1 Construction of pJOE with Homologous Arms of the Target Gene

Genomic DNA of *Pseudomonas* sp. 102515 was isolated by genomic DNA extraction kit (Transgen Biotech) and used as template for the amplification of upstream and downstream homologous arms of the *crtX*, *crtY* and *crtZ* genes by PCR. Amplified upstream and downstream homologous arms of the genes were purified from agarose gel by Gel Extraction Kit (Favorgen), hybridized and amplified by OE PCR by using upstream forward and downstream reverse primers. pJOE_pvdJ plasmid was digested with BamHI and PmlI restriction digestion enzymes (ThermoFisher Scientific). Digested pJOE_pvdJ and hybridized upstream-downstream homologous arms were purified from gel and ligated by Gibson Assembly (TakaraBio In-Fusion Cloning).

2.2.2 Construction of pgRNAtet with N20 Sequence of the Target Gene

For the construction of pgRNAtet, two different strategies were followed. First, the N20 sequence of *crtX* gene on the pgRNAtet-IvaA plasmid was changed via primer and obtained 3.5 kb PCR product was self-ligated by T4 DNA ligase (ThermoFisher

Scientific). Secondly, pgRNAtet plasmid was amplified by PCR as 2 fragments and N20 sequence was changed again by primers. First, pgRNAtet-F and pgRNAtet-R primer pair was used, and 1.6 kb fragment obtained. Then, pgRNAtet-CrtYZ-R primer was used with pgRNAtet-CrtY-F and 1.9 kb fragment obtained with specific N20 sequence for *crtY* gene. These two PCR products were purified from agarose gel and ligated by Gibson Assembly (TakaraBio In-Fusion Cloning). The same protocol was followed for *crtZ* gene by using pgRNAtet-CrtZ-F primer.

2.2.3 Construction of Overexpression Plasmids

CaZEP was amplified from pUC_{lac}-KBS5000-CaZEP via PCR with primers 28 and 29 and purified from gel. The blunt-ended PCR product was first cloned into pJET1.2, which was cut by EcoRV restriction enzyme (ThermoFisher Scientific), by T4 DNA ligase (ThermoFisher Scientific) to yield pNAr16. For the ligation, 50-100 ng vector, 5:1 vector/insert molar ratio insert, 1 µL 10x T4 ligase buffer, 1 µL PEG buffer (for blunt-end ligations), 0.5 µL T4 DNA ligase and dH_2O up to 10 µL was added and the ligation reactions were incubated on ice for 30 min and then, incubated at 18˚C overnight. The construct, pNAr16, and vector pMiS1-MVA-Ges were cut by PmeI and HindIII (ThermoFisher Scientific) and required bands collected and purified from gel. Sticky-end *CaZEP* obtained from restriction digestion of pNAr16 was inserted into pMiS1 vector via T4 DNA ligase and pNAr17 was constructed.

crtW gene was synthesized as gene block and amplified by PCR with primer 26-27 and first cloned into pJET1.2, as described for *CaZEP*, to yield pNAr11. pNAr11 and pNAr17 were cut by PmeI-SpeI and result in sticky-end *crtW* as insert and vector pMiS1 that were ligated by T4 DNA ligase and yielded pNAr18. On the other hand, $CaCCS_{m40}$ was amplified from pMF541 with primers 30-31 and cloned into pJET1.2 by following the same protocol for pNAr11 and pNAr16 and resulted in pNAr12. pNAr12 and pNAr17 were cut by SpeI-HindIII and resulted in sticky-end $CaCCS_{m40}$ as insert and vector pMiS1-*CaZEP* that were ligated by T4 DNA ligase and yielded pNAr20.

2.3 Transformations and Genetic Engineering of *Pseudomonas* sp. 102515

E. coli Top10 and BL21(DE3) cells were made chemically competent by $CaCl_2$ treatment according to Sambrook et al. [71]. The transformation of plasmids into *E. coli* chemically competent cells were done by heat-shock method. Briefly, a small amount of the plasmids/ligation reaction was added to 150 µL competent cells and incubated on ice for 30 min. Then, cells were kept in a 42°C water bath for 1 min. After the water bath, cells were incubated on ice for 1 min and 1 mL LB medium was added for the recovery of cells and incubated at 37°C for 30 min. Finally, transformed cells were spread on LB Agar plates which contain proper antibiotic for the selection of transformed cells. Plates were incubated at 37°C overnight.

Transformations to *Pseudomonas* sp. 102515 cells were done by electroporation. Electrocompetent cells were prepared according to literature [72]. Briefly, growth of *Pseudomonas* sp. 102515 cells was tracked until OD_{600} reached 0.4 and after this point, all the steps carried on ice or +4˚C. Cells were harvested by centrifugation and washed three times with 300 mM sucrose solution. 100 µL of sucrose solution was used to resuspend cells and cells were mixed with plasmid, transferred to ice-cooled cuvettes. After 10 min incubation on ice, electroporation was performed according to settings: voltage - 2.5 kV (12.5 kV/cm); capacitor - 25 µF. 1 mL of LB medium was immediately added to cells and mixed. Mixture was transferred into a culture tube and incubated at 28˚C; with 220 rpm agitation for 2 h. Cells were spread on LB Agar plates which contain proper antibiotic for the selection of transformed cells and incubated at 28˚C for 2 days. Colonies were subcultured into a fresh plate and growing colonies were inoculated into LB medium with appropriate antibiotics for further analysis.

For the transformations of CRISPR-Cas9 components for λRed/Cas9 recombineering, electroporation was done in 2-step according to Pfleger et al. [67]. *Pseudomonas* sp. 102515 cells containing pCas9 plasmid were transformed with pJOE, which carries the homologous arms of the target gene, by electroporation and transformed cells were selected by Gen35+Kan30 LB agar plates. One of the colonies was inoculated into 5 mL LB medium supplemented with Gen35+Kan30 and incubated at 28˚C with

shaking for 2 days. 50 mL culture was started with 1% inoculation of 2-day seed culture and growth was observed until OD_{600} reached 0.4. Then, 0.2% L-arabinose added for induction and culture was incubated for 15 min. Cells were harvested and made electrocompetent by described protocol. These cells were subjected to transformation of pgRNAtet plasmid by electroporation and transformed cells were selected by Gen35+Tet25 LB agar plates.

After knockout strains were obtained, CRISPR-Cas9 components were removed from the cells by inoculating into antibiotic free LB medium and then, spreading on both antibiotic containing and antibiotic free LB agar plates. The procedure of inoculation and spreading was continuously performed until there was no growth observed on antibiotic containing plates. Overexpression plasmids were transformed to plasmid free *Pseudomonas* sp. 102515Δ*crtX* cells as described above, with one step. Selection of the transformants were done via Kan30 LB agar plates.

2.4 Shake Flask Cultivation for Carotenoid Production

For *E. coli* BL21(DE3) cells carrying pAC-LYCipi, pAC-Betaipi, pAC-Zeaxipi or pAC-VIOL, a single colony was inoculated into 5 mL LB medium containing Chl25 and incubated at 37˚C with 220 rpm agitation overnight. 100 mL cultures were started in shake flasks with 0.5% inoculation of overnight seed culture in LB medium with Chl25. Cultures were incubated at 37˚C with 220 rpm agitation for 2 days until extraction.

For *Pseudomonas* sp. 102515 strains, a single colony was inoculated into 5 mL LB medium, antibiotic supplemented if necessary and incubated at 28˚C with 220 rpm agitation for 2 days. 50 mL, 100 mL or 200 mL cultures were started in shake flasks with 0.5% inoculation of 2-day seed culture and proper antibiotic was added. After 6 h, 0.2% L-rhamnose was added for induction during astaxanthin production from Δ*crtX*/pNAr18, violaxanthin production from Δ*crtX*/pNAr17 and capsanthin/capsorubin production from Δ*crtX*/pNAr20. Cultures were incubated at 28˚C with 220 rpm agitation for 5 days until extraction.

2.5 PCR Confirmation

Genomic DNA of wild type *Pseudomonas* sp. 102515 and knockout strains of *Pseudomonas* sp. 102515 were isolated by genomic DNA extraction kit (Transgen Biotech) and used as templates for the confirmation of knockout of *crtX*, *crtY* and *crtZ* genes in the genome. PCR was performed for wild type and knockout genomic DNA with the same primer pair such as ColonyPCR-CrtX-F and ColonyPCR-CrtX-R (found in Table 2.2) and obtaining a shorter DNA fragment from knockout strains was aimed since the gene was removed. It was also applied to the other knockout strains with the same manner and listed primer pairs in Table 2.2 .

2.6 Carotenoid Extraction

5-day cultures were centrifuged at 6,000 g for 10 min to harvest cells. Supernatant was removed and an equal amount of acetone:methanol:chloroform (4:3:3, v/v/v) mixture was added. Sonication was applied for 1 min/50 mL culture to disrupt cell membrane and extract carotenoids. Samples were centrifuged again at 8,000 g for 15 min to remove cell debris. Supernatants were collected and extracts were dried by rotary evaporator. Residues were collected by acetone:methanol:chloroform (4:3:3) solvent mixture for further analysis.

2.7 TLC and HPLC Analysis

Thin layer chromatography (TLC) was performed for separation of carotenoids with silica gel coated with fluorescent indicator F254 (Merck). Developing solvent was used as acetone:n-hexane:dH_2O (9:9:1, v/v/v). Standards were used for zeaxanthin (Solarbio), β-carotene (Solarbio), lycopene (Solarbio), astaxanthin (Solarbio) and capsanthin (Naturewill Biotechnology Co.) along with the extracts from BL21(DE3) strains which produce carotenoids via the transformation of pAC based plasmids.

Extracted carotenoids were determined by HPLC analysis. The analyses were performed on a reserve-phase C18 analytical column with 250 × 4.6 mm diameter, 5 μm

particle size (Hypersil ODS, ThermoFisher Scientific). The HPLC instrument (LC-20AD auto sampler, DGU20A_{5R}, Shimadzu) was equipped with photodiode array detector (SPD-M20A, Shimadzu) and chromatograms were detected at 454 nm. Analysis of extracted carotenoids were done by an isocratic elution of acetonitrile:methanol:isopropanol (5:3:2, v/v/v) with 1 mL/min flow rate and oven temperature at 40˚C.

Chapter 3

Results

3.1 Results for Knockout Strains

3.1.1 Construction of pJOE with Homologous Arms of the Target Gene

As a starting point of the project, genomic DNA of *Pseudomonas* sp. 102515 was isolated and used as a template to amplify the upstream and downstream homologous arms of the target gene. Firstly, upstream and downstream homologous arms of *crtX* gene were amplified by PCR, as described in the method part, via primer pairs 1-2 and 3-4 (Table 2.2). PCR reactions were loaded to 0.8% agarose gel and run at 100 V for 30 min (see Figure 3.1 A) and expected bands (1 kb for upstream and 900 bp for downstream) were cut from gel and amplified PCR products were purified by gel extraction kit. Small amounts of purified products were loaded to 0.8% agarose gel to check purity (see Figure 3.1 B). Purified products were used as template in OE PCR and hybridized by the protocol explained in the method part using primers 1 and 4. Hybridization of upstream and downstream homologous arms via OE PCR was confirmed by visualizing on agarose gel electrophoresis (see Figure 3.1 C) and the corresponding band (1.9 kb) collected and purified (see Figure 3.1 D) for further cloning steps as insert.

For the construction of pNAr7, pJOE_pvdJ was cut by BamHI and PmlI and 5.1 kb vector obtained after purification from gel (see Figure 3.2 A). Construction of pNAr7 was done by Gibson Assembly and reaction mixture was transformed into *E. coli* Top10 chemically competent cells by heat-shock. Transformed colonies were selected by Kan50 plate and they were used for plasmid isolation. Isolated plasmids were subjected to restriction digestion by BamHI and PmlI to confirm the construct. As seen in Figure 3.2 B, sample 2 was confirmed as pNAr7.

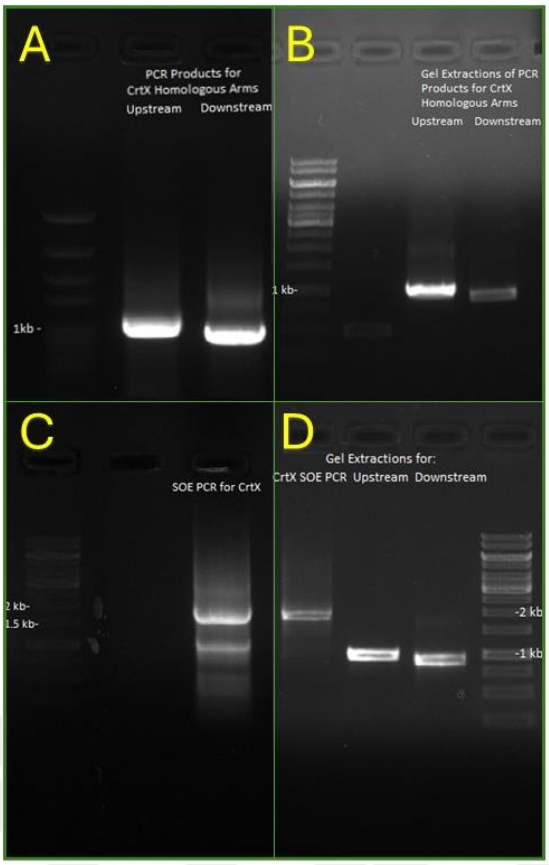

Figure 3.1 Agarose gel electrophoresis results for the construction of pJOE with homologous arms of *crtX* gene (pNAr7). A) PCR amplification of upstream and downstream homologous arms, B) Gel extraction results for amplified homologous arms, C) Hybridization of homologous arm by overlapping-extension PCR, D) Gel extraction results for hybridized homologous arms and amplified individual homologous arms.

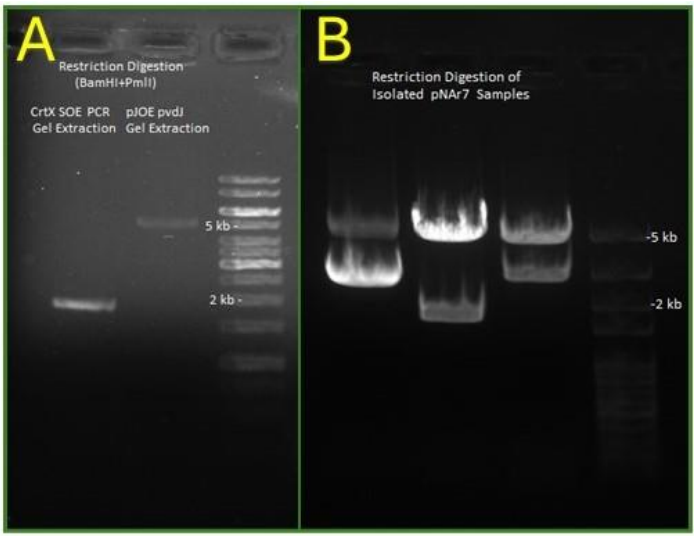

Figure 3.2 Agarose gel electrophoresis results for the construction and confirmation of pJOE with homologous arms of *crtX* gene (pNAr7). A) Gel extraction of hybridized homologous arms of *crtX* and pJOE vector obtained by BamHI-PmlI, B) Confirmation of isolated plasmids via BamHI-PmlI restriction digestions.

The same steps were followed for the construction of pNAr10 with homologous arms of *crtY* and pNAr14 with homologous arms of *crtZ* genes (see Figure A.1 and Figure A.2). Confirmations of pNAr7, pNAr10 and pNAr14 were done by different restriction digestions (see Figure 3.3). First, BamHI and PmlI were used for all these constructs since hybridized homologous arms were inserted by these sites. Expected bands were 5.1 kb (vector backbone) and 1.9 kb (insert). For further confirmation, EcoRV was used to digest constructs hence EcoRV cuts pJOE_pvdJ at two different positions but when pvdJ was removed and only pJOE was used as vector backbone, EcoRV can cut from only one site and restriction digestion yields only one band at 7 kb for pNAr7, pNAr10 and pNAr14. Samples were confirmed by both BamHI-PmlI and EcoRV restriction digestions. Constructs were also confirmed by sequencing and alignments of sequencing result and our target sequence for pNAr7, pNAr10 and pNAr14 is shown in Figure A.13. Plasmid maps for the constructs are attached in Figure A.8 .

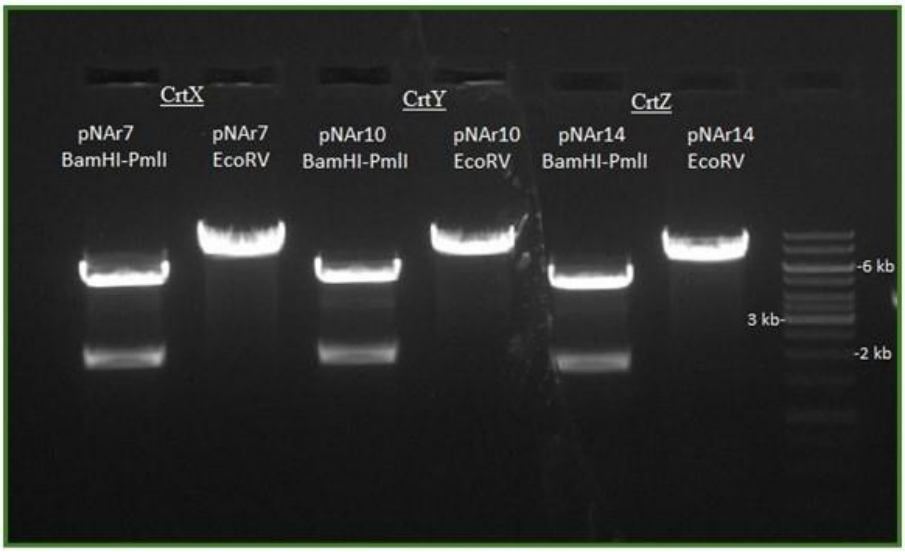

Figure 3.3 Confirmation of pJOE constructs which carry the homologous arms of the target gene *crtX* (pNAr7), *crtY* (pNAr10) and *crtZ* (pNAr14) by restriction digestion enzymes.

3.1.2 Construction of pgRNAtet with N20 Sequence of the Target Gene

Two different strategies were developed for the construction of pgRNAtet with unique N20 sequence to target genes *crtX*, *crtY* and *crtZ*, individually. The first strategy was applied to target *crtX* gene by constructing pNAr8, that focused on changing the N20 sequence via primers and amplifying the whole plasmid (3.5 kb) by PCR. In Figure 3.4,

amplified pgRNAtet via PCR and unique N20 sequence to target *crtX* is seen. The obtained PCR product was linear and thus, it was self-ligated via T4 DNA ligase to construct pNAr8. Since the only difference between pgRNAtet and pNAr8 was N20 sequence, the confirmation of pNAr8 was done by transformation to *Pseudomonas* sp. 102515 and TLC analysis of the extracted carotenoids from the transformed strain. In addition, positive pNAr8 construct from TLC result was sequenced and aligned with unique N20 sequence of *crtX* gene that was confirmed pNAr8 (see Figure A.14 A).

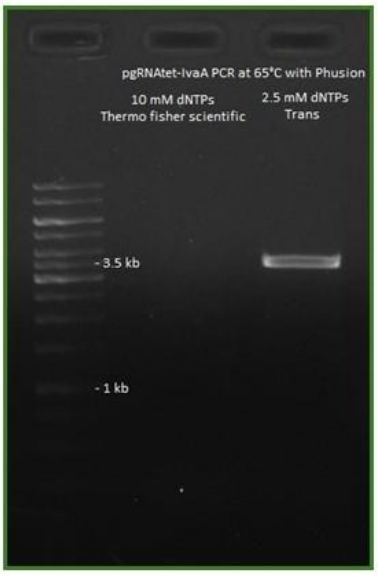

Figure 3.4 Agarose gel electrophoresis results for construction of pgRNAtet with *crtX* N20 sequence (pNAr8).

Construction and confirmation of pgRNAtet with the first strategy required excessive work thus, another strategy was developed that includes the amplification of the plasmid as two fragments and ligation of these fragments via Gibson assembly. For the construction of pNAr9 to target *crtY* and pNAr15 to target *crtZ*, the second strategy was followed and N20 sequence was changed with primer while also one of the two SpeI restriction sites was eliminated via another primer to make confirmation of the construct easier. Fragment 1 has a size of 1.6 kb and amplified by primers 15-16, that was common part of both pNAr9 and pNAr15. One of the SpeI sites on the pgRNAtet was removed from fragment 1. Fragment 2 has a size of 1.9 kb that includes the specific N20 sequence which was changed by primers 18 (for *crtY*) and 19 (for *crtZ*).

In Figure 3.5 A and B, amplification and gel extractions of the two fragments for pNAr9 has shown. After the construction of pNAr9 via Gibson assembly and

transformation to *E. coli* Top10 chemically competent cells by heat-shock, transformed colonies were selected by Tet10 plate. The colonies were used for plasmid isolation. Isolated plasmids were subjected to restriction digestion by SpeI hence one of the two sites was removed in the construct. In Figure 3.5 C, restriction digestion by SpeI of two isolates from pNAr9 construction was shown and sample 2 was confirmed since the plasmid was only linearized by single cut of SpeI. Construction of pNAr15 and amplification of fragment 1 were seen in Figure A.3 . Furthermore, pNAr9 and pNAr15 constructs were sequenced and the results aligned with unique N20 sequences of *crtY* and *crtZ* genes to confirm the constructs (see Figure A.14). Plasmid maps for all pgRNAtet constructs are shown in Figure A.9 .

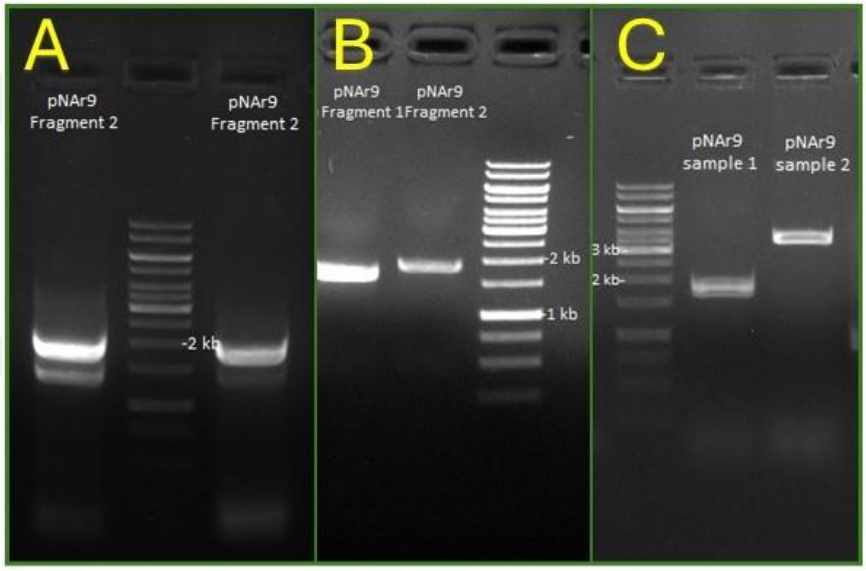

Figure 3.5 Agarose gel electrophoresis results for the construction and confirmation of pgRNAtet with N20 sequence of *crtY* gene (pNAr9). A) PCR amplification of fragment 2, B) Gel extraction results for amplified fragments, C) Confirmation of the construct by SpeI restriction digestion.

3.1.3 Electroporation of CRISPR-Cas9 Components for Knockouts

The components of CRISPR-Cas9 system for knockout includes pCas9, pJOE with homologous arms of the target gene and pgRNAtet with specific N20 sequence. pCas9 is a ready-to-use component and was not subjected to any change while pJOE and pgRNAtet were constructed for each gene specifically. At the beginning, pCas9 was transformed to wild type *Pseudomonas* sp. 102515 by electroporation and transformed colonies were selected by Gen35 plate (see Figure 3.6 A). Colonies were subcultured into a fresh Gen35

plate (see Figure 3.6 B) to avoid from false positive colonies and glycerol stocks prepared from these cells for the use in further electroporation experiments.

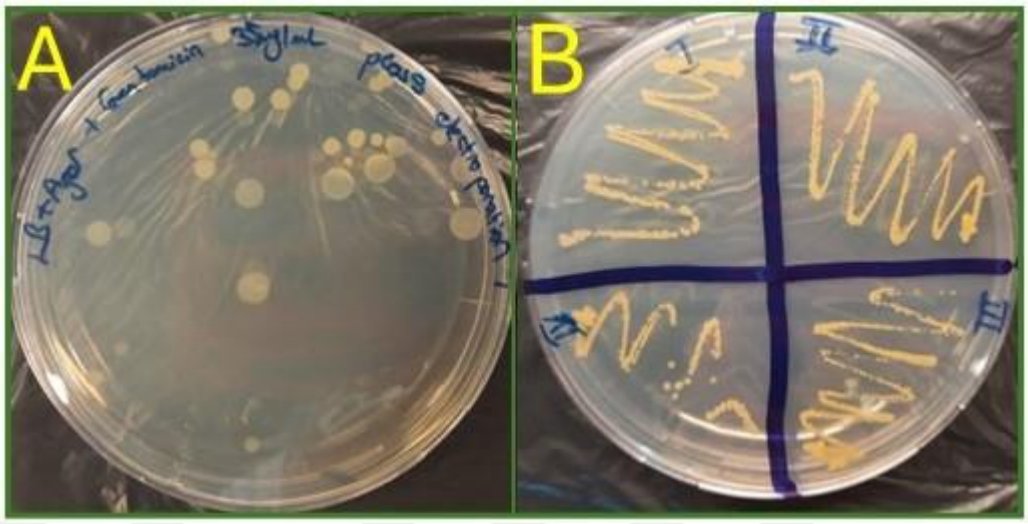

Figure 3.6 Electroporation of pCas9 plasmid into *Pseudomonas* sp. 102515. A) Selection of transformed cells after electroporation, B) Subculturing of transformants in a fresh plate.

Secondly, pJOE constructs with homologous arms (pNAr7, pNAr10 and pNAr14) were separately transformed to *Pseudomonas* sp. 102515/pCas9 by electroporation, as described in the method, for the donation of template during double strand repair by homology directed repair (HDR). In Figure 3.7 , it has shown that the electroporation of pNAr7 to *Pseudomonas* sp. 102515/pCas9 and selection of the transformed colonies via Gen35+Kan30 plates. Same procedure was followed for the transformation of pNAr10 (see Figure A.4) and pNAr14 (see Figure A.6) with different volumes of plasmids.

Lastly, pgRNAtet constructs (pNAr8, pNAr9 and pNAr15) were transformed to *Pseudomonas sp*. 102515/pCas9-pJOE construct. At this step, 50 mL culture was started with 1% seed inoculation into LB medium supplemented with Gen35+Kan30 for *Pseudomonas* sp. 102515/pCas9-pNAr7, *Pseudomonas* sp. 102515/pCas9-pNAr10 and *Pseudomonas* sp. 102515/pCas9-pNAr14. OD_{600} was tracked until 0.4 and culture was induced by 0.2% L-arabinose for the expression of λ-Red recombination proteins. Induced culture was incubated at 28˚C with 220 rpm shaking for 15 minutes and electrocompetent cells prepared. Different amounts of different pNAr8 isolates were transformed to *Pseudomonas* sp. 102515/pCas9-pNAr7 cells and selection was done by Gen35+Tet25 plates (see Figure 3.8) since pNAr7 donated the template for HDR and

was not replicated anymore in the cells. Different amounts of pNAr9 were transformed to *Pseudomonas* sp. 102515/pCas9-pNAr10 (see Figure A.5) and pNAr15 to *Pseudomonas* sp. 102515/pCas9-pNAr14 (see Figure A.7).

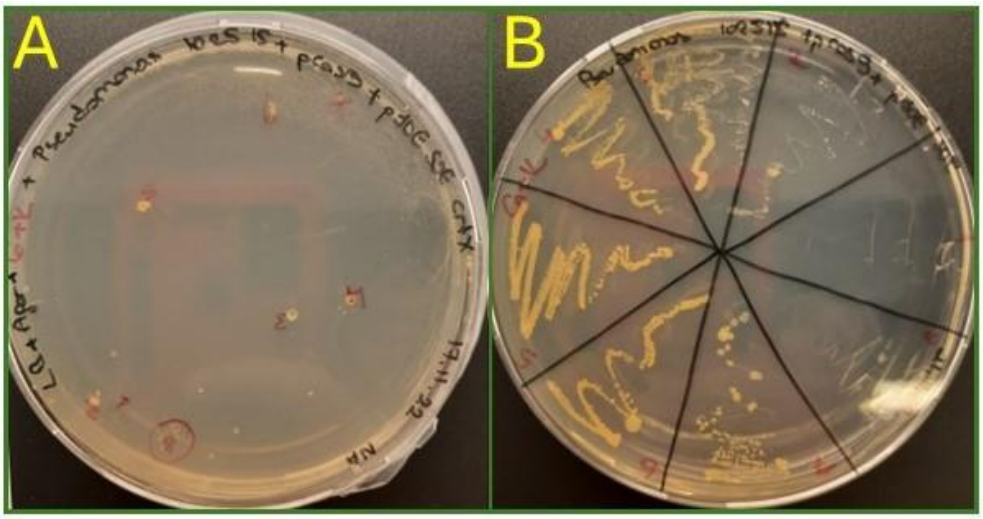

Figure 3.7 Electroporation of pNAr7 plasmid to *Pseudomonas* sp. 102515/pCas9. A) Selection of transformed cells after electroporation, B) Subculturing of transformants in a fresh plate.

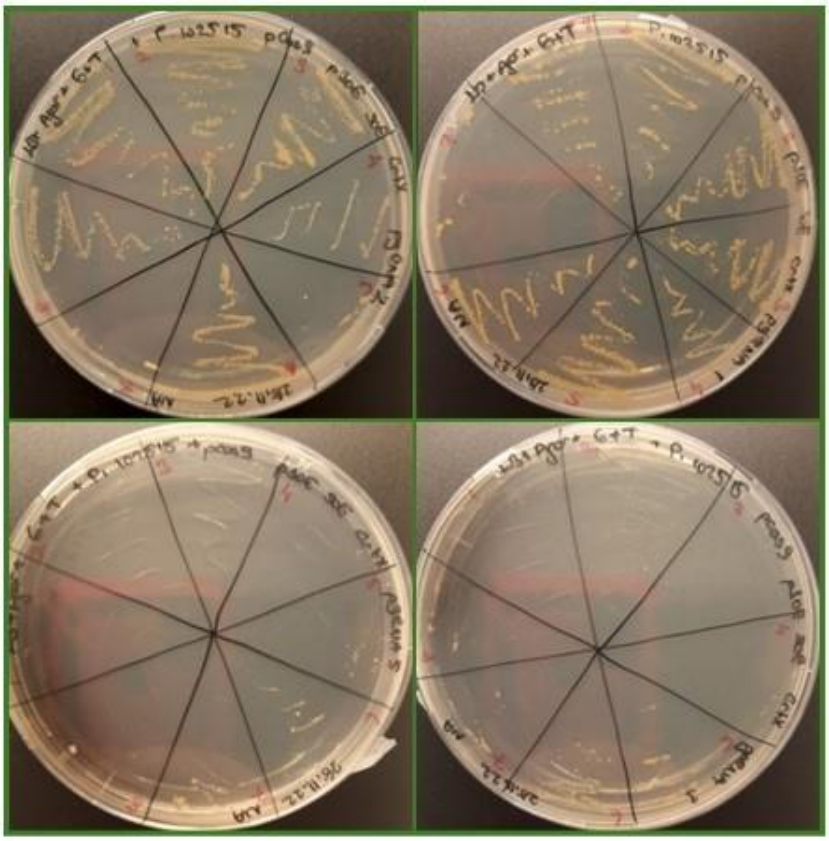

Figure 3.8 Electroporation of pNAr8 plasmid to *Pseudomonas* sp. 102515/pCas9-pNAr7, subculturing of transformants in fresh plates.

It has been showed that λ-Red recombineering increases the efficiency of homologous recombination for damage repair in the genome of *Pseudomonas putida* cells [73]. Depending on this result, λ-Red recombinases were included in pCas9 that can be inducible by L-arabinose, in the study conducted by Pfleger. et al for genome editing of *P. putida* [67]. In addition, it has been showed that two-step electroporation of pJOE and pgRNAtet yielded higher number of transformants with higher editing efficiency compared to one-step electroporation where pJOE and pgRNAtet constructs were transformed at the same time [67]. Since *Pseudomonas* sp. was used in this study, the same steps were followed, and successful results were achieved.

3.1.4 PCR Confirmation of Knockout Strains

In the previous steps, CRISPR-Cas9 components were transformed to wild type *Pseudomonas* sp. 102515 to knockout *crtX*, *crtY* and *crtZ* genes via HDR. For this purpose, homologous arms of the target gene were amplified and hybridized by PCR. This PCR product served as a template to repair double strand break created by Cas9 enzyme that was led to target site via pgRNAtet construct. Since the gene was removed from the genome by repairing the damaged site with the upstream and downstream homologous arms, knockouts can be confirmed by PCR.

Genomic DNA of wild type *Pseudomonas* sp. 102515 and *Pseudomonas* sp. 102515Δ*crtX*, *Pseudomonas* sp. 102515Δ*crtY* and *Pseudomonas* sp. 102515Δ*crtZ* were isolated by genomic DNA extraction kit and used as template for PCR. Primers were designed from the upstream and downstream regions of the target gene, and it was expected to get a shorter PCR product from knockout strains compared to wild type. In Figure 3.9 A, PCR confirmation of *crtX* knockout strain was shown. *crtX* gene in the wild type *Pseudomonas* sp. 102515 genome is 1.2 kb long. PCR with primers 20-21 resulted in ~1.4 kb product from wild type genomic DNA and ~600 bp product from *crtX* knockout strain that indicates 800 bp was removed from *crtX* gene and *Pseudomonas* sp. 102515Δ*crtX* is confirmed.

Same results were obtained for *Pseudomonas* sp. 102515Δ*crtY* with primers 22-23 and seen in Figure 3.9 B. *crtY* gene in the wild type *Pseudomonas* sp. 102515 genome is

also 1.2 kb long and again, almost 800 bp shorter product obtained from *Pseudomonas* sp. 102515Δ*crtY* genomic DNA and confirmed the knockout. *crtZ* gene has a size of 525 bp in wild type *Pseudomonas* sp. 102515 genome and therefore, the difference of the PCR products with primers 24-25 for confirmation of *Pseudomonas* sp. 102515Δ*crtZ* was ~300 bp (see Figure 3.9 C).

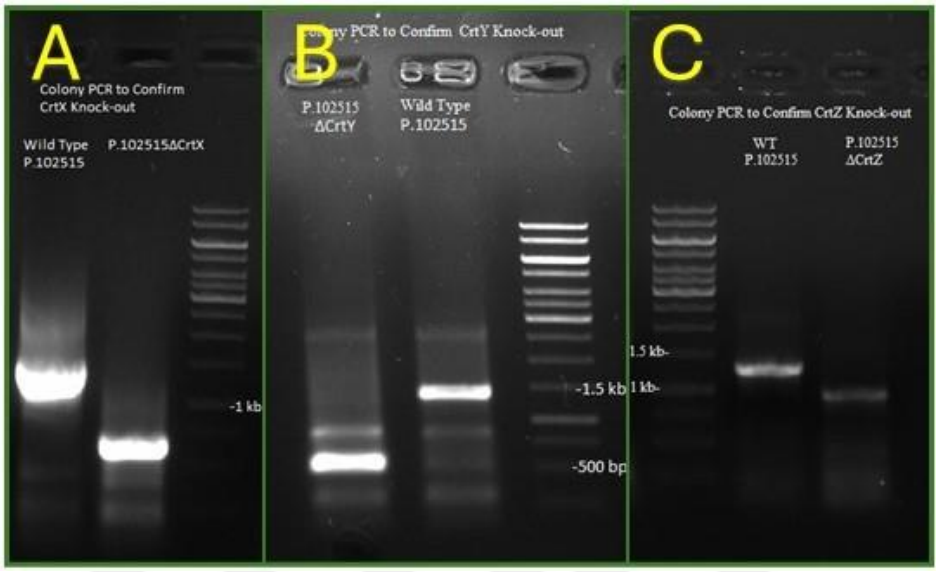

Figure 3.9 Agarose gel electrophoresis result for PCR confirmation of knockout strains. A) Confirmation of Δ*crtX*, B) Confirmation of Δ*crtY*, C) Confirmation of Δ*crtZ*.

3.1.5 TLC Analysis for the Extracts of Knockout Strains

After electroporation of CRISPR-Cas9 components and selection of transformed cells, a higher volume of cultures was started in shake flasks to extract the synthesized carotenoids. Carotenoids were extracted and analyzed by TLC as described in method. Since the pNAr8 construct could not be confirmed by restriction digestion, different isolates of pNAr8 were transformed and the extracts were used to confirm the construct. In Figure 3.10 A, TLC analysis of 8 different pNAr8 transformants is shown. As a negative control, extract from wild type *Pseudomonas* sp. 102515 was used while positive control was the extract from *E. coli* BL21(DE3)/pAC-ZEAXipi. It is seen that the banding pattern of extracts from *Pseudomonas* sp. 102515Δ*crtX* were matched with the positive control while the others were still wild type *Pseudomonas* sp. 102515. Three of confirmed *Pseudomonas* sp. 102515Δ*crtX* mutants were selected and their extracts were analyzed by TLC with negative control and positive control, seen in Figure 3.10 B.

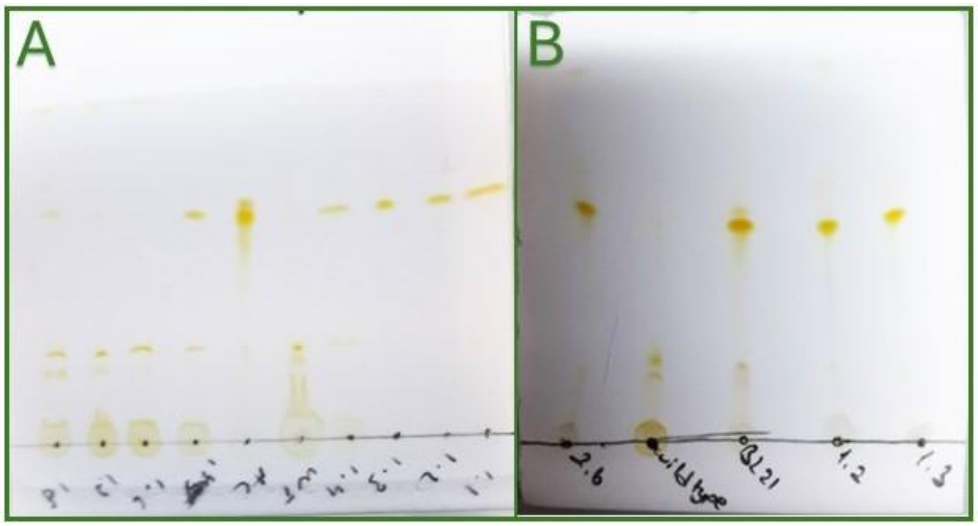

Figure 3.10 TLC analysis for extracts from *crtX* knockouts by different pNAr8 constructs with positive and negative controls. A) TLC for screening for all pNAr8 transformants, B) TLC for positive pNAr8 constructs.

Analysis of the other knockouts (Δ*crtY* and Δ*crtZ*) was easier, hence the construction of pgRNAtet strategy was changed that have a simpler confirmation of the constructs pNAr9 and pNAr15 via SpeI restriction digestion. In Figure 3.11 and Figure 3.12 , TLC results for the extracts from all knockouts are shown with negative control as wild type *Pseudomonas* sp. 102515 extract and positive controls *E. coli* BL21(DE3)/pAC-based plasmid extract and standard of the expected carotenoids. For the *Pseudomonas* sp. 102515Δ*crtX*, additional orange band was observed on the upper part

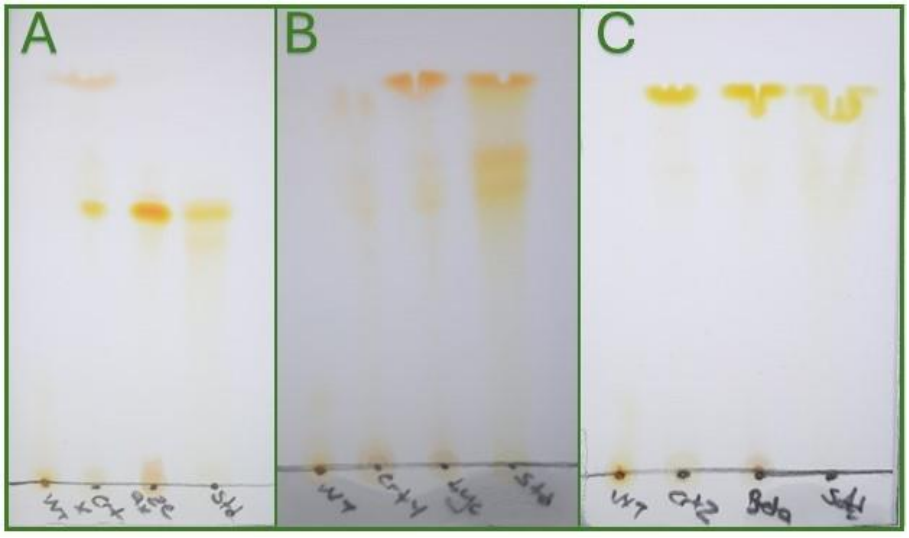

Figure 3.11 TLC analysis of extracts from knockouts with positive and negative controls. A) TLC for extract of *Pseudomonas* sp. 102515Δ*crtX*, B) TLC for extract of *Pseudomonas* sp. 102515Δ*crtY*, C) TLC for extract of *Pseudomonas* sp. 102515Δ*crtZ*.

of TLC plate that matches with lycopene. It leads us to assume that knockout of *crtX* gene had influenced the conversion of lycopene into following carotenoids or increased the synthesis of lycopene. Beta carotene and lycopene could not be separated with the developing solvent acetone:n-hexane:dH_2O (9:9:1) since they have similar polarity. Different developing solvents were tested but better separation could not be achieved, extracts were further analyzed by HPLC and confirmed.

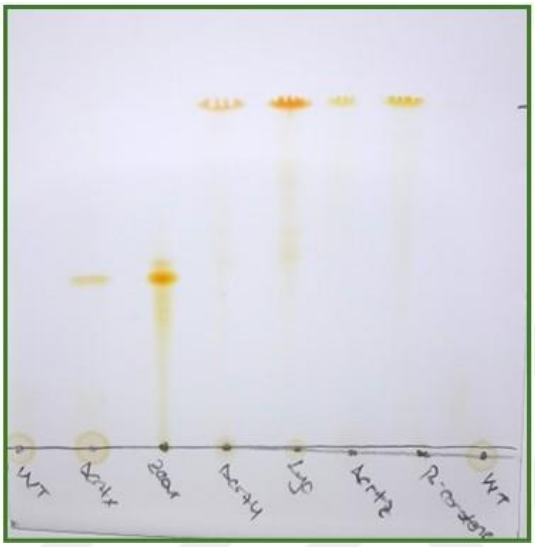

Figure 3.12 TLC analysis for knockouts with positive control as standards and negative control as wild type.

3.1.6 HPLC Analysis for the Extracts of Knockout Strains

Extracts from knockout strains were analyzed by isocratic elution of acetonitrile:methanol:isopropanol (5:3:2, v/v/v). First, *Pseudomonas* sp. 102515Δ*crtX* mutant was obtained and its extract was analyzed by HPLC. *E. coli* BL21(DE3)/pAC-ZEAXipi extract, and zeaxanthin standard were analyzed as positive control. The chromatogram is seen in Figure 3.13 . All the samples were eluted with retention time of 3.53-3.92 min as two peaks. In addition to retention time, UV profiles of the peaks (see Figure 3.14, Figure 3.15 and Figure 3.16) were examined to confirm that the peaks are belonging to carotenoids. Since the two peaks have quite close retention times and same UV profiles, the results suggest that the peaks are both zeaxanthin isomers. The HPLC analysis of *Pseudomonas* sp. 102515Δ*crtX* extract have an additional peak at 9.64 min (see Figure 3.15) that have a unique UV profile for lycopene and this result is consistent with TLC analysis.

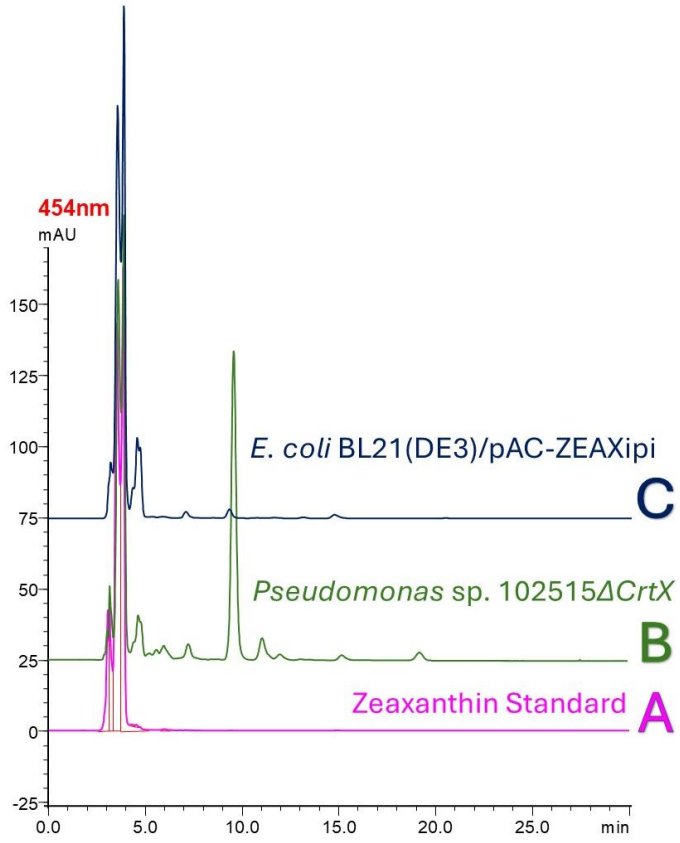

Figure 3.13 HPLC chromatograms for confirmation of *crtX* knockout. A) Zeaxanthin standard, B) *Pseudomonas* sp. 102515Δ*crtX* and C) *E. coli* BL21(DE3)/pAC-ZEAXipi.

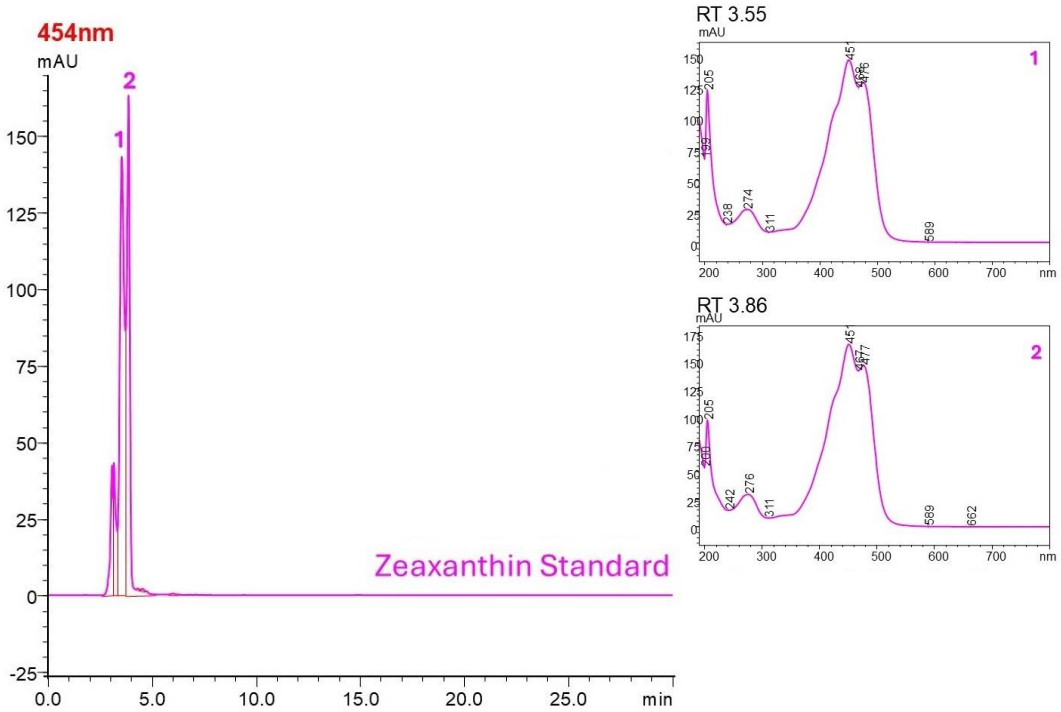

Figure 3.14 UV profiles of peaks from HPLC analysis of zeaxanthin standard.

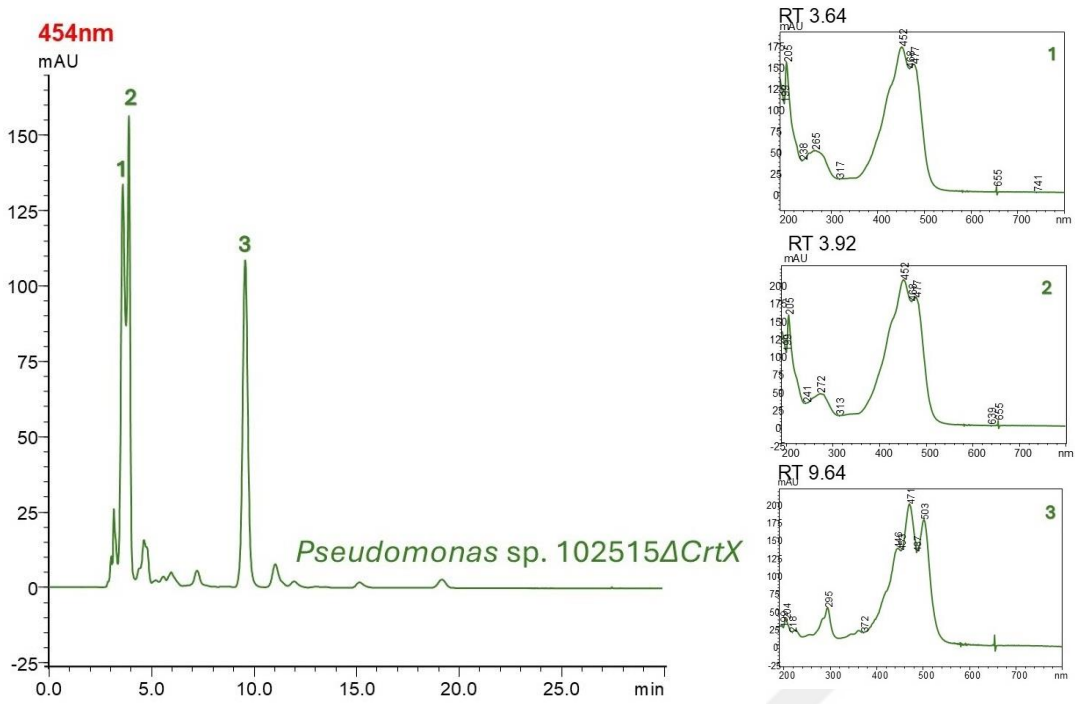

Figure 3.15 UV profiles of peaks from HPLC analysis of *Pseudomonas* sp. 102515Δ*crtX* extract.

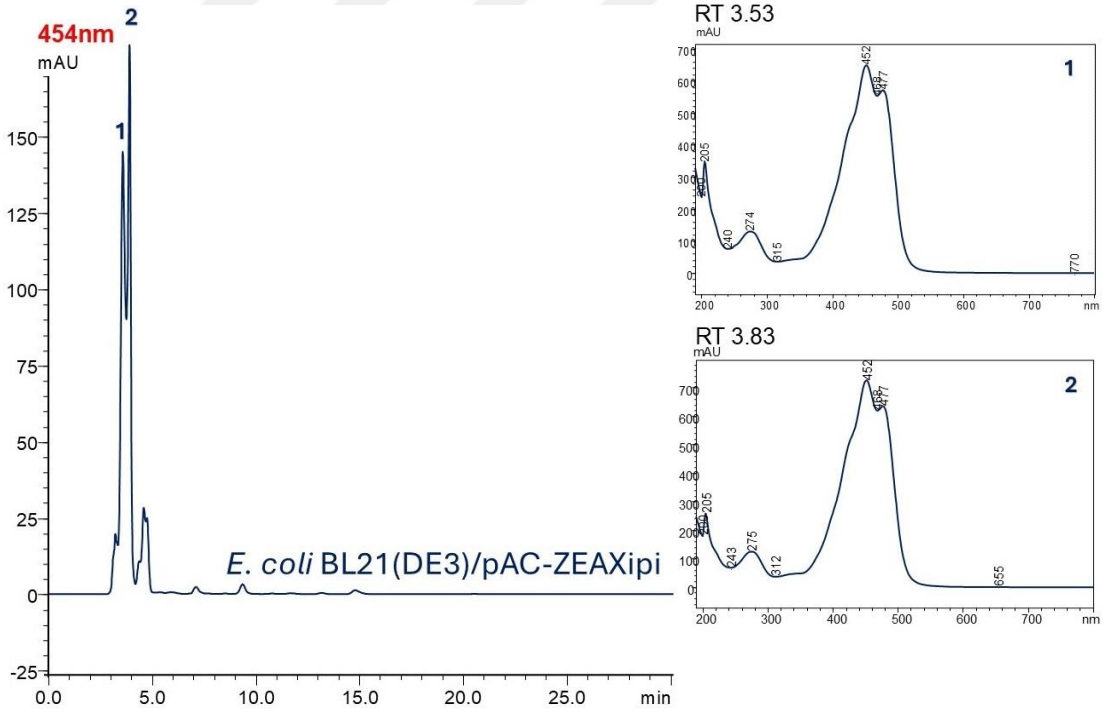

Figure 3.16 UV profiles of peaks from HPLC analysis of *E. coli* BL21(DE3)/pAC-ZEAXipi extract.

Pseudomonas sp. 102515Δ*crtY* and *Pseudomonas* sp. 102515Δ*crtZ* extracts were also analyzed by the same method. In Figure 3.17, HPLC chromatogram for the confirmation of *crtY* gene knockout was shown. Lycopene standard and *E. coli* BL21(DE3)/pAC-LYCipi extract were analyzed as positive control along with *Pseudomonas* sp. 102515Δ*crtY* extract. The corresponding lycopene peak from all the samples eluted with retention times of 9.34-9.54 min and UV profiles of the peaks were shown in Figure 3.17. Two shouldered UV profiles of the peaks with maxima point at 471 nm were consistent with lycopene from the literature and all the findings confirm the knockout of *crtY* gene as well as the synthesis of lycopene.

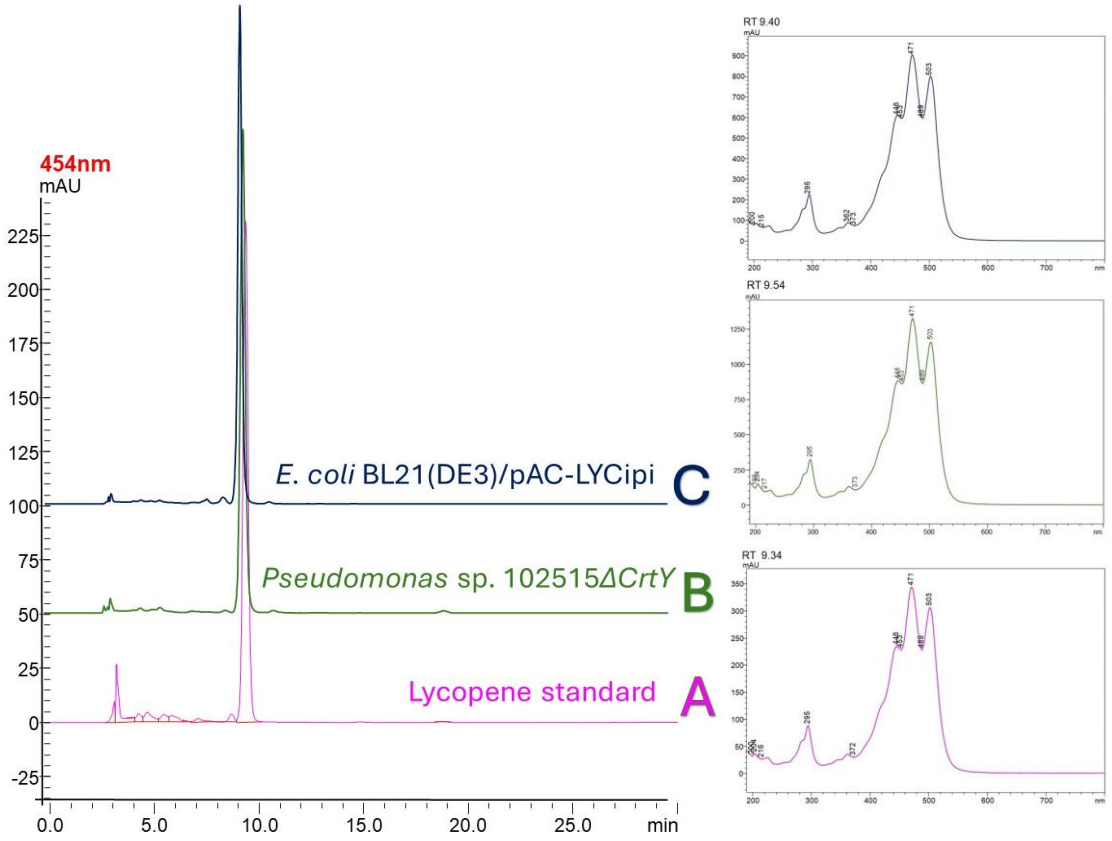

Figure 3.17 HPLC chromatograms and UV profiles of the peaks for confirmation of *crtY* knockout. A) Lycopene standard, B) *Pseudomonas* sp. 102515Δ*crtY* extract, C) *E. coli* BL21(DE3)/pAC-LYCipi extract.

Similarly, *Pseudomonas* sp. 102515Δ*crtZ* extract was analyzed with positive controls, β-carotene standard and *E. coli* BL21(DE3)/pAC-BETAipi extract. β-carotene peak was eluted with retention times of 14.89-15.36 min (see Figure 3.18). Carotenoid specific and matching UV profiles were observed for all the peaks with maxima point at 452 nm. HPLC analysis confirms the knockout of *crtZ* gene. β-carotene and lycopene are

both nonpolar carotenoids. β-carotene is slightly less polar than lycopene [74] that results in elution of β-carotene with later retention time depending on mobile phases. Since the polarity difference is very small, elution of lycopene might be observed with later retention times based on mobile phases' polarity.

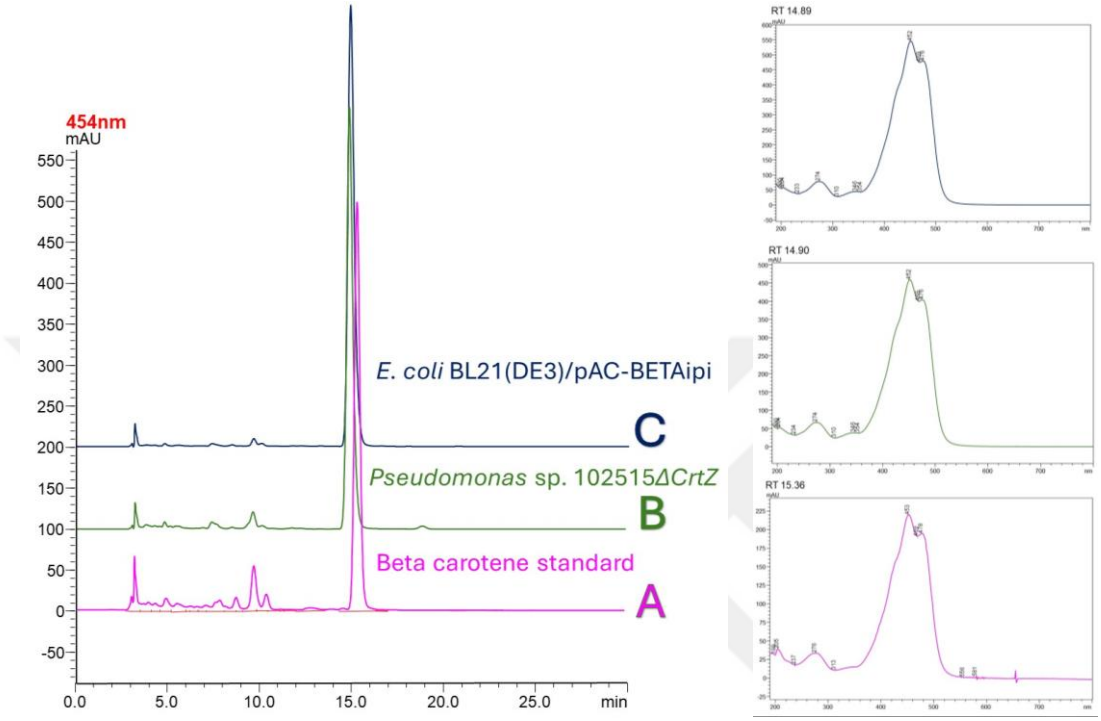

Figure 3.18 HPLC chromatograms and UV profiles of the peaks for confirmation of *crtZ* knockout. A) Beta carotene standard, B) *Pseudomonas* sp. 102515Δ*crtZ* extract, C) *E. coli* BL21(DE3)/pAC-BETAipi extract.

3.2 Results for Overexpression Strains

3.2.1 Construction of pMiS1-CaZEP (pNAr17)

Construction of the overexpression plasmids was started with the construction of pNAr17. *ZEP* gene of *Capsicum annuum*, with 1.9 kb size, was amplified by primers 28-29 from pUC_{lac}-KBS5000-CaZEP plasmid (see Figure 3.17A). On the other site, pSUN113 was cut by EcoRV to yield pJET1.2 cloning vector with 3 kb size (Figure 3.17B). Both vector pJET1.2 and insert CaZEP bands were collected from gel and

purified by kit (Figure 3.17C) and ligated via T4 DNA ligase. The construct carrying CaZEP as insert with pJET1.2 vector backbone was named pNAr16.

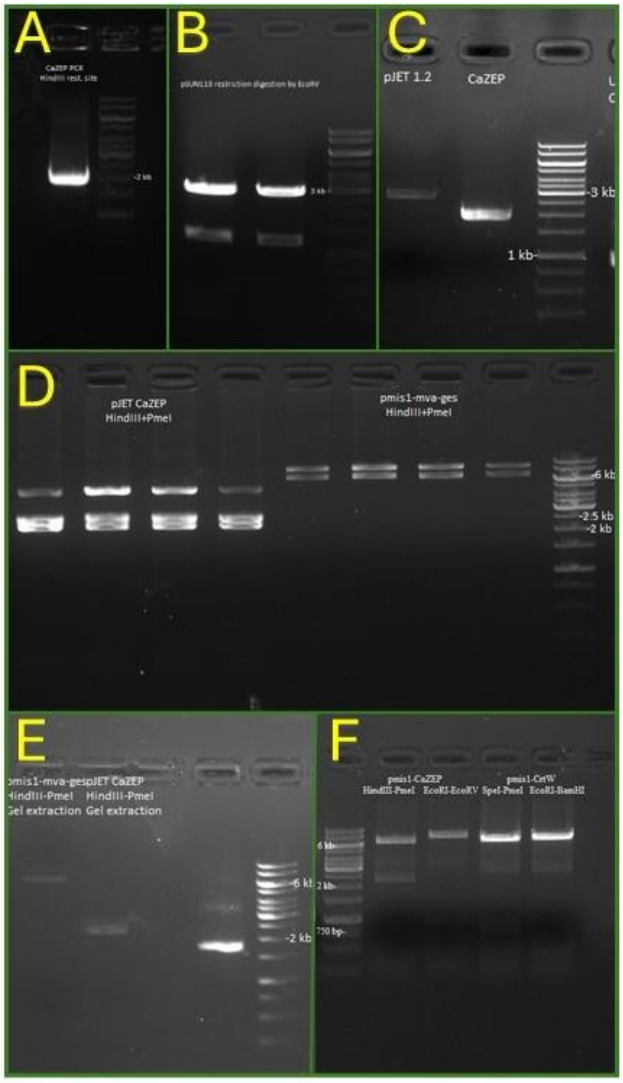

Figure 3.19 Agarose gel electrophoresis result for construction and confirmation of pJET-CaZEP (pNAr16) and pMiS1-CaZEP (pNAr17). A) PCR amplification of blunt-end CaZEP, B) Restriction digestion of pSUN113 to have linearized pJET1.2, C) Gel extractions of pJET1.2 and CaZEP, D) Confirmation of pNAr16 and sticky-end vector (pMiS1)/insert(CaZEP) preparation by restriction digestion, E) Gel extractions of pMiS1 and CaZEP, F) Confirmation of pNAr17 and pNAr18 by restriction digestion.

pNAr16 and pMiS1-MVA-ges plasmids were digested by PmeI and HindIII to obtain insert (CaZEP, 1.9 kb) and vector (pMiS1, 6.4 kb) with sticky-ends (Figure 3.17D). Vector and insert were purified from gel (Figure 3.17E) and T4 DNA ligase was again used to ligate sticky-end CaZEP and pMiS1 that yields pNAr17. For the confirmation of pNAr17, PmeI-HindIII (6.4 kb+ 1.9 kb) and EcoRI-EcoRV (7.2 kb+ 900 bp+200 bp) were used to cut construct (Figure 3.17F). pNAr16 was sequenced to confirm the

construct and sequencing result was aligned with *CaZEP* gene sequence in Figure A.10 . Plasmid maps for pNAr16 and pNAr17 are shown in Figure A.10 .

3.2.2 Construction of pMiS1-crtW (pNAr18)

crtW gene was synthesized as gene block. The synthesized gene block was used as template for the amplification of *crtW*. Primers 26-27 were used and introduced PmeI and SpeI restriction sites to PCR product's 5' and 3' ends, respectively. Amplified *crtW* gene (800 bp) was cut from the gel and purified via kit (see Figure 3.18 A and B). *crtW* gene was first cloned into pJET1.2 vector with the same manner of CaZEP and the construct named pNAr11, confirmed by PmeI-SpeI restriction digestion that should give 2.6 kb+800 bp+ 400 bp bands. In Figure 3.18 C, it is shown that sample 2 was confirmed while the sample 1 was a self-ligation product of pJET1.2.

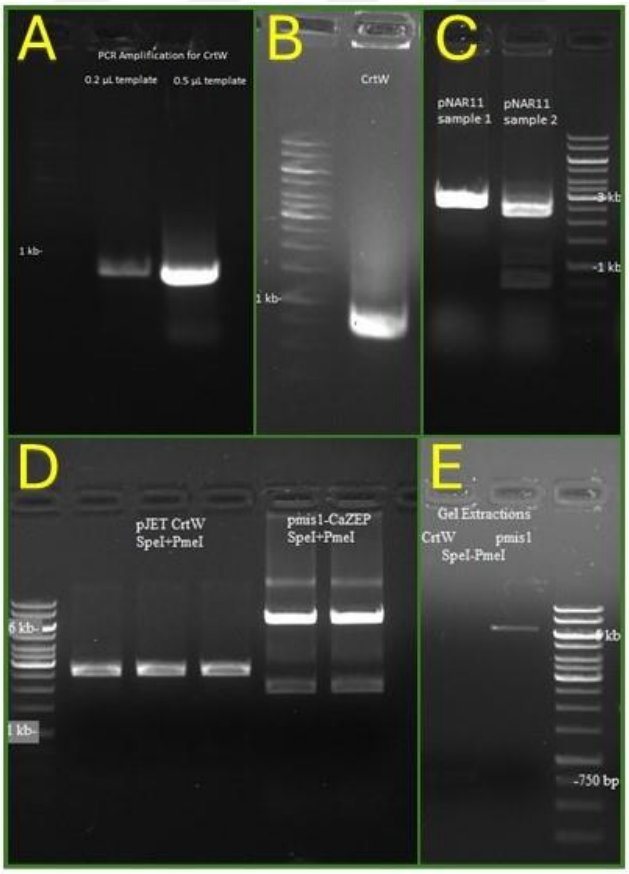

Figure 3.20 Agarose gel electrophoresis result for construction and confirmation of pJET-*crtW* (pNAr11) and pMiS1-*crtW* (pNAr18). A) PCR amplification of blunt-end *crtW*, B) Gel extraction of *crtW*, C) Confirmation of pNAr11, D) Sticky-end vector (pMiS1)/insert (*crtW*) preparation by restriction digestion, E) Gel extractions of pMiS1 and *crtW*.

In Figure 3.18 D, pNAr11 and pNAr17 were cut by PmeI and SpeI to yield sticky-end insert *crtW* (800 bp) and vector pMiS1 (6.4 kb). Corresponding bands collected and purified from gel (see Figure 3.18 E) and *crtW* gene was cloned into pMiS1 vector via T4 DNA ligase to yield pNAr18. Confirmation of pNAr18 was done by PmeI-SpeI (6.4 kb+800 bp) and EcoRI-BamHI (6.7 kb+460 bp) and is shown in Figure 3.17 F. Sequencing result of pNAr11 was aligned with *crtW* gene sequence and is shown in Figure A.16 . Plasmid maps for pNAr11 and pNAr18 are shown in Figure A.11 .

3.2.3 Construction of pMiS1-CaZEP-CaCCS$_{m40}$ (pNAr20)

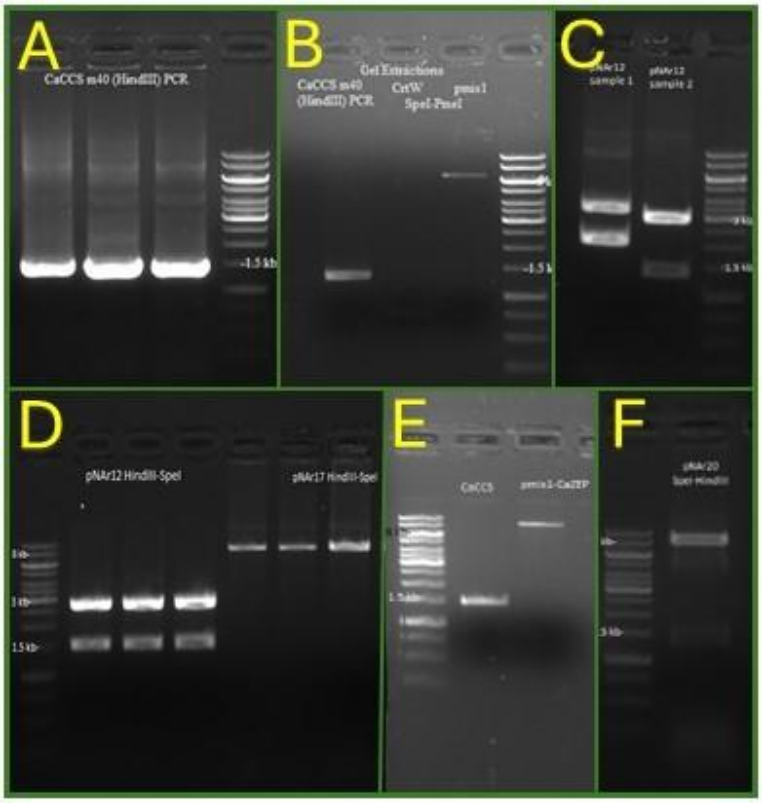

Figure 3.21 Agarose gel electrophoresis result for construction and confirmation of pJET-CaCCS$_{m40}$ (pNAr12) and pMiS1-CaZEP-CaCCS$_{m40}$ (pNAr20). A) PCR amplification of blunt-end *CaCCS*$_{m40}$, B) Gel extraction of *CaCCS*$_{m40}$, C) Confirmation of pNAr12, D) Sticky-end vector (pNAr17)/insert (*CaCCS*$_{m40}$) preparation by restriction digestion, E) Gel extractions of pNAr17 and *CaCCS*$_{m40}$, F) Confirmation of pNAr20.

CCS gene of *Capsicum annuum* (1.4 kb) was amplified from pMF541 via primers 30-31 with SpeI and HindIII restriction sites (see Figure 3.19 A). Similar to *CaZEP* and *crtW* genes, *CaCCS*$_{m40}$ was first purified from gel (Figure 3.19 B) and then cloned into pJET1.2 by T4 DNA ligase. The resulted construct named pNAr12 and confirmed by

SpeI-HindIII restriction digestion that should give 2.7 kb+1.4 kb+260 bp as shown in Figure 3.19 C, sample 2. pNAr12 and pNAr17 were cut by SpeI and HindIII to have sticky end insert *CaCCS*$_{m40}$ (1.4 kb) and linearized pMiS1-CaZEP (8.4 kb) as vector (see Figure 3.19 D). Insert and vector were cut from the gel and purified by gel extraction kit (Figure 3.19 E) and then, ligated by T4 DNA ligase to construct pMiS1-CaZEP-CaCCS$_{m40}$, named as pNAr20. Confirmation of pNAr20 was done by SpeI-HindIII restriction digestion that yields 8.4 kb+1.4 kb bands as seen in Figure 3.19 F. pNAr12 was sequenced and resulting sequence was aligned with *CaCCS* gene sequence in Figure A.17. In addition, plasmid maps are shared in Figure A.12 for pNAr12 and pNAr20.

In a previous study, different sources of *ZEP* gene were tested and *CaZEP* was found to be most efficient one in terms of violaxanthin production with minimum zeaxanthin [69]. Therefore, *CaZEP* was chosen for this study. The same study was also showed that despite the high expression levels of *CaCCS*$_{m40}$, the synthesis of capsanthin/capsorubin was very low [69]. *CaCCS* gene exhibits dual activity as lycopene-β-cyclase and capsanthin/capsorubin synthase. A previous study has shown that linking *CaCCS* with *CaZEP* increases the efficiency of *CaCCS* as capsanthin/capsorubin synthase to produce capsanthin and/or capsorubin [75].

3.2.4 Electroporation of Overexpression Plasmids to *Pseudomonas* sp. 102515Δ*crtX*

After the construction of overexpression plasmids pNAr17, pNAr18 and pNAr20, the plasmids were transformed to *Pseudomonas* sp. 102515Δ*crtX* by electroporation as described in the method. Different amounts from each construct were transformed and selection was done by Kan30 plates. Transformed colonies were subcultured into fresh Kan30 plates and all of them were shown in Figure 3.22 . The color change from yellow to orange was observed in subculturing plates for colonies of pNAr20 and pNAr18.

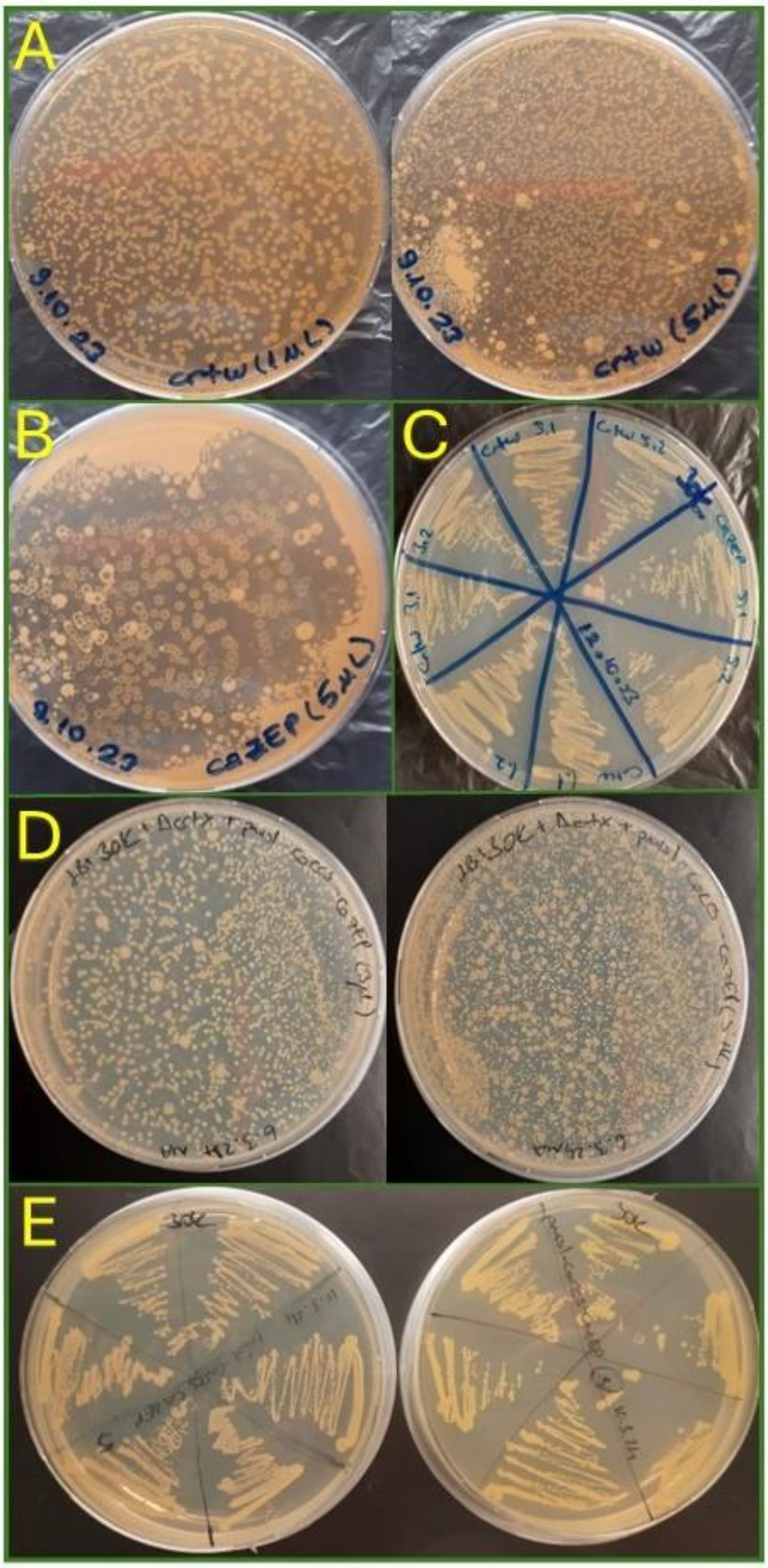

Figure 3.22 Electroporation of overexpression plasmids to *Pseudomonas* sp. 102515Δ*crtX*. A) Transformation of pNAr18, B) Transformation of pNAr17, C) Subculturing of pNAr18 and pNAr17 transformants into a fresh plate, D) Transformation of pNAr20, E) Subculturing of pNAr20 transformants into fresh plates.

3.2.5 TLC Analysis for the Extracts of Overexpression Strains

Carotenoids were extracted from *Pseudomonas* sp. 102515Δ*crtX*/pNAr18 and *Pseudomonas* sp. 102515Δ*crtX*/pNAr17 cultures after induction. Extracts were first analyzed by TLC. In Figure 3.21A, astaxanthin producing *Pseudomonas* sp. 102515Δ*crtX*/pNAr18 strain extracts were analyzed with negative control as *Pseudomonas* sp. 102515Δ*crtX* extract and zeaxanthin standard. There were yellow and orange colonies that had grown to extract carotenoids. All cells exhibit different banding patterns than negative controls, only yellow colonies were also yellow band that matches with zeaxanthin. Further, *Pseudomonas* sp. 102515Δ*crtX*/pNAr18 extract was analyzed by TLC with positive control (astaxanthin standard) and negative controls (see Figure 3.21B). On the same TLC plate, *Pseudomonas* sp. 102515Δ*crtX*/pNAr17 extract was analyzed along with negative control as *Pseudomonas* sp. 102515Δ*crtX* extract and positive control *E. coli* BL21(DE3)/pAC-VIOL extract (Figure 3.21B). Additional bands were observed for *Pseudomonas* sp. 102515Δ*crtX*/pNAr17 extract.

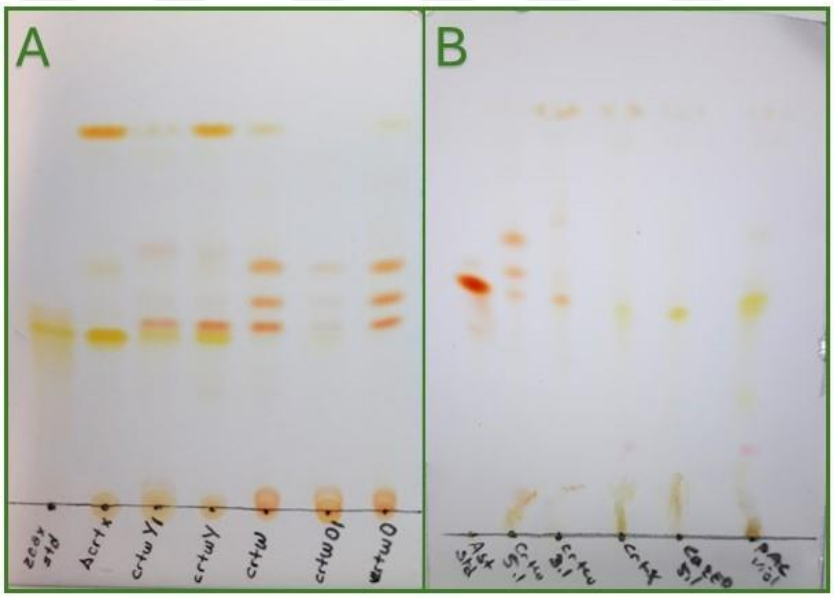

Figure 3.23 TLC analysis for overexpression strains *Pseudomonas* sp. 102515Δ*crtX*/pNAr17 and *Pseudomonas* sp. 102515Δ*crtX*/pNAr18. A) TLC for extract from pNAr18 transformed cells with negative control, B) TLC for extracts from pNAr18 and pNAr17 transformed cells with positive and negative controls.

Pseudomonas sp. 102515Δ*crtX*/pNAr17 extract was analyzed again with higher amount of the sample (see Figure 3.24 A) and there were three bands observed that will turn into green after a few hours (Figure 3.24 B), could be due to degradation of

violaxanthin. One of the three bands was matching with the band from *E. coli* BL21(DE3)/pAC-VIOL extract.

Extract from *Pseudomonas* sp. 102515Δ*crtX*/pNAr20 strain has a reddish color and analyzed by TLC with positive control (capsanthin standard) and negative control *Pseudomonas* sp. 102515Δ*crtX* extract in Figure 3.24 A. Several bands observed for capsanthin standard since the purity of the standard >85% and some of bands were matching with *Pseudomonas* sp. 102515Δ*crtX*/pNAr20 extract. HPLC analysis is required for both *Pseudomonas* sp. 102515Δ*crtX*/pNAr18 and *Pseudomonas* sp. 102515Δ*crtX*/pNAr20 extracts to confirm the synthesis of violaxanthin and capsanthin/capsorubin certainly.

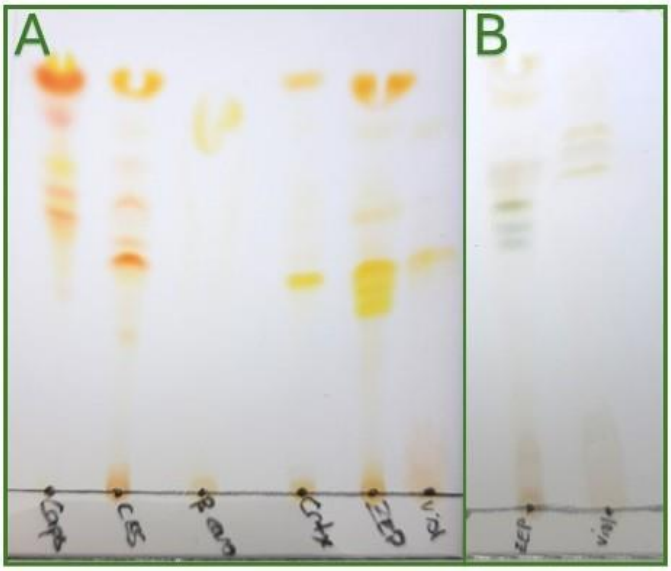

Figure 3.24 TLC analysis for overexpression strains *Pseudomonas* sp. 102515Δ*crtX*/pNAr17 and *Pseudomonas* sp. 102515Δ*crtX*/pNAr20. A) TLC for extracts from pNAr17 and pNAr20 transformed cells with negative control and positive controls, B) TLC for extracts from pNAr17 with positive control after a few hours.

3.2.6 HPLC Analysis for the Extracts of Overexpression Strains

Pseudomonas sp. 102515Δ*crtX*/pNAr18 extract was analyzed by HPLC along with the astaxanthin standard as positive control (Figure 3.25). Purity of astaxanthin standard was observed high in both TLC and HPLC, only one peak eluted at 3.75 min. HPLC analysis of *Pseudomonas* sp. 102515Δ*crtX*/pNAr18 extract resulted in elution of 2 peaks, one at 3.70 min and its UV profile was matching with astaxanthin standard with maxima

point at 475 nm. The other peak was eluted with retention time of 9.29 min and UV profile indicates that this peak was belonging to lycopene. Synthesis of astaxanthin from *Pseudomonas* sp. 102515Δ*crtX*/pNAr18 strain was confirmed by HPLC results. Extracts from *Pseudomonas* sp. 102515Δ*crtX*/pNAr17 and *Pseudomonas* sp. 102515Δ*crtX*/pNAr20 will be analyzed by HPLC to confirm the production of violaxanthin and capsanthin/capsorubin.

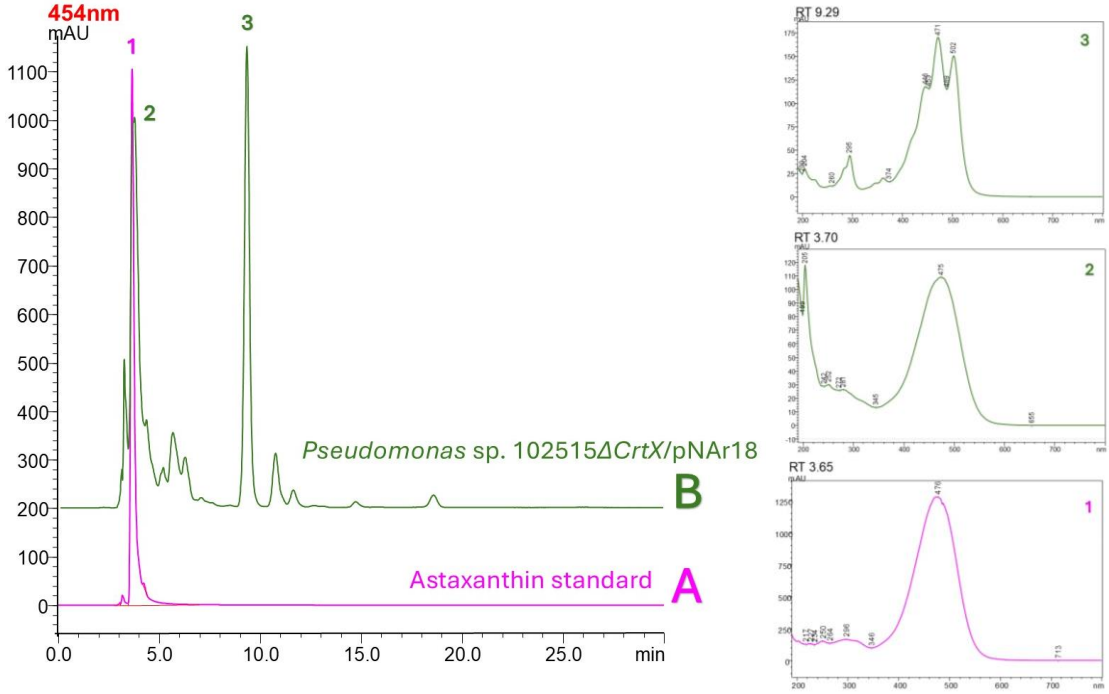

Figure 3.25 HPLC chromatograms and UV profiles of the peaks for the confirmation of astaxanthin production. A) Astaxanthin standard, B) *Pseudomonas* sp. 102515Δ*crtX*/pNAr18 extract.

Chapter 4

Conclusions and Future Prospects

4.1 Conclusions

Carotenoids are secondary metabolites synthesized mainly by photosynthetic organisms such as plants, algae, and certain bacterial species. They are synthesized from IPP and DMAPP through the catalysis of several enzymes and have a conjugated polyene chain in their structure. The conjugated polyene chain provides carotenoids with antioxidant activities to scavenge free radicals, ROS, and quench singlet oxygen. Since animals and humans cannot synthesize carotenoids, they must obtain them through their diet. Carotenoids exhibit various biological activities such as anticancer, neuroprotective, anti-atherosclerotic due to primarily their antioxidant activity. Therefore, carotenoids are beneficial to human health for both the prevention and treatment of various diseases.

In this thesis, we have focused on microbial biosynthesis of six different carotenoids: lycopene, β-carotene, zeaxanthin, astaxanthin, violaxanthin and capsanthin/capsorubin. For this purpose, the genome of an endophytic bacteria isolated from the leaves of *Taxus chinensis*, identified as *Pseudomonas* sp. 102515, was engineered by CRISPR-Cas9 technology and overexpression plasmids were introduced. The synthesized carotenoids were extracted from engineered stains and analyzed by TLC and HPLC analysis.

The biosynthesis of carotenoids occurs through different microorganisms exhibiting unique advantages and disadvantages in their production capabilities. Mainly, yeast, microalgae and bacteria species have been used for carotenoid production. These microorganisms can be native producers for a carotenoid but also, genetic engineering allows to introduce carotenogenic genes to biosynthesize various carotenoids from different microorganisms including non-carotenoid producers. Since the cultivation of

microorganisms is time and cost effective than plants, microbial biosynthesis has gained attention for industrial scale production. However, required cultivation media for the growth of microorganisms results in higher cost than chemical synthesis. At this point, agro-industrial residues might be considered as an alternative to cultivation media to reduce the cost due to their high nutrient potential [76].

In the literature, there are several studies for the biosynthesis of these carotenoids from algae, yeast, and bacteria species [70,77-85]. Also, there are studies that uses endophytic bacteria species for microbial synthesis of carotenoids [86-88]. However, this is the first study that focuses on microbial synthesis of six different carotenoids from one specific endophytic bacterium by engineering its genome. In addition, capsanthin is a unique carotenoid to red pepper and biosynthesis of capsanthin was achieved in only one study with a low yield [69]. This study is promising for high yield capsanthin biosynthesis due to the current findings, and it will be proven when capsanthin biosynthesis is confirmed by HPLC analysis.

Zeaxanthin epoxidase (ZEP) is found in different organisms. Takemura *et al.* investigated the efficiency of seven different ZEP in *E. coli* for the biosynthesis of violaxanthin [70]. It has been found that ZEP from *Capsicum annuum* (CaZEP) shows the highest conversion efficiency of zeaxanthin to antheraxanthin/violaxanthin. In addition, findings of Furubayashi *et al.* in a different study were supported that CaZEP exhibits higher conversion efficiency than *Arabidopsis thaliana* ZEP (AtZEP) [69]. It has been also investigated that the truncated versions of CaZEP and AtZEP at similar points. However, full length CaZEP resulted in the highest conversion efficiency compared to AtZEP and truncated versions. Therefore, non-truncated full length CaZEP was used in this study. Further, capsanthin/capsorubin synthase from *C. annuum* (CaCCS) was investigated for capsanthin production in *E. coli*. Full length CaCCS showed lycopene β-cyclase activity while 40 amino acids truncated $CaCCS_{m40}$ was exhibiting high level of expression and slight increase in capsanthin production when it was introduced with CaZEP on the same plasmid. These findings provide a valuable insight into our study and thus, CaZEP and $CaCCS_{m40}$ were used to biosynthesize violaxanthin and capsanthin with the same strategy.

4.2 Societal Impact and Contribution to Global Sustainability

In this study, biosynthesis of high value-added carotenoids was aimed via engineered microorganisms. Mainly, zeaxanthin, lycopene, β-carotene, astaxanthin and capsanthin/capsorubin have been biosynthesized successfully. Carotenoids have health benefits due to their both antioxidant properties and provitamin A activities. Depending on these biological activities, the biosynthesis of carotenoids supports the "Good Health and Well-being" goal of the United Nations Sustainable Development Goals, as well as the objectives outlined in sub-goals 3.3 and 3.4 with the potential of being effective in the treatment and prevention of both infectious and non-infectious diseases. Microbial biosynthesis of carotenoids creates an alternative for production of carotenoid-rich products that can provide a healthier diet to humans and lowers the cost of healthcare.

Microbial biosynthesis is a biotechnological approach that will eliminate the disadvantages of alternative methods such as extraction from plants and chemical synthesis for carotenoid production. Besides, microbial biosynthesis offers environmentally friendly procedures to produce carotenoids, unlike chemical synthesis, by avoiding the use of harmful organic solvents. In addition, microbial biosynthesis of carotenoids offers a more sustainable alternative compared to extraction from plants since it requires less land and less use of water. Less land requirement allows the preservation of natural habitat and biodiversity as well as supporting agriculture while less use of water preserves our natural sources.

Also, it is a time-effective and lower-cost method compared to other methods. The lower cost of carotenoid synthesis is important to produce carotenoid-rich products and profit by their biological activities. In general, this thesis can contribute to the advancement of biotechnology's sustainable practices, the enhancement of human health, and the promotion of economic growth in a manner consistent with the objectives of global sustainability.

4.3 Future Prospects

In the study, the strains have been engineered by gene knockouts and introduction of overexpression plasmids to produce certain carotenoids. Six different strains have been engineered to synthesize zeaxanthin, lycopene, β-carotene, astaxanthin, violaxanthin and capsanthin/capsorubin. Following this part of the project, the titers for each carotenoid synthesized from the engineered strains will be determined and culture conditions will be optimized to reach the maximum yield by these engineered strains. In addition, bioreactors will be used to optimize yield at an industrial scale.

On the other hand, another plasmid is under construction which encodes for MVA pathway. Since the MVA pathway provides the precursors (IPP and DMAPP) for carotenoid synthesis, it is expected that the introduction of this plasmid will improve the overall yield for all the strains. In addition, in the study conducted by Chen *et al.*, glycosylated of astaxanthin biosynthesis from *Yarrowia lipolytica* was achieved by introducing *crtX* gene to increase the water solubility, bioavailability and stability of astaxanthin [89]. To investigate the biosynthesis of glycosylated astaxanthin from *Pseudomonas* sp. 102515, pNAr18 has also been transformed into the wild type strain by electroporation.

BIBLIOGRAPHY

[1] V. Böhm, "Carotenoids," *Antioxidants*, vol. 8, no. 11, p. 516, Oct. 2019, doi: 10.3390/antiox8110516.

[2] A. S. Fernandes, T. C. do Nascimento, E. Jacob-Lopes, V. V. De Rosso, and L. Q. Zepka, "Introductory Chapter: Carotenoids - A Brief Overview on Its Structure, Biosynthesis, Synthesis, and Applications," in *Progress in Carotenoid Research*, L. Q. Zepka, E. Jacob-Lopes, and V. V. De Rosso, Eds., IntechOpen, 2018. doi: 10.5772/intechopen.79542.

[3] A. Westphal and V. Böhm, "Carotenoids. Properties, distribution, bioavailability, metabolism and health effects," *Ernahrungs Umschau International*, vol. 62, no. 11, pp. 196–207, Jun. 2015, doi: 10.4455/eu.2015.036.

[4] A. V. Rao and L. G. Rao, "Carotenoids and human health," *Pharmacol Res*, vol. 55, no. 3, pp. 207–216, Mar. 2007, doi: 10.1016/j.phrs.2007.01.012.

[5] R. J. Cogdell and A. T. Gardiner, "[18] Functions of Carotenoids in Photosynthesis," *Methods Enzymol*, vol. 214, pp. 185–193, 1993, doi: 10.1016/0076-6879(93)14065-Q.

[6] R. M. Russell and S. A. R. Paiva, "β-Carotene and Other Carotenoids as Antioxidants," *J Am Coll Nutr*, vol. 18, no. 5, pp. 426–433, Jun. 1999, doi: 10.1080/07315724.1999.10718880.

[7] A. J. Meléndez-Martínez, "An Overview of Carotenoids, Apocarotenoids, and Vitamin A in Agro-Food, Nutrition, Health, and Disease," *Mol Nutr Food Res*, vol. 63, no. 15, Jun. 2019, doi: 10.1002/mnfr.201801045.

[8] F. Grodstein, J. H. Kang, R. J. Glynn, N. R. Cook, and J. M. Gaziano, "A randomized trial of beta carotene supplementation and cognitive function in men: The physicians' health study II," *Arch Intern Med*, vol. 167, no. 20, pp. 2184–2190, Nov. 2007, doi: 10.1001/archinte.167.20.2184.

[9] P. D. Fraser and P. M. Bramley, "The biosynthesis and nutritional uses of carotenoids," *Prog Lipid Res*, vol. 43, no. 3, pp. 228–265, May 2004, doi: 10.1016/j.plipres.2003.10.002.

[10] J. Rico *et al.*, "Exploring natural biodiversity to expand access to microbial terpene synthesis," *Microb Cell Fact*, vol. 18, no. 1, Feb. 2019, doi: 10.1186/s12934-019-1074-4.

[11] T. Kuzuyama and H. Seto, "Two distinct pathways for essential metabolic precursors for isoprenoid biosynthesis," *Proc Jpn Acad Ser B Phys Biol Sci*, vol. 88, no. 3, pp. 41–52, 2012, doi: 10.2183/pjab.88.41.

[12] L. Tao, J. Wilczek, J. M. Odom, and Q. Cheng, "Engineering a β-carotene ketolase for astaxanthin production," *Metab Eng*, vol. 8, no. 6, pp. 523–531, Nov. 2006, doi: 10.1016/j.ymben.2006.06.001.

[13] Y. Yang *et al.*, "Complete biosynthetic pathway of the C50 carotenoid bacterioruberin from lycopene in the extremely halophilic archaeon Haloarcula japonica," *J Bacteriol*, vol. 197, no. 9, Apr. 2015, doi: 10.1128/JB.02523-14.

[14] X. H. Mo *et al.*, “Characterization of C30 carotenoid and identification of its biosynthetic gene cluster in Methylobacterium extorquens AM1,” *Synth Syst Biotechnol*, vol. 8, no. 3, pp. 527–535, Sep. 2023, doi: 10.1016/j.synbio.2023.08.002.

[15] A. J. Meléndez-Martínez *et al.*, “A comprehensive review on carotenoids in foods and feeds: status quo, applications, patents, and research needs,” *Crit Rev Food Sci Nutr*, vol. 62, no. 8, pp. 1999–2049, Jan. 2022, doi: 10.1080/10408398.2020.1867959.

[16] S. Y. Leong and I. Oey, “Effects of processing on anthocyanins, carotenoids and vitamin C in summer fruits and vegetables,” *Food Chem*, vol. 133, no. 4, pp. 1577–1587, Aug. 2012, doi: 10.1016/j.foodchem.2012.02.052.

[17] G. Britton and F. Khachik, “Carotenoids in Food,” in *Carotenoids*, vol. 5, G. Britton, H. Pfander, and S. Liaaen-Jensen, Eds., Birkhäuser Basel, 2009, pp. 45–66. doi: 10.1007/978-3-7643-7501-0_3.

[18] A. Sass-Kiss, J. Kiss, P. Milotay, M. M. Kerek, and M. Toth-Markus, “Differences in anthocyanin and carotenoid content of fruits and vegetables,” *Food Research International*, vol. 38, no. 8–9, pp. 1023–1029, Mar. 2005, doi: 10.1016/j.foodres.2005.03.014.

[19] A. López, G. A. Javier, J. Fenoll, P. Hellín, and P. Flores, “Chemical composition and antioxidant capacity of lettuce: Comparative study of regular-sized (Romaine) and baby-sized (Little Gem and Mini Romaine) types,” *Journal of Food Composition and Analysis*, vol. 33, no. 1, pp. 39–48, Feb. 2014, doi: 10.1016/j.jfca.2013.10.001.

[20] B. Beltrán, R. Estévez, C. Cuadrado, S. Jiménez, and B. Olmedilla Alonso, “[Carotenoid data base to assess dietary intake of carotenes, xanthophyls and vitamin A; its use in a comparative study of vitamin A nutritional status in young adults].,” *Nutr Hosp*, vol. 27, no. 4, pp. 1334–1343, 2012.

[21] M. G. Dias *et al.*, “Comprehensive Database of Carotenoid Contents in Ibero-American Foods. A Valuable Tool in the Context of Functional Foods and the Establishment of Recommended Intakes of Bioactives,” *J Agric Food Chem*, vol. 66, no. 20, Apr. 2018, doi: 10.1021/acs.jafc.7b06148.

[22] J. Shi and M. Le Maguer, “Lycopene in tomatoes: Chemical and physical properties affected by food processing,” *Crit Rev Food Sci Nutr*, vol. 40, no. 1, pp. 1–42, Jun. 2000, doi: 10.1080/10408690091189275.

[23] R. K. Saini *et al.*, “Carotenoids: Dietary Sources, Extraction, Encapsulation, Bioavailability, and Health Benefits—A Review of Recent Advancements,” *Antioxidants*, vol. 11, no. 4, p. 795, Apr. 2022, doi: 10.3390/antiox11040795.

[24] J. Müller-Maatsch, J. Sprenger, J. Hempel, F. Kreiser, R. Carle, and R. M. Schweiggert, “Carotenoids from gac fruit aril (Momordica cochinchinensis [Lour.] Spreng.) are more bioaccessible than those from carrot root and tomato fruit,” *Food Research International*, vol. 99, no. 2, pp. 928–935, Sep. 2017, doi: 10.1016/j.foodres.2016.10.053.

[25] E. Y. Ko, R. K. Saini, Y. S. Keum, and B. K. An, “Age of laying hens significantly influences the content of nutritionally vital lipophilic compounds in eggs,” *Foods*, vol. 10, no. 1, Dec. 2021, doi: 10.3390/foods10010022.

[26] Y. J. Aguillón-Páez and G. J. Díaz, “Lutein and zeaxanthin content in corn imported from three countries of the American continent and in corn cultivated in Colombian territory,” *Arq Bras Med Vet Zootec*, vol. 75, no. 3, Jun. 2023, doi: 10.1590/1678-4162-12786.

[27] M. Mrowicka, J. Mrowicki, E. Kucharska, and I. Majsterek, “Lutein and Zeaxanthin and Their Roles in Age-Related Macular Degeneration—Neurodegenerative Disease,” *Nutrients*, vol. 14, no. 4, p. 827, Feb. 2022, doi: 10.3390/nu14040827.

[28] J. Hempel, C. N. Schädle, J. Sprenger, A. Heller, R. Carle, and R. M. Schweiggert, “Ultrastructural deposition forms and bioaccessibility of carotenoids and carotenoid esters from goji berries (Lycium barbarum L.),” *Food Chem*, vol. 218, pp. 525–533, Mar. 2017, doi: 10.1016/j.foodchem.2016.09.065.

[29] R. Veberic, J. Jurhar, M. Mikulic-Petkovsek, F. Stampar, and V. Schmitzer, “Comparative study of primary and secondary metabolites in 11 cultivars of persimmon fruit (Diospyros kaki L.),” *Food Chem*, vol. 119, no. 2, pp. 477–483, Mar. 2010, doi: 10.1016/j.foodchem.2009.06.044.

[30] A. G. Pereira *et al.*, “Xanthophylls from the Sea: Algae as Source of Bioactive Carotenoids,” *Mar Drugs*, vol. 19, no. 4, p. 188, Mar. 2021, doi: 10.3390/MD19040188.

[31] M. Guerin, M. E. Huntley, and M. Olaizola, “Haematococcus astaxanthin: Applications for human health and nutrition,” *Trends Biotechnol*, vol. 21, no. 5, pp. 210–216, May 2003, doi: 10.1016/S0167-7799(03)00078-7.

[32] F. Camacho, A. Macedo, and F. Malcata, “Potential industrial applications and commercialization of microalgae in the functional food and feed industries: A short review,” *Mar Drugs*, vol. 17, no. 6, p. 312, May 2019, doi: 10.3390/md17060312.

[33] K. N. C. Murthy, A. Vanitha, J. Rajesha, M. M. Swamy, P. R. Sowmya, and G. A. Ravishankar, “In vivo antioxidant activity of carotenoids from Dunaliella salina - A green microalga,” *Life Sci*, vol. 76, no. 12, pp. 1381–1390, Feb. 2005, doi: 10.1016/j.lfs.2004.10.015.

[34] G. D. López, G. Álvarez-Rivera, C. Carazzone, E. Ibáñez, C. Leidy, and A. Cifuentes, “Bacterial Carotenoids: Extraction, Characterization, and Applications,” *Crit Rev Anal Chem*, vol. 53, no. 6, pp. 1239–1262, Dec. 2023, doi: 10.1080/10408347.2021.2016366.

[35] D. Asker, T. S. Awad, T. Beppu, and K. Ueda, “Screening, isolation, and identification of zeaxanthin-producing bacteria,” in *Microbial Carotenoids*, vol. 1852, C. , B. JL. Barreiro, Ed., New York: Humana Press, 2018. doi: 10.1007/978-1-4939-8742-9_11.

[36] C. Joshi and R. S. Singhal, “Modelling and optimization of zeaxanthin production by Paracoccus zeaxanthinifaciens ATCC 21588 using hybrid genetic algorithm techniques,” *Biocatal Agric Biotechnol*, vol. 8, pp. 228–235, Oct. 2016, doi: 10.1016/j.bcab.2016.10.004.

[37] K. Hirasawa and A. Tsubokura, “Method for separating carotenoid,” 8853460B2, Oct. 07, 2014

[38] O. Fidan and J. Zhan, “Discovery and engineering of an endophytic Pseudomonas strain from Taxus chinensis for efficient production of zeaxanthin diglucoside,” *J Biol Eng*, vol. 13, no. 1, p. 66, Aug. 2019, doi: 10.1186/s13036-019-0196-x.

[39] G. Britton, “Structure and properties of carotenoids in relation to function.,” *The FASEB Journal*, vol. 9, no. 15, pp. 1551–1558, Dec. 1995, doi: 10.1096/fasebj.9.15.8529834.

[40] A. Vershinin, “Biological functions of carotenoids - Diversity and evolution,” *BioFactors*, vol. 10, no. 2–3, pp. 99–104, Dec. 1999, doi: 10.1002/biof.5520100203.

[41] K. S. Cho, M. Shin, S. Kim, and S. B. Lee, “Recent advances in studies on the therapeutic potential of dietary carotenoids in neurodegenerative diseases,” *Oxid Med Cell Longev*, vol. 2018, pp. 1–13, Apr. 2018, doi: 10.1155/2018/4120458.

[42] J. Nordberg and E. S. J. Arnér, “Reactive oxygen species, antioxidants, and the mammalian thioredoxin system,” *Free Radic Biol Med*, vol. 31, no. 11, pp. 1287–1312, Dec. 2001, doi: 10.1016/S0891-5849(01)00724-9.

[43] C. C. R. Nogueira, I. C. N. D. P. Paixão, and V. L. Teixeira, “Antioxidant activity of natural products isolated from red seaweeds,” *Nat Prod Commun*, vol. 9, no. 7, Jun. 2014, doi: 10.1177/1934578x1400900737.

[44] B. Halliwell, “Biochemistry of oxidative stress,” *Biochem Soc Trans*, vol. 35, no. 5, pp. 1147–1150, Nov. 2007, doi: https://doi.org/10.1042/BST0351147.

[45] G. W. Burton and K. U. Ingold, “β-Carotene: An unusual type of lipid antioxidant,” *Science (1979)*, vol. 224, no. 4649, pp. 569–573, May 1984, doi: 10.1126/science.6710156.

[46] D. A. Cooper, A. L. Eldridge, and J. C. Peters, “Dietary carotenoids and certain cancers, heart disease, and age-related macular degeneration: A review of recent research,” *Nutr Rev*, vol. 57, no. 7, pp. 201–214, Jun. 1999, doi: 10.1111/j.1753-4887.1999.tb06944.x.

[47] J. Chaudière and R. Ferrari-Iliou, “Intracellular antioxidants: From chemical to biochemical mechanisms,” *Food and Chemical Toxicology*, vol. 37, no. 9–10, pp. 949–962, Oct. 1999, doi: 10.1016/S0278-6915(99)00090-3.

[48] K. Jørgensen and L. H. Skibsted, “Carotenoid scavenging of radicals,” *Z Lebensm Unters Forsch*, vol. 196, no. 5, pp. 423–429, Oct. 1993, doi: 10.1007/bf01190806.

[49] K. Fukuzawa, Y. Inokami, A. Tokumura, J. Terao, and A. Suzuki, “Rate constants for quenching singlet oxygen and activities for inhibiting lipid peroxidation of carotenoids and α-tocopherol in liposomes,” *Lipids*, vol. 33, no. 8, pp. 751–756, Aug. 1998, doi: 10.1007/s11745-998-0266-y.

[50] R. Edge, D. J. McGarvey, and T. G. Truscott, “The carotenoids as anti-oxidants - A review,” *J Photochem Photobiol B*, vol. 41, no. 3, pp. 189–200, Dec. 1997, doi: 10.1016/S1011-1344(97)00092-4.

[51] J. H. Tinkler, F. Böhm, W. Schalch, and T. G. Truscott, “Dietary carotenoids protect human cells from damage,” *J Photochem Photobiol B*, vol. 26, no. 3, pp. 283–285, Dec. 1994, doi: 10.1016/1011-1344(94)07049-0.

[52] F. Khachik, “Distribution and metabolism of dietary carotenoids in humans as a criterion for development of nutritional supplements,” *Pure and Applied*

Chemistry, vol. 78, no. 8, pp. 1551–1557, Jan. 2006, doi: 10.1351/pac200678081551.

[53] G. van Poppel, "Carotenoids and cancer: An update with emphasis on human intervention studies," *Eur J Cancer*, vol. 29, no. 9, pp. 1335–1344, Feb. 1993, doi: 10.1016/0959-8049(93)90087-V.

[54] R. G. Ziegler, "A review of epidemiologic evidence that carotenoids reduce the risk of cancer," *Journal of Nutrition*, vol. 119, no. 1, pp. 116–122, Jan. 1989, doi: 10.1093/jn/119.1.116.

[55] J. L. Rowles, K. M. Ranard, C. C. Applegate, S. Jeon, R. An, and J. W. Erdman, "Processed and raw tomato consumption and risk of prostate cancer: a systematic review and dose–response meta-analysis," *Prostate Cancer Prostatic Dis*, vol. 21, no. 3, pp. 319–336, Jan. 2018, doi: 10.1038/s41391-017-0005-x.

[56] K. Vijay *et al.*, "Low-dose doxorubicin with carotenoids selectively alters redox status and upregulates oxidative stress-mediated apoptosis in breast cancer cells," *Food and Chemical Toxicology*, vol. 118, pp. 675–690, Aug. 2018, doi: 10.1016/j.fct.2018.06.027.

[57] X. Wen *et al.*, "Neuroprotective effect of astaxanthin against glutamate-induced cytotoxicity in HT22 cells: Involvement of the Akt/GSK-3β pathway," *Neuroscience*, vol. 303, pp. 558–568, Sep. 2015, doi: 10.1016/j.neuroscience.2015.07.034.

[58] X. S. Zhang *et al.*, "Astaxanthin alleviates early brain injury following subarachnoid hemorrhage in rats: Possible involvement of Akt/bad signaling," *Mar Drugs*, vol. 12, no. 8, pp. 4291–4310, Jul. 2014, doi: 10.3390/md12084291.

[59] E. J. Johnson *et al.*, "Relationship between serum and brain carotenoids, α - tocopherol, and retinol concentrations and cognitive performance in the oldest old from the georgia centenarian study," *J Aging Res*, vol. 2013, pp. 1–13, Apr. 2013, doi: 10.1155/2013/951786.

[60] D. Nguyen, T. Thrimawithana, T. J. Piva, D. Grando, and T. Huynh, "Benefits of plant carotenoids against age-related macular degeneration," *J Funct Foods*, vol. 106, May 2023, doi: 10.1016/j.jff.2023.105597.

[61] W. Stahl and H. Sies, "β-Carotene and other carotenoids in protection from sunlight," *American Journal of Clinical Nutrition*, vol. 96, no. 5, pp. 1179S-1184S, Nov. 2012, doi: 10.3945/ajcn.112.034819.

[62] F. Hajizadeh-Sharafabad, Z. Ghoreishi, V. Maleki, and A. Tarighat-Esfanjani, "Mechanistic insights into the effect of lutein on atherosclerosis, vascular dysfunction, and related risk factors: A systematic review of in vivo, ex vivo and in vitro studies," *Pharmacol Res*, vol. 149, p. 104477, Nov. 2019, doi: 10.1016/j.phrs.2019.104477.

[63] R. K. Saini, K. R. R. Rengasamy, F. M. Mahomoodally, and Y. S. Keum, "Protective effects of lycopene in cancer, cardiovascular, and neurodegenerative diseases: An update on epidemiological and mechanistic perspectives," *Pharmacol Res*, vol. 155, p. 104730, May 2020, doi: 10.1016/j.phrs.2020.104730.

[64] R. K. Saini and Y. S. Keum, "Microbial platforms to produce commercially vital carotenoids at industrial scale: an updated review of critical issues," *J Ind*

Microbiol Biotechnol, vol. 46, no. 5, pp. 657–674, May 2019, doi: 10.1007/s10295-018-2104-7.

[65] N. Mezzomo and S. R. S. Ferreira, "Carotenoids functionality, sources, and processing by supercritical technology: A review," *J Chem*, vol. 2016, p. 164312, Mar. 2016, doi: 10.1155/2016/3164312.

[66] V. Ashokkumar *et al.*, "Technological advances in the production of carotenoids and their applications– A critical review," *Bioresour Technol*, vol. 367, p. 128215, Jan. 2023, doi: 10.1016/j.biortech.2022.128215.

[67] T. B. Cook, J. M. Rand, W. Nurani, D. K. Courtney, S. A. Liu, and B. F. Pfleger, "Genetic tools for reliable gene expression and recombineering in Pseudomonas putida," *J Ind Microbiol Biotechnol*, vol. 45, no. 7, pp. 517–527, Jul. 2018, doi: 10.1007/s10295-017-2001-5.

[68] J. Mi *et al.*, "De novo production of the monoterpenoid geranic acid by metabolically engineered Pseudomonas putida," *Microb Cell Fact*, vol. 13, no. 1, p. 170, Dec. 2014, doi: 10.1186/s12934-014-0170-8.

[69] M. Furubayashi *et al.*, "Capsanthin Production in Escherichia coli by Overexpression of Capsanthin/Capsorubin Synthase from Capsicum annuum," *J Agric Food Chem*, vol. 69, no. 17, pp. 5076–5085, Apr. 2021, doi: 10.1021/acs.jafc.1c00083.

[70] M. Takemura *et al.*, "Pathway engineering for efficient biosynthesis of violaxanthin in Escherichia coli," *Appl Microbiol Biotechnol*, vol. 103, no. 23–24, pp. 9393–9399, Oct. 2019, doi: 10.1007/s00253-019-10182-w.

[71] J. Sambrook and D. W. Russell, *Molecular Cloning: A Laboratory Manual*, Third edition. United States: Cold Spring Harbor Laboratory Press., 2001.

[72] K. Iwasaki, H. Uchiyama, O. Yagi, T. Kurabayashi, K. Ishizuka, and Y. Takamura, "Transformation of Pseudomonas putida by Electroporation," *Biosci Biotechnol Biochem*, vol. 58, no. 5, pp. 851–854, Jan. 1994, doi: 10.1271/bbb.58.851.

[73] X. Luo, Y. Yang, W. Ling, H. Zhuang, Q. Li, and G. Shang, "Pseudomonas putida KT2440 markerless gene deletion using a combination of λ Red recombineering and Cre/loxP site-specific recombination," *FEMS Microbiol Lett*, vol. 363, no. 4, p. fnw014, Jan. 2016, doi: 10.1093/femsle/fnw014.

[74] H. G. Daood, G. Bencze, G. Palotás, Z. Pék, A. Sidikov, and L. Helyes, "HPLC analysis of carotenoids from tomatoes using cross-linked C18 column and MS detection," *J Chromatogr Sci*, vol. 52, no. 9, pp. 985–991, Sep. 2014, doi: 10.1093/chromsci/bmt139.

[75] J. I. Hattan, M. Furubayashi, T. Maoka, M. Takemura, and N. Misawa, "Reconstruction of the Native Biosynthetic System of Carotenoids in E. coli─Biosynthesis of a Series of Carotenoids Specific to Paprika Fruit," *ACS Synth Biol*, vol. 12, no. 4, pp. 1072–1080, Mar. 2023, doi: 10.1021/acssynbio.2c00578.

[76] P. Sundararajan and S. P. Ramasamy, "Current perspectives on industrial application of microbial carotenoid as an alternative to synthetic pigments," 2024. doi: 10.1016/j.scp.2023.101353.

[77] D. Xinrui, L. Bo, B. Yihong, L. Weifeng, and T. Yong, "Metabolic engineering of Escherichia coli for high-level production of violaxanthin," *Microb Cell Fact*, vol. 22, no. 1, p. 115, Jun. 2023, doi: 10.1186/s12934-023-02098-y.

[78] D. D. Qi, J. Jin, D. Liu, B. Jia, and Y. J. Yuan, “In vitro and in vivo recombination of heterologous modules for improving biosynthesis of astaxanthin in yeast,” *Microb Cell Fact*, vol. 19, no. 1, p. 103, May 2020, doi: 10.1186/s12934-020-01356-7.

[79] G. Chen *et al.*, “Molecular mechanisms of the coordination between astaxanthin and fatty acid biosynthesis in Haematococcus pluvialis (Chlorophyceae),” *Plant Journal*, vol. 81, no. 1, pp. 95–107, Jan. 2015, doi: 10.1111/tpj.12713.

[80] A. Shaish, A. Ben-Amotz, and M. Avron, “Biosynthesis of β-carotene in Dunaliella,” *Methods Enzymol*, vol. 213, pp. 439–444, 1992, doi: 10.1016/0076-6879(92)13145-N.

[81] J. Yang and L. Guo, “Biosynthesis of β-carotene in engineered E. coli using the MEP and MVA pathways,” *Microb Cell Fact*, vol. 13, no. 1, p. 160, Nov. 2014, doi: 10.1186/s12934-014-0160-x.

[82] C. Schwartz, K. Frogue, J. Misa, and I. Wheeldon, “Host and pathway engineering for enhanced lycopene biosynthesis in Yarrowia lipolytica,” *Front Microbiol*, vol. 8, p. 2233, Nov. 2017, doi: 10.3389/fmicb.2017.02233.

[83] M. H. Hussain *et al.*, “Rationally optimized generation of integrated Escherichia coli with stable and high yield lycopene biosynthesis from heterologous mevalonate (MVA) and lycopene expression pathways,” *Synth Syst Biotechnol*, vol. 6, no. 2, pp. 85–94, Jun. 2021, doi: 10.1016/j.synbio.2021.04.001.

[84] H. Beuttler *et al.*, “Biosynthesis of zeaxanthin in recombinant Pseudomonas putida,” *Appl Microbiol Biotechnol*, vol. 89, no. 4, pp. 1137–1147, Oct. 2010, doi: 10.1007/s00253-010-2961-0.

[85] Y. Xie, S. Chen, and X. Xiong, “Metabolic Engineering of Non-carotenoid-Producing Yeast Yarrowia lipolytica for the Biosynthesis of Zeaxanthin,” *Front Microbiol*, vol. 12, Oct. 2021, doi: 10.3389/fmicb.2021.699235.

[86] A. Pachaiyappan, G. Sadhasivam, M. Kumar, and A. Muthuvel, “Biomedical Potential of Astaxanthin from Novel Endophytic Pigment Producing Bacteria Pontibacter korlensis AG6,” *Waste Biomass Valorization*, vol. 12, no. 4, pp. 2119–2129, Jul. 2020, doi: 10.1007/s12649-020-01169-0.

[87] N. S. A. Hagaggi and U. M. Abdul-Raouf, “Production of bioactive β-carotene by the endophytic bacterium Citricoccus parietis AUCs with multiple in vitro biological potentials,” *Microb Cell Fact*, vol. 22, no. 1, p. 90, May 2023, doi: 10.1186/s12934-023-02108-z.

[88] M. Singh and K. D. Pandey, “Endophytic bacterial strains modulated synthesis of lycopene and bioactive compounds in Solanum lycopersicum L. fruit,” *Biocatal Agric Biotechnol*, vol. 35, p. 102088, Aug. 2021, doi: 10.1016/j.bcab.2021.102088.

[89] J. Chen, R. Zhang, G. Zhang, Z. Liu, H. Jiang, and X. Mao, “Heterologous Expression of the Plant-Derived Astaxanthin Biosynthesis Pathway in Yarrowia lipolytica for Glycosylated Astaxanthin Production,” *J Agric Food Chem*, vol. 71, no. 6, 2023, doi: 10.1021/acs.jafc.2c08153.

APPENDIX

Additional Results

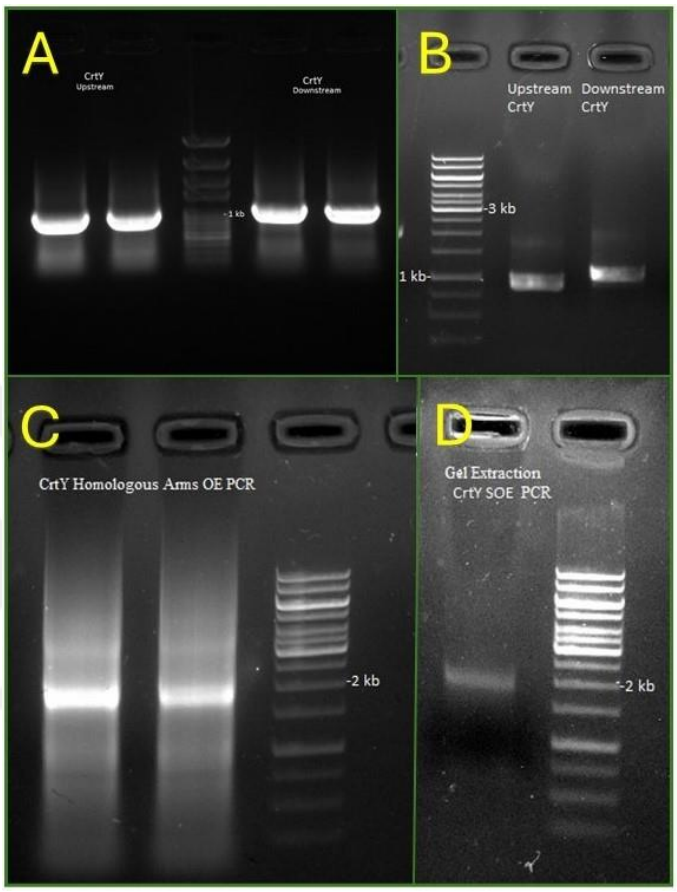

Figure A.1 Agarose gel electrophoresis results for the construction of pJOE with homologous arms of *crtY* gene. A) PCR amplification of upstream and downstream homologous arms, B) Gel extraction results for amplified homologous arms, C) Hybridization of homologous arm by OE PCR, D) Gel extraction results for hybridized homologous arms.

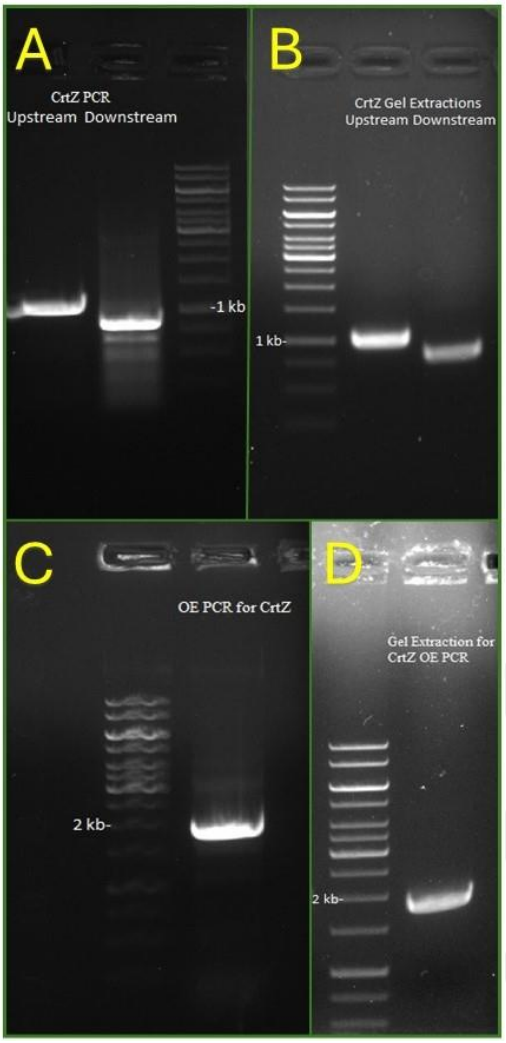

Figure A.2 Agarose gel electrophoresis results for the construction of pJOE with homologous arms of *crtZ* gene. A) PCR amplification of upstream and downstream homologous arms, B) Gel extraction results for amplified homologous arms, C) Hybridization of homologous arm by OE PCR, D) Gel extraction results for hybridized homologous arms.

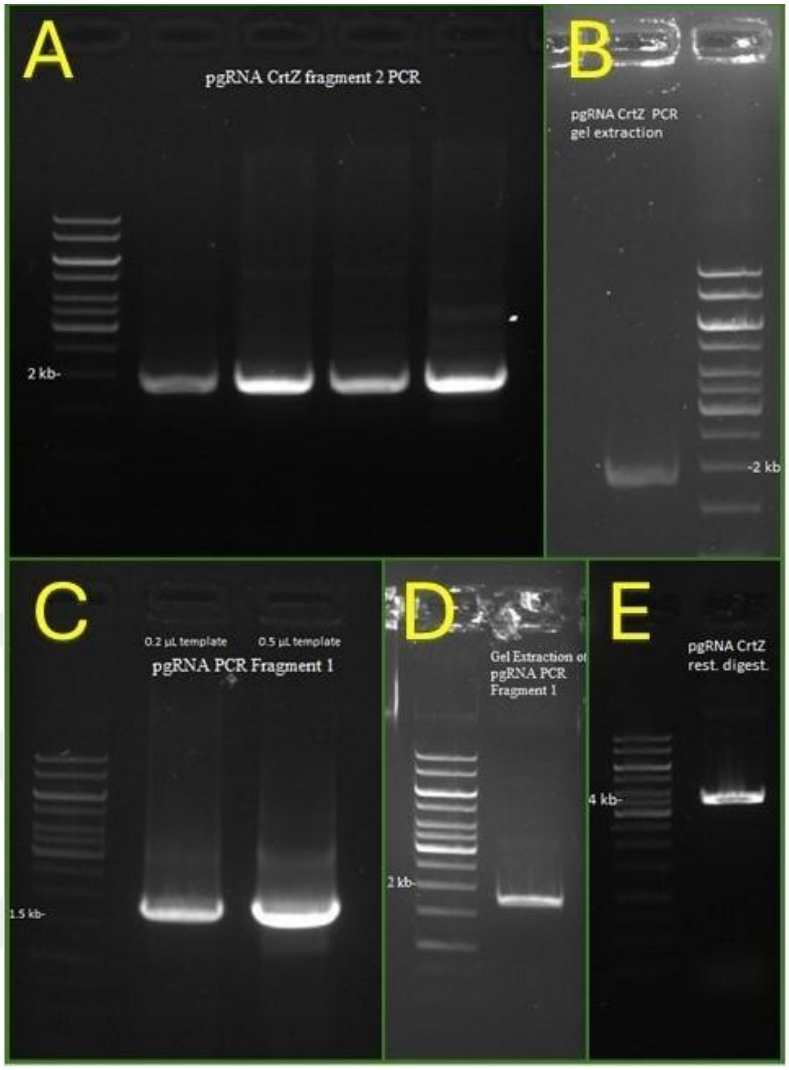

Figure A.3 Agarose gel electrophoresis results for the construction of pgRNAtet with N20 sequence of *crtZ* gene (pNAr15). A) PCR amplification of fragment 2, B) Gel extraction result for amplified fragment 2, C) PCR amplification of fragment 1, D) Gel extraction result for amplified fragment 1, E) Confirmation of the construct by SpeI restriction digestion.

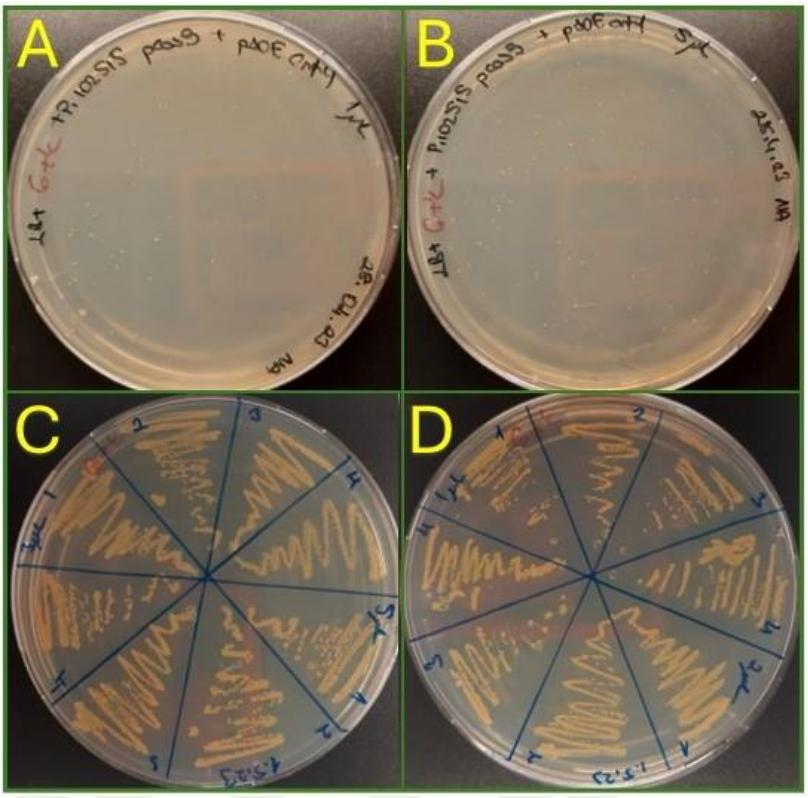

Figure A.4 Electroporation of pNAr10 plasmid to *Pseudomonas* sp. 102515/pCas9. A) and B) Selection of transformed cells after electroporation, C) and D) Subculturing of transformants in fresh plates.

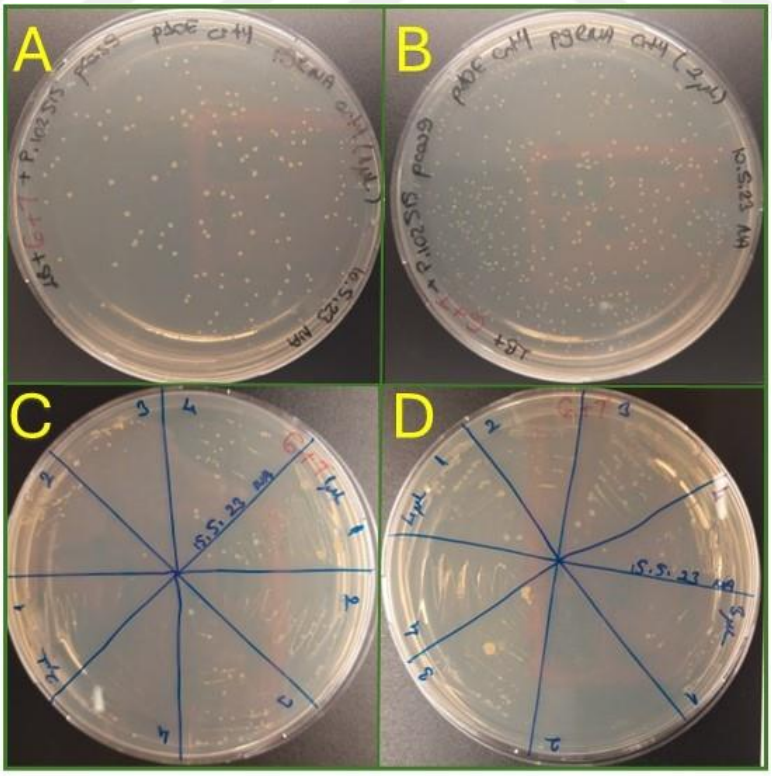

Figure A.5 Electroporation of pNAr9 plasmid to *Pseudomonas* sp. 102515/pCas9-pNAr10. A) and B) Selection of transformed cells after electroporation, C) and D) Subculturing of transformants in fresh plates.

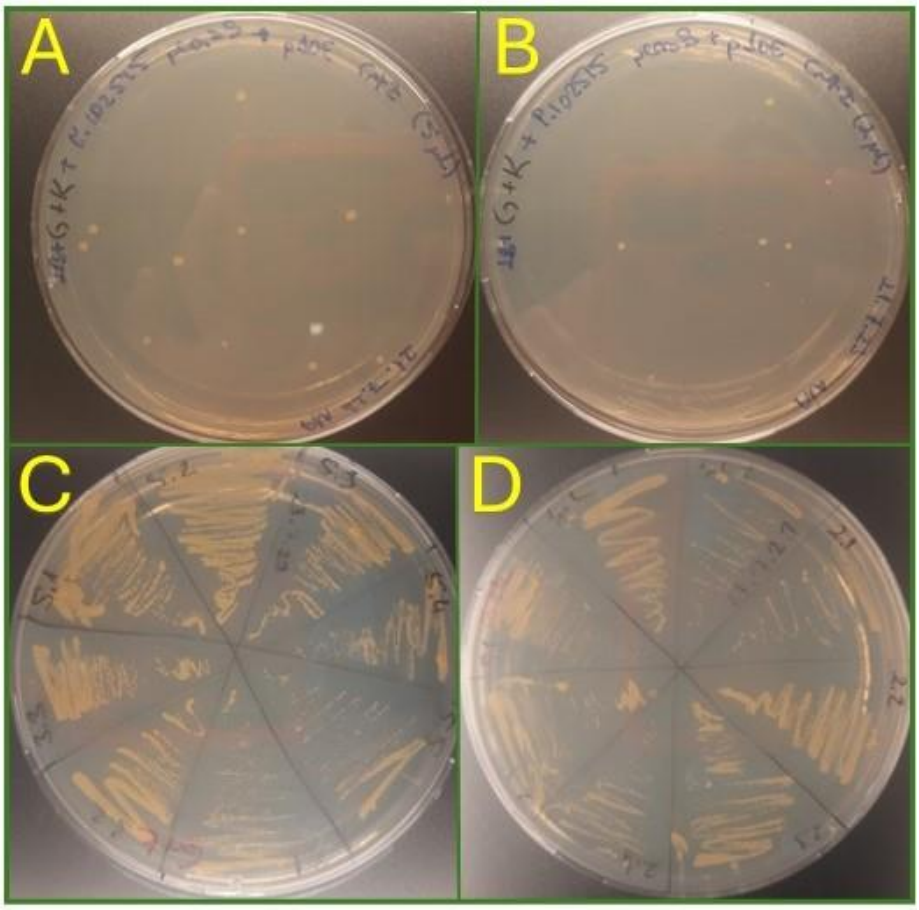

Figure A.6 Electroporation of pNAr14 plasmid to *Pseudomonas* sp. 102515/pCas9. A) and B) Selection of transformed cells after electroporation, C) and D) Subculturing of transformants in fresh plates.

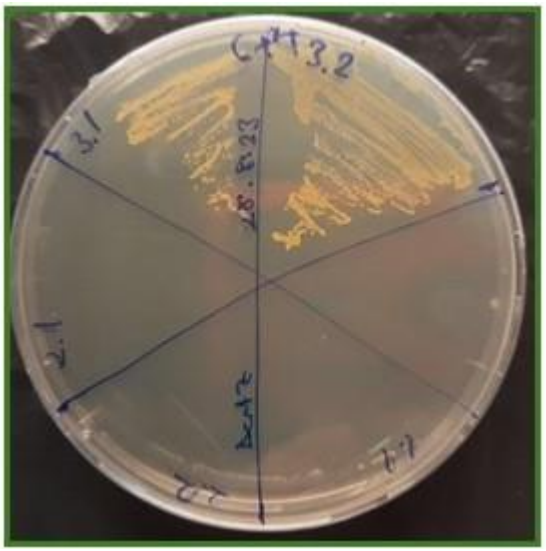

Figure A.7 Electroporation of pNAr15 plasmid to *Pseudomonas* sp. 102515/pCas9-pNAr14, subculturing of transformants in a fresh plate.

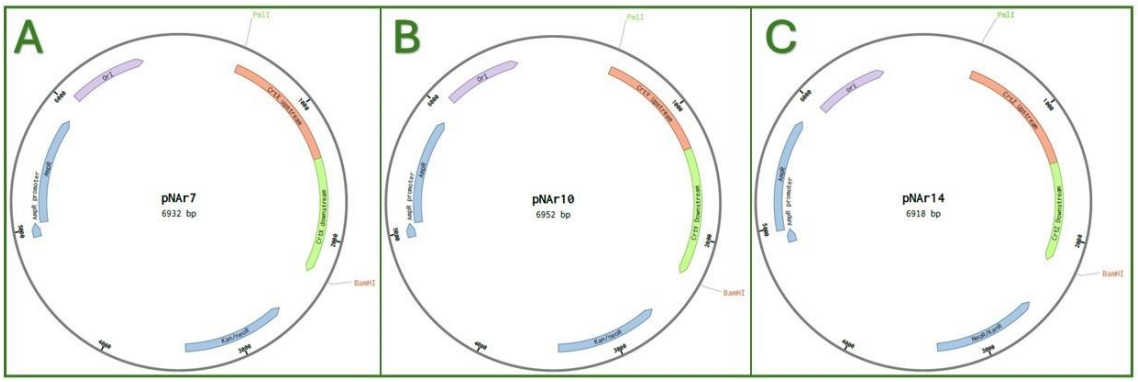

Figure A.8 Plasmid maps for pJOE constructs with hybridized homologous arms of target gene, upstream annotated with orange and downstream annotated with green. A) pNAr7 for *crtX*, B) pNAr10 *crtY*, C) pNAr14 *crtZ*.

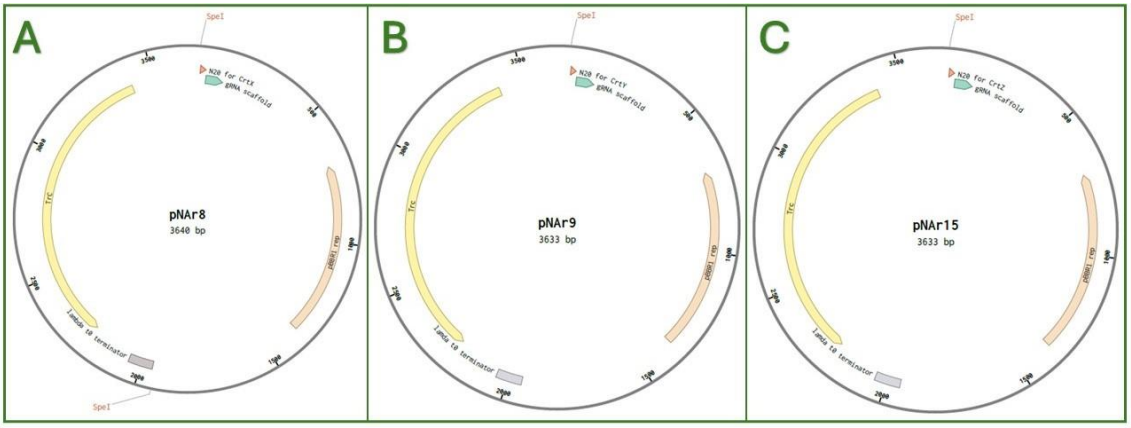

Figure A.9 Plasmid maps for pgRNAtet constructs with unique N20 sequence (annotated orange) of target gene. A) pNAr8 for *crtX*, B) pNAr9 *crtY*, C) pNAr15 *crtZ*.

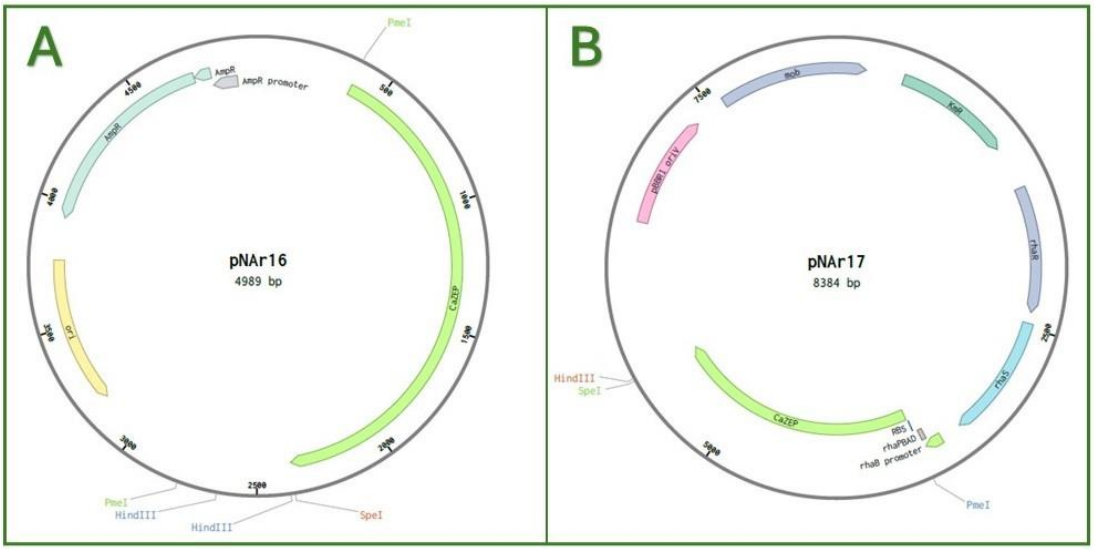

Figure A.10 Plasmid maps for *CaZEP* (annotated green) encoding constructs. A) pNAr16 with pJET1.2 backbone, B) pNAr17 with pMiS1 backbone.

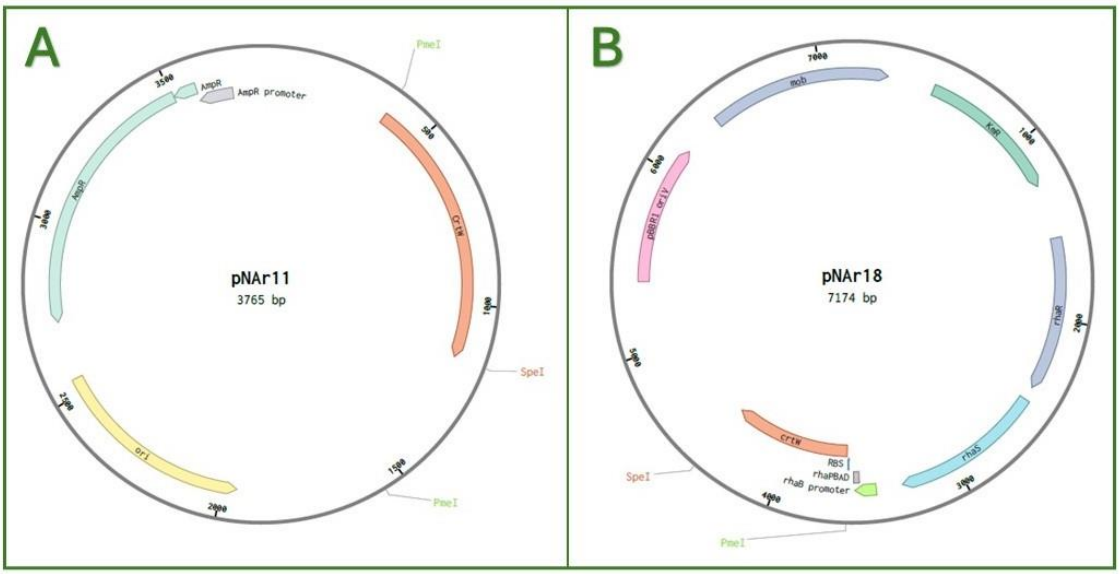

Figure A.11 Plasmid maps for *crtW* (annotated orange) encoding constructs. A) pNAr11 with pJET1.2 backbone, B) pNAr18 with pMiS1 backbone.

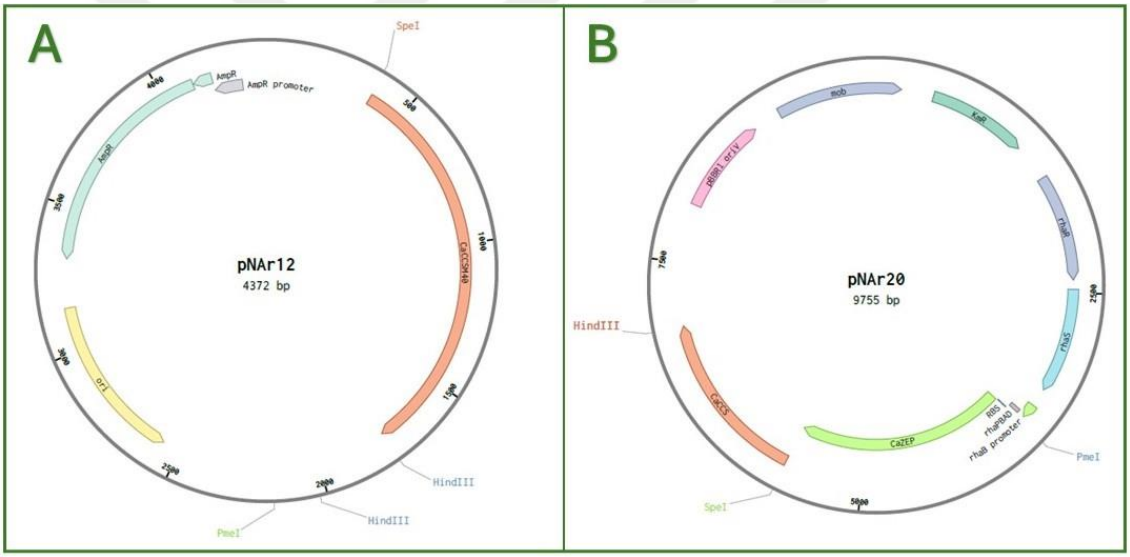

Figure A.12 Plasmid maps for *CaCCS* (annotated orange) encoding constructs. A) pNAr12 with pJET1.2 backbone, B) pNAr20 with pMiS1-CaZEP backbone.

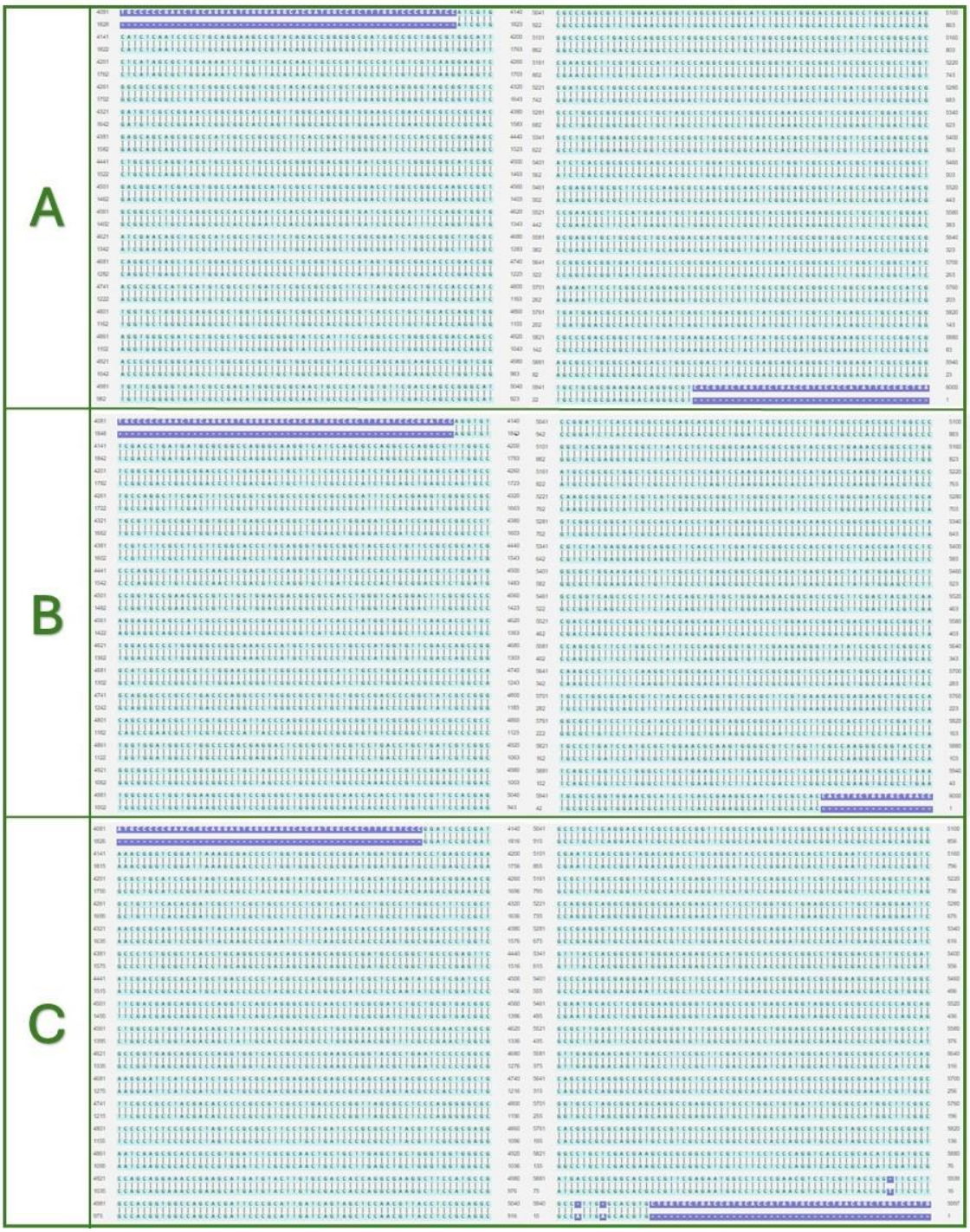

Figure A.13 Sequence alignment results for hybridized homologous arms of target genes with sequence 1 as sequencing result and sequence 2 as in silico designed sequence, aligned regions are blue. A) Alignment for *crtX* homologous arms in pNAr7, B) Alignment for *crtY* homologous arms in pNAr10, C) Alignment for *crtZ* homologous arms in pNAr14.

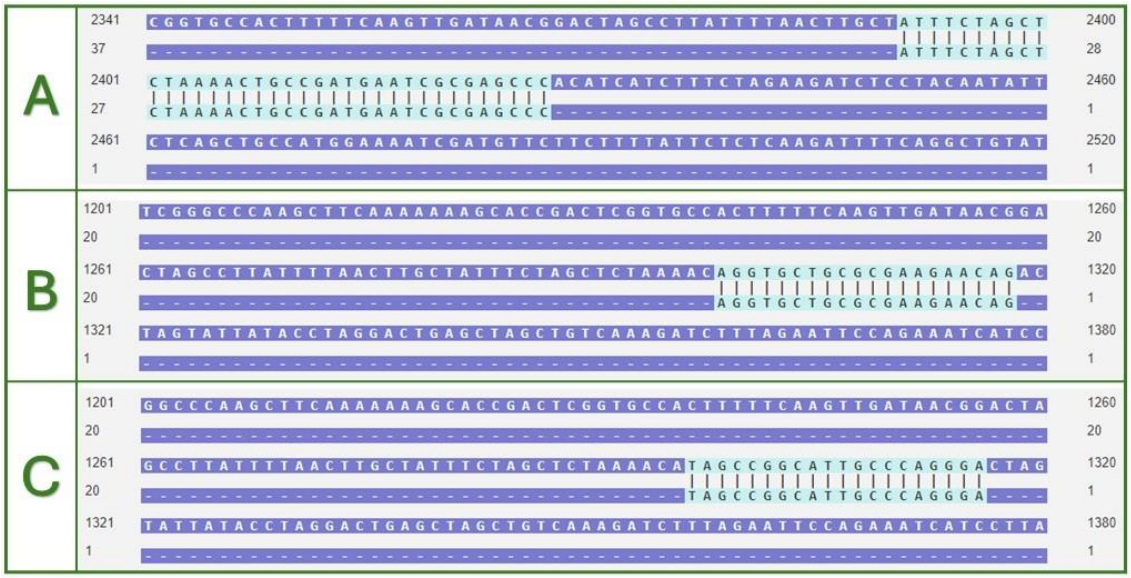

Figure A.14 Sequence alignment results unique N20 sequence of target genes with sequence 1 as sequencing result and sequence 2 as N20 sequence, aligned regions are blue. A) Alignment for *crtX* N20 sequence in pNAr8, B) Alignment for *crtY* N20 sequence in pNAr9, C) Alignment for *crtZ* N20 sequence in pNAr15.

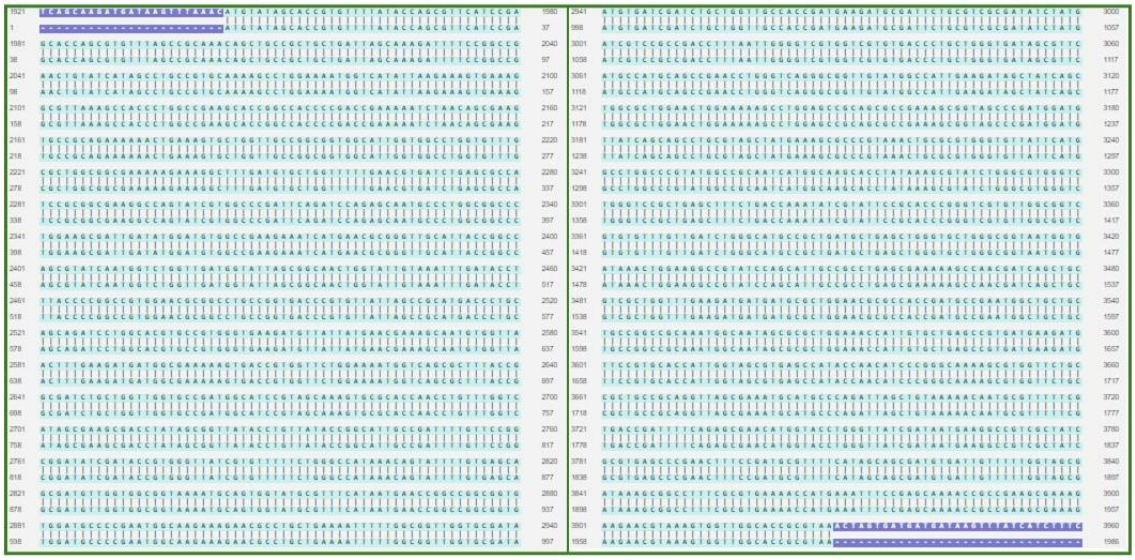

Figure A.15 Sequence alignment results for *CaZEP* gene with sequence 1 as sequencing result from pNAr16 and sequence 2 as *CaZEP* gene, aligned regions are blue..

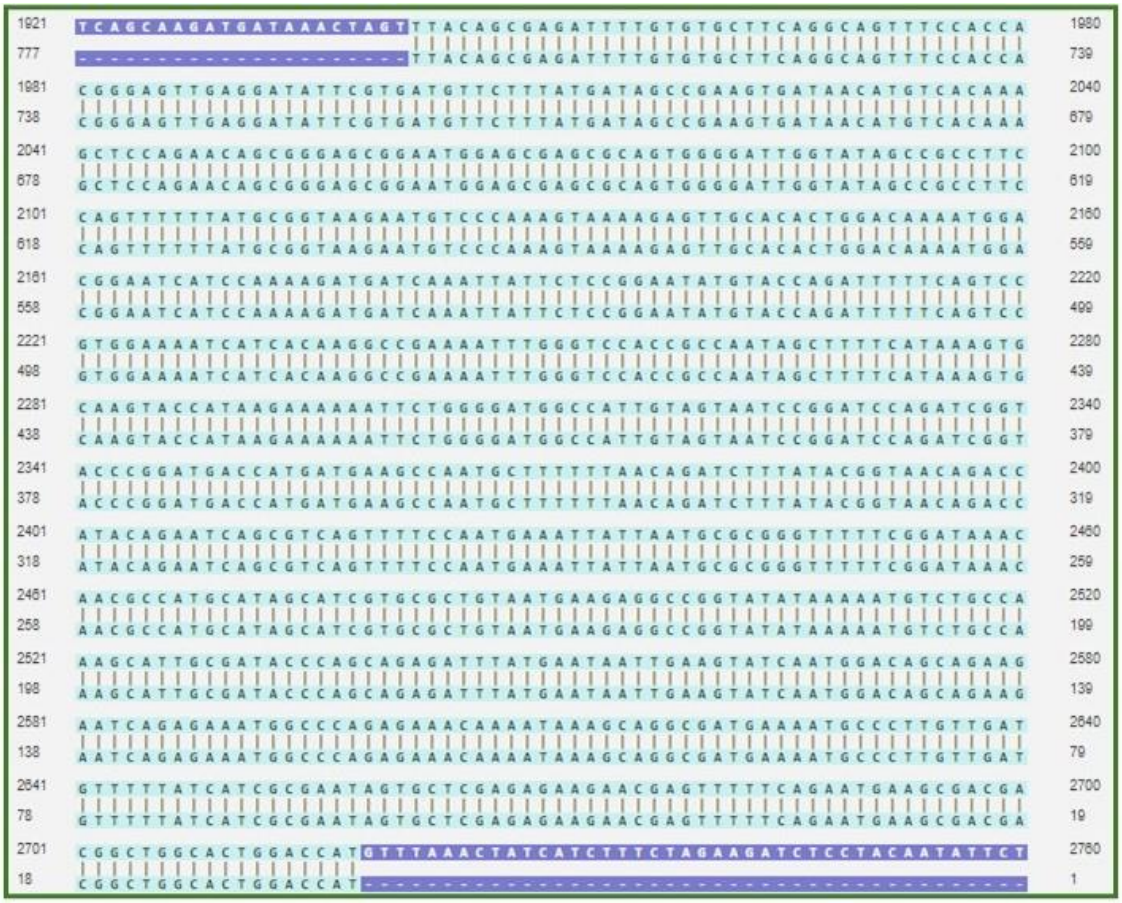

Figure A.16 Sequence alignment results for *crtW* gene with sequence 1 as sequencing result from pNAr11 and sequence 2 as *crtW* gene, aligned regions are blue.

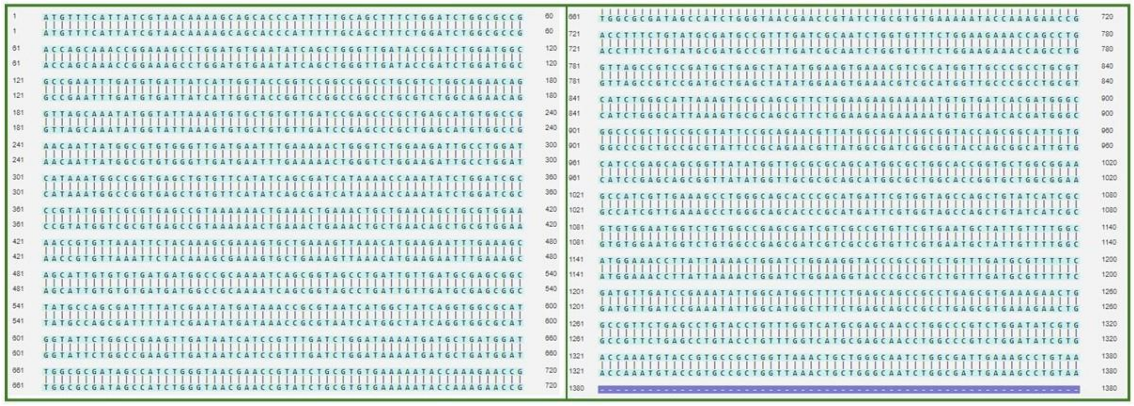

Figure A.17 Sequence alignment results for *CaCCS* gene with sequence 1 as sequencing result from pNAr12 and sequence 2 as *CaCCS* gene, aligned regions are blue.

Curriculum Vitae

EDUCATIONAL BACKGROUND

2022 – 2024: Abdullah Gül University
Department of Bioengineering, Master of Science
GPA: 3.96 / 4.00

2017 – 2021: Canakkale Onsekiz Mart University,
Department of Molecular Biology and Genetics, Bachelor of Science
GPA: 3.52 / 4.00

2021 January - June: University of Jyväskylä,
Department of Biological and Environmental Sciences,
Erasmus+ Student Mobility Program

PROJECTS

- **Production of High Value-Added Carotenoids in Engineered Microorganisms (2022 – 2024, 24 months)**

  Genome editing of an endophytic carotenoid producing *Pseudomonas* sp. by CRISPR-Cas9 system and construction of overexpression plasmids.

  Asst. Prof. Dr. Ozkan Fidan, Nuriye Arslansoy

  Metabolic Engineering and Synthetic Biology Laboratory, Department of Bioengineering, Abdullah Gül University, Türkiye

- **Investigation of the Potential Therapeutic Effect of Dietary Changes in the *C. elegans* Model Organism with patr-1 Mutation (2023–2024, 10 months)**

  Feeding the model organism with isolated soil bacteria species, probiotic, pathogen bacteria strains and carotenoid producing *Pseudomonas* sp. and observation of the movement capabilities of *C. elegans* with patr-1 mutation.

  Asst. Prof. Ozkan Fidan, Sara Luna Al-Banna, Sumiah Mazed, Nuriye Arslansoy

  Metabolic Engineering and Synthetic Biology Laboratory, Department of Bioengineering, Abdullah Gül University, Türkiye

- **Valorization of Waste Cooking Oil by Recombinant Enzyme Production (2022 – 2023, 10 months)**

  Recombinant enzyme production via molecular cloning and biotransformation of waste cooking oil to obtain high value-added product.

  Asst. Prof. Dr. Ozkan Fidan, Fatma Sener, Melisa Zülal Karaman, Hatice Yılmaz, Sena Yüksel, Nuriye Arslansoy

  Metabolic Engineering and Synthetic Biology Laboratory, Department of Bioengineering, Abdullah Gül University, Türkiye

- **Isolation of Soil Bacteria from Sultan Marshes to Investigate Their Antifungal Activities (2022–2023, 10 months)**

  Bacteria isolation from soil samples and identification via 16s rRNA sequences, testing bacterial species against 5 different fungi strains which causes plant diseases.

  Asst. Prof. Dr. Ozkan Fidan, Ahsen Beyza Yigit, Fatma Begendik, Nurzülal Erden, Nuriye Arslansoy

  Metabolic Engineering and Synthetic Biology Laboratory, Department of Bioengineering, Abdullah Gül University, Türkiye

- **Investigation of Natural Products to Prevent Human Body Malodor Formation (2022–2023, 10 months)**

  After in silico analyses, testing 3 natural products and tracking the formation 3M3SH that causes human body malodor, investigating antibacterial activity of tested natural products.

  Asst. Prof. Dr. Ozkan Fidan, Ayse Anaz, Ayse Doga Karipcin, Ayse Hamide Kose, Beyza Nur Demirsoy, Nuriye Arslansoy

  Metabolic Engineering and Synthetic Biology Laboratory, Department of Bioengineering, Abdullah Gül University, Türkiye

- **Cell-free Expression of 1433-0 Protein (2021 – 2022, 4 months)**

  Cell-free expression of 1433-0 protein via transformation of pIX30 plasmid to *E.coli* (DH5α) after cloning of 1433-0 gene, and purification of synthetic 1433-0 proteins.

  Prof. Dr. Gerhard Obermeyer, Nuriye Arslansoy

  Membrane Biophysics Laboratory, Department of Biosciences, Paris-Lodron Universität Salzburg, Austria

PUBLICATIONS

• Fidan, O.*, Karipcin, A.D., Köse, A.H., Anaz, A., Demirsoy, B.N., **Arslansoy, N.,** Sun, L., Mujwar, S. **(2024).** Discovery of a C-S lyase inhibitor for the prevention of human body malodor formation: tannic acid inhibits the thioalcohol production in *Staphylococcus hominis*. *International Microbiology* https://doi.org/10.1007/s10123-024-00551-5

• **Arslansoy, N.**, & Fidan, O.* **(2024).** Carotenoids and Their Antioxidant Power. In A. N. Barros & A. C. Santos Abraão (Eds.), *The Power of Antioxidants - Unleashing Nature's Defense Against Oxidative Stress*. https://doi.org/10.5772/intechopen.1006082

PRESENTATIONS

• **Oral Presentation**: Fidan, O.*, **Arslansoy, N. (2023)** Biosynthesis of high value-added carotenoids by engineered microorganisms. 6th International Eurasian Conference on Biological and Chemical Sciences, Ankara, Türkiye, October 11-13.

• **Poster Presentation**: Karakas Metin, O., **Arslansoy, N., (2021)** Plant genome editing via CRISPR-Cas9 system. Canakkale Onsekiz Mart University Special Topics Course Presentations, Canakkale, Türkiye, January 13.